Master Thesis

Rasmus Arvidson & Jørgen Torp

Subsurface mapping of Revdalen

Telemark University College

Faculty of Arts and Sciences

HØGSKOLEN I TELEMARK

Master thesis in nature, health and environmental studies.

Subsurface mapping of Revdalen

Rasmus Arvidson & Jørgen Torp

15.05.2015

Subsurface mapping of Revdalen using geophysical instruments.

Høgskolen i Telemark

Avdeling for allmennvitenskapelige fag

Institutt for natur-, helse- og miljøfag

Hallvard Eikas plass

3800 Bø i Telemark

http://www.hit.no

Acknowledgements

We would like to thank our near family members for their support and patience in this study, which has had a durance of 15 months. Thank you, Professor Klempe, who has worked close with us all these months. We would also like to thank the Telemark University College (TUC) for making it possible to work with such equipment and staff.

Sammendrag

I Revdalen i Bø kommune har det vært forsket mye på den mulige forurensningen av grunnvannet og grunnvannsbrønner som blir brukt av husholdninger i området. Forurensningen er knyttet til avfallsdeponiet ved Djupegrop. Kartleggingen av grunnforholdene i området har vært vanskelig grunnet overflateforholdene. Sammen med bruk av tidligere data, har denne studien brukt to geofysiske metoder, ground penetrating radar og resistivitetsmålinger, med hovedvekt på resistivitetsmålinger, for å forsøke å forbedre kunnskapen om grunnforholdene, spesielt avstand til fjellgrunnen. Resistivitetsmetoden er ny for Høgskolen i Telemark, så studien har i tillegg hatt et fokus på å få erfaringer med bruken av denne geofysiske metoden, samt erfaringer av bruken av programvaren Geographic Information System for å behandle dataen fra kartleggingen

Abstract

In Revdalen in Bø county there has been a lot of research of the possible contamination of the ground water, and the ground water wells which are used by the households in the area. The contamination is connected to the landfill found at Djupegrop. The subsurface mapping of this area has been difficult due to the surficial conditions. Together with the use of earlier data, this study has used two geophysical methods, ground penetrating radar and resistivity measurements, with emphasis on resistivity measurements, to try to enhance the knowledge of the subsurface conditions, especially depth to bedrock. The method of resistivity measurements is new to the Telemark University College, so an additional focus of the study has been to gain experience of the use of the geophysical method, and to gain experience in the use of the software Geographic Information System to process the data of the subsurface mapping.

Key words: geophysical instruments; subsurface mapping; GPR; resistivity measurements.

Content

Introduction

Area description

The Bø municipality is situated in Telemark County, approximately 150 km west of Oslo.

The Revdalen area is located 4 km Northeast of Bø centrum. Revdalen is situated between the valley-sides that form the Bø-valley area. The area in which this study was conducted currently consists of farmland and forested land, with scattered domestic homes and farms. There is also a gravel pit and a rock quarry operating in the Revdalen area.

Revdalen Landfill

From 1958-1974 the Djupegrop landfill was active. From 1974-1997 the Revdalen landfill was active. January 1st 1997 the landfill was closed for dumping and later in the summer the landfill was covered by a layer of clay.

Djupegrop is a natural kettle hole, and is still visible in the terrain. The dump site is now covered by pine trees that are subject to forestry operations.

In 1989 continuous groundwater observations were undertaken by the Telemark University College and Bø municipality. Observations were undertaken with several test wells throughout the area. The observations show a high concentration of contamination in the area (Klempe, 1999).

The study area can be seen on figure 1.1 on page6. It consists of an area of 0,465 km^2 and is divided into two equally sized study areas. Study area 1 includes resistivity profiles 6-20 and has a size of 0,220 km^2 and study area 2, which includes profiles 26-42 and has a size of 0,245 km^2.

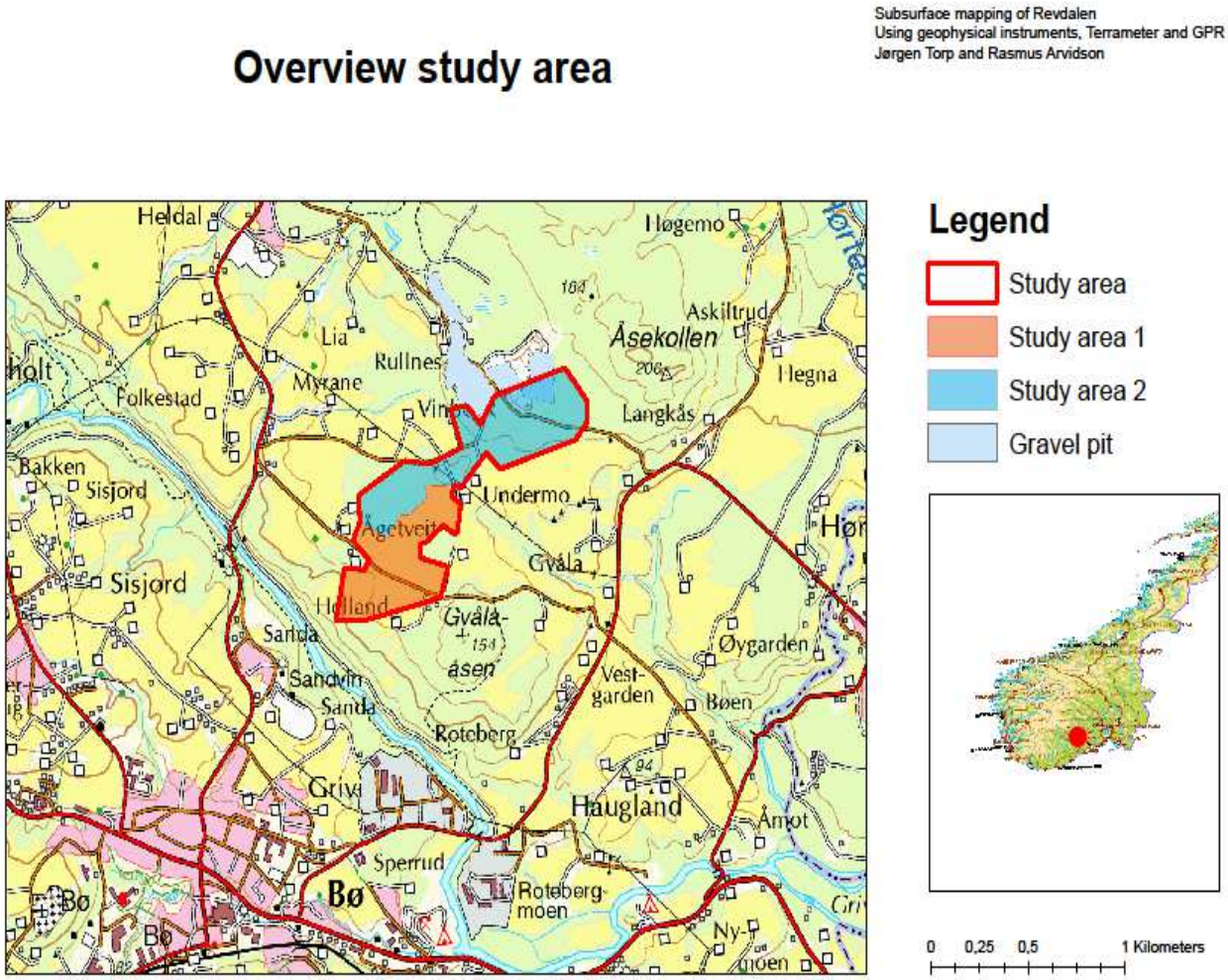

Figure 1.1: Overview of study area

Study area 1

This study area consists of relatively flat farmland, with a few hedgerows. It is situated north and south of the farm Ågetveit, as seen in figure 1.1 on page6. With natural property boundaries forming the edges of the study area.

The reason for separating the two study areas was the surface conditions, where study area 1 consists of farmland and was subject to agricultural work, which limited the time frame in which measurements could be taken.

Measurements in this area were undertaken in the timeperiod March 2014-May2014.

Study area 2

Study area 2 is situated north of study area 1 and consists predominantly of forested areas, with a few wet patches and bogs. Study area 2 is also situated in an area with forest roads that were subject to heavy traffic. Study area 2 streches out over an area with the Hellestad Sandtak and the old Revdalen landfill forming the northern boundary and the farms Ågetveit and Valen forming the southern and western boundaries as seen in figure 1.1 on page6.

Measurements in study area 2 were undertaken in April 2014- June 2014.

Revdalen Gravel Pit – Hellestad Sandtak

The gravel pit *Hellestad Sandtak* has been operating in the Revdalen Area since 1952. It delivers a varied amount of sand and gravel resources for use in several purposes throughout the Telemark area (Sandtak, 2015).

Bedrock and geology

The geology in the Telemark area was built in the Precambrian era (1500-900 mill. years ago). Originally the bedrock in Telemark was produced by sediments and volcanic activity in the Precambrian but it has since been subject to metamorphosis with intensive folding (Jansen, 1986).

In the Telemark area the bedrock consists of gneiss-granite with excerpts of quartzite and amphibolite's. Strike-zones are predominantly east-west oriented (Jansen, 1982).

The topography in the region is mainly influenced by the deformations in bedrock that occurred due to geomorphologic movements. The area has many faults and fractures that are still visible. Erosion and ice movement has formed the U-shaped valleys that are predominant in the area. The Bø-valley is one of such (Bergstrøm, 1999).

The geology in the Revdalen area, which is situated approximately in the center of the Telemark area is described as part of the Lifjell area. But the bedrock in Revdalen distinguishes itself as different from the quartzite-dominated Lifjell area by having predominantly gneiss-granite bedrock. Between the Lifjell area and the Revdalen area an amphibolite rich zone separates the two areas (Jansen 1983).

Quaternary geology

The deposits in Revdalen were produced in the Weichsel. The Weichsel lasted from approximately 115000 years B.P. to approximately 9000 years B.P. The peak of expansion was approximately 23000 years B.P. where the ice-cap covered most of Fennoscandia and Denmark, Germany and Poland. In the Telemark area the ice was melted down approximately 9500 years B.P. (Bergstrøm, 1999).

The main ice movement direction in the Telemark area is south-southeast or south-east, with several halts and advances along the retreat pattern. After the ice had retreated to the Geiteryggen stage at 11000-10600 years B.P., the main ice flow directions focused on southeastern movements in the established valleys and fjords in Telemark (Bergstrøm, 1999).

With the ice retreating, several landscape features were created. In the following a few of the landscape features that are present in the Revdalen area will be described.

As the ice melted sediments were deposited along and in front of the glacier.

In the study area, Jansen (1986) describes the Revdalen area as part of the Oterholt-Eika-Folkestadmogane, with a connection to the Akkerhaugen-stage of deglaciation. The material deposited in the area comes from this deglaciation stage. The Akkerhaugen deglaciation stage can be seen on figure 1.2 on page9.

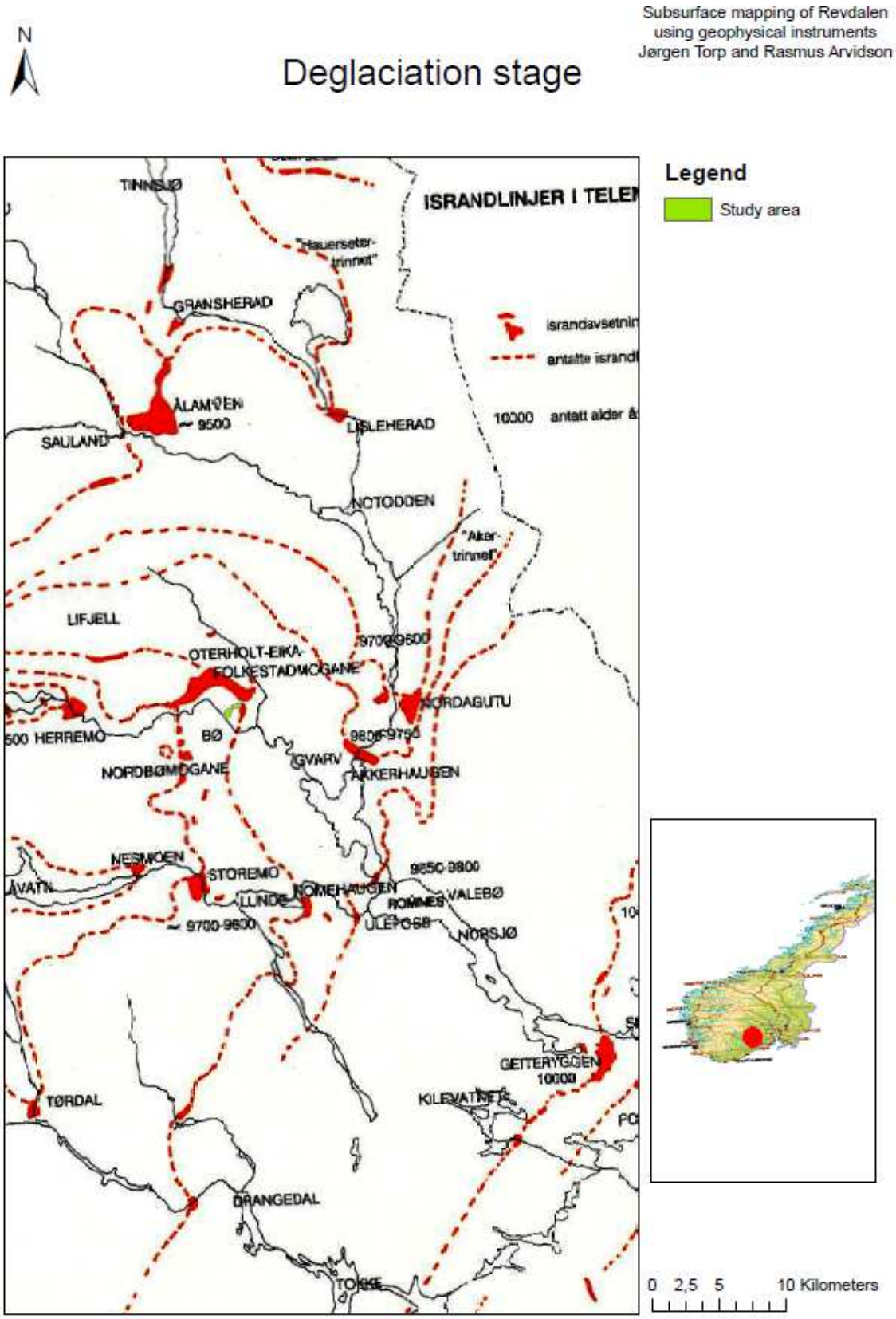

Figure 1.2: Deglaciation of Telemark (Jansen, 1986).

The Revdalen area is a front deposit. As the ice was benched in the sea, a delta was formed in front of the glacier. Material was transported out to the delta by glacial rivers, and was gradually built up in front of the glacier (Trømborg, 2006). Gradually as the ice retreated in the Bø area, several delta deposits were built up in front of the ice and along the bedrock hillside. As the sea rose, waves washed in over these delta deposits and sorted the material producing shore sediments (Jansen, 1986). At Revdalen the marine limit was situated approximately 150 m above today's sea-level (Bergstrøm, 1999).

As the ice melted a system of subglacial rivers formed what is known as an esker system shaping the terrain and creating hilly ridges with stone, sand and gravel (Jansen, 1986). The subglacial rivers would transport material beneath the ice, gradually slowing down towards the topographical bottom of the terrain. As the rivers slowed down, further sediments were deposited, forcing the subglacial river to carve upwards into the ice, and continuously build up new sediments. When the ice was completely retreated from the area, the formed ridges would collapse on both sides, leaving behind a system of ridges up to 20 m height visible in the terrain. An esker system can be seen in the northern part of the study area. (Jansen 1983)

A kettle hole is a landscape feature that is present in the study area. Kettle holes are a hole in the terrain created as the ice retreated. Big chunks of ice were often separated from the glacier, and covered by glaciofluvial deposits, lying protected in the terrain as a remnant of the glacier. When the ice chunks finally melted, material would collapse inwards creating a hole in the terrain. Kettle holes vary in size depending on the size of the ice chunk (Trømborg, 2006). Djupegrop is a kettle hole and is still visible in the terrain. Another visible kettle hole in the study area is Olavsbekk.

Part of the study area is an end moraine. This material was created in the melting periods of the last ice age (Klempe, 1988). In melting periods, a melt-out moraine may be created. When the ice cap retreats due to a warmer period, the retreat process will go slower if the ice cap meets the bedrock, which is believed to be the case at north-west in Revdalen (Klempe, 1988). In this situation there will be an accumulation of diamict if there are periods of colder climate in between the warmer periods, something which was also the case for Revdalen (Klempe, 1988). The colder periods made the ice cap expand, thus pushing the

material of the bottom of the ice cap in front of the ice. Now the melt-out moraine is transformed to a push-moraine. If this happens several times over the same location, a heap of end-moraine material would be build up.

The delta deposits were made by deposition from glacial rivers. This sorted material makes up for what is today used as a gravel resource. The majority of the rivers forming the Revdalen area, came from Lifjell, and carried meltwater and sorted material down where it is settled today (Jansen, 1986, and Jansen, 1983).

In the figure 1.3 seen below, is a map of the sedimentology in Revdalen. Pink is exposed bedrock. Orange is glaciofluvial delta deposits. Blue is marine deposits.

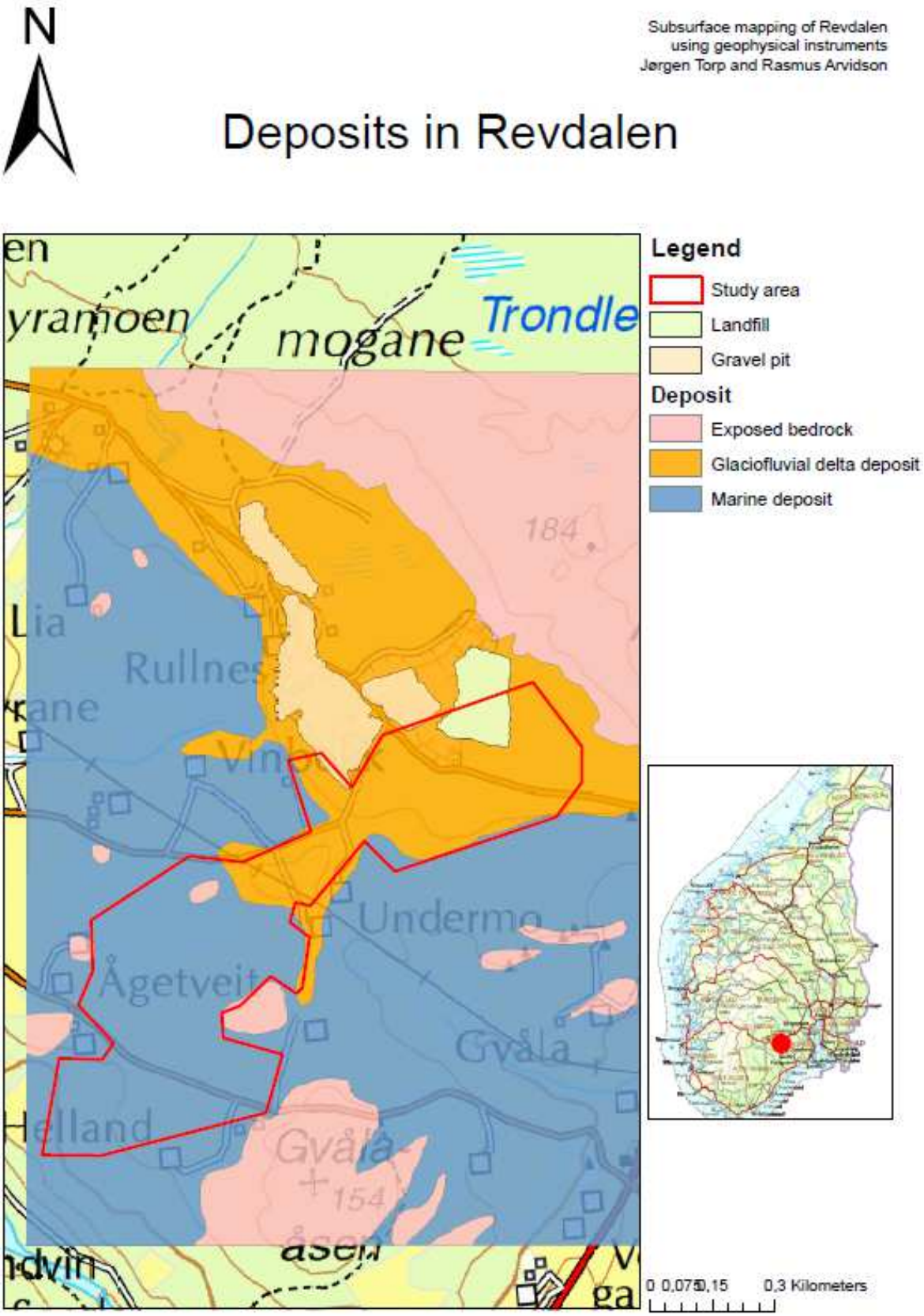

Figure 1.3: Sedimentology in Revdalen.

Earlier research

Jansen (1983) mapped the sand resources in the northern part of our study area. The area has been mapped subsurface, with different methods: drilling, GPR and seismic. Klempe (2004) also did some research in the northern part of our study area. From GPR profiles and drillings he made a database to examine the subsurface conditions. Many of the data from this research data are unpublished. Børresen et al. (1990) surveyed this area for their BSC Thesis. We have used some of their drillings from this area. Data from all of these has been used when interpreting the resistivity results, with good results. With both drillings, GPR data and several resistivity measurements from our research in the research area, the certainty of the interpretation of the resistivity measurements should be greatly enhanced. We have included data from these studies in our database, something which has increased the number of data points for the GIS data. The location of the data points, depth to bedrock values, and other information, are found in the result chapter, together with the interpretation of the relevant resistivity profiles.

Problems and purpose

There has been a lot of research in the area. Most of it has been connected to the landfill at Djupegrop and the investigation of the landfill's possible contamination of several ground water wells used by the households in the area. This research has met problems due to the subsurface sediment's attributes: in many places it has been difficult to perform drillings because of the compact and compressed surface sediments; GPR (ground penetrating radar) and seismic has encountered problems due to the thickness and unsaturated zone in the area. It has also been difficult to identify the cleft situated below Djupegrop (Klempe, 2004). The purposes for this thesis are to see whether results from a subsurface mapping with 2D-resistivity measurements can enhance the understanding of the subsurface of Revdalen. Especially will the depth to bedrock be analyzed, combining data from the resistivity measurements with data from earlier research done in the area. The study will emphasize the use of instruments and software used at TUC – 2D-resistivity measurements, GPR and GIS – in order to get valuable experience and know-how for the institution, using instruments and software already widely used in the study courses. The purposes are summarized in the table 1.1 below:

Table 1.1: Study aims.

Main study aim.	**Partial study aim.**
1) Subsurface mapping of Revdalen.	1-1) Using resistivity measurements to map the subsurface. Use other sources of information such as GPR and earlier data.
1) Subsurface mapping of Revdalen.	1-2) Creating a database from resistivity measurements readings and available data from TUC's geological and geophysical surveys.
2) Get experiences with the use of resistivity measurements by experimenting.	2-1) Get experiences with different subsurface conditions: resistivity profiles alone; combining TUC's two available geophysical instruments.

Methods

2D-Resistivity measurements

Choice of geophysical method

Resistivity measurements is a method that is non-invasive, in which it does not demand large field work and equipment such as drilling, and does not disturb the surface in any great manner or the subsurface conditions at all. This makes the method suitable for projects with limitations in budget, time or nature vulnerability, all of which were limiting factors in this study. The ability to use this geophysical method is therefore useful for TUC, and our study is an experimental study in order to get experience in use of this geophysical instrument.

History

The method of using current to understand the subsurface conditions has been used since the 1920's (Loke 2004). From the 1950's the method was used for mineral exploration, with four electrodes and limited computer capabilities (Loke 2004). In the 1990's, due to strongly enhanced computer capabilities, one started experimenting with many electrodes instead of only four. After this, the use has greatly increased and the method is now used in several different research fields, such as hydrogeological, geotechnical and in environmental surveys (Loke, 2004).

Geophysical theory

The general theory of resistivity measurements is that current is transmitted through the ground and the change in potential, described in terms of voltage, is measured (Loke, 2004). There are four electrodes which are active, two that transmit current and two that read voltage. Since different mediums have different ability to transmit current, one can deduce the sediment from its resistivity value (Loke, 2004).

When doing resistivity measurements, there are two ways the current moves. The first is by electronic conduction, which is when the sediment has electrons that can be easily transmitted, which is the case for many metallic elements (Loke 2004.). This is common when conductive minerals are present (Loke 2004.). The second way is by electrolytic conduction, which is when the current flow is caused by the movement of ions in the

groundwater (Loke 2004). This is common for environmental and engineering surveys (Loke 2004).

When the electrodes, having equal electrode distance, are moved horizontally one step further down on the line, keeping the spacing between the electrodes equal, a new resistivity value is found horizontally but with the same depth (Solberg et al., 2010). This is seen in figure 2.1 on page 16. When the spacing between the electrodes increases, a resistivity measurement for a level with greater depth is taken (Solberg et al., 2010). This is demonstrated in figure 2.2 on page 16.

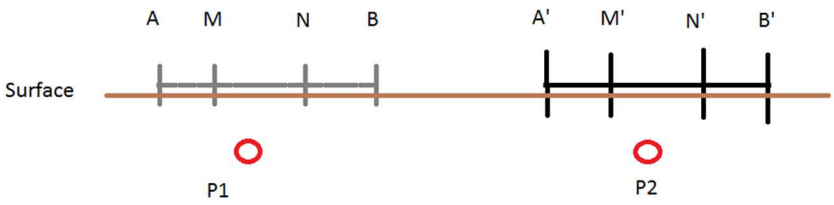

Figure 2.1: Measuring resistivity values horizontally. When current electrodes A and B and potential electrodes M and N are used, we get a resistivity value for P1. When these are moved to A', B', M' and N', thus moving the electrodes in the same direction while keeping the same electrode distance, we get a resistivity value for P2.

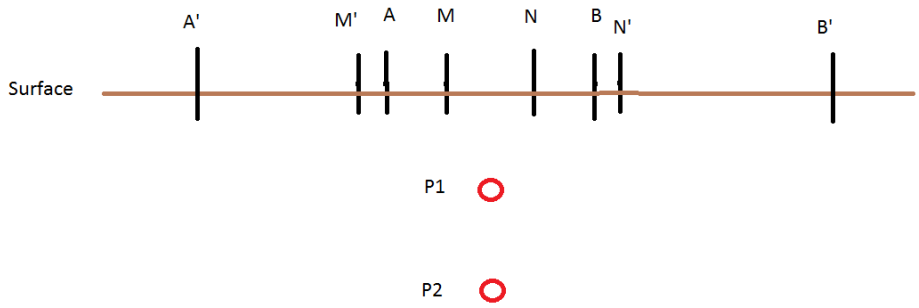

Figure 2.2: Measuring resistivity values vertically. When current electrodes A and B and potential electrodes M and N are used, we get a resistivity value for P1. When these are moved to A', B', M' and N', thus increasing the electrode distance for the electrodes, we get a resistivity value for P2.

The resistivity values are found using Ohm's law and a geometrical factor. Ohm's law is U = R x I, where U = voltage, R = resistance and I = current (Loke, 2004). The resistance, R, is then

multiplied by a geometrical factor, K, and we then get ρ_a, apparent resistivity (Loke, 2004). The ρ_a is found by calculating an average of resistances, as seen in figure 2.3 below.

$$K = 2\pi[\frac{1}{AM} - \frac{1}{MB} - \frac{1}{AN} + \frac{1}{NB}]^{-1} \qquad [\text{m}]$$

$$\rho_a = RK \qquad [\ \Omega\text{m}]$$

$$R = \frac{\delta V}{I} \qquad [\ \Omega] \quad \delta V \text{ is difference in voltage(V), I is electric charge(A)}$$

Figure 2.3: Calculation of resistivity values. Translated from Solberg et al. (2010, p. 24).

From all the resistivity values combined we get a pseudo section, which reflects the qualitative subsurface resistivity (Solberg et al., 2010). The specific resistivity, ρ, is found by using a data program to invert the pseudo section. This will be further explained in the next section.

Data processing

In order to find the true resistivity (ρ), from the apparent resistivity (ρ_a), an inversion must be made. This can be done with the program res2dinv (Loke, 2004). The profile is divided into blocks, which are given a specific resistivity value, and the data program is trying to match the pseudo section to a theoretical model (Loke, 2004). This match between the theoretical model and the measured values is given by a root-mean-square value (RMS) (Loke 2004). The data program tries to improve the RMS value by inverting the data several times, but after 6-7 inversions, the RMS cannot be enhanced (Solberg et al., 2010). The lower the RMS value is, the better is the match between the theoretical model and the measured values (Solberg et al., 2010).

The top layer have blocks with thickness at 0.5 of the electrode distance as a default value, and the following layers increases with 10 % (Solberg et al., 2010). As such, the top layers have the densest resolution, and the smaller the electrode distance, the better the resolution.

There are a number of different configurations that can be made when inverting. The most important are type of inversion, horizontal/vertical filter and topography. There are mainly two inversion types, least-square method and robust method (Loke, 2004). The most used method is least-square, since this is the method that gives the most plausible inversion of the two (Solberg et al., 2010). The robust method gives sharper boundaries which are not always fully geological plausible, and is used mostly for enhancing the understanding of the least-square inversion (Solberg et al., 2010). The horizontal/vertical filter gives an inversion more suited to respectively horizontal or vertical layering (Loke, 2004). The topography affects the way the current flow, so topography information must be added when it may affect the current flow (Loke 2004). The program then solves the inversion by either the finite difference method or the finite element method (Loke, 2004), thus solving each equation stepwise (Anderson and Woessner 2002).

Electrode configurations

There are several types of electrode configurations, and the choice of electrode configuration may give different resistivity results (Loke, 2004). The four most common configurations are schlumberger, wenner, dipole-dipole and gradient (Solberg et al., 2010). Each of them has its strengths and weaknesses in factors such as time consumption, sensibility to noise, vertical resolution and depth penetration (Solberg et al., 2010). Both gradient and wenner are configurations that are well suited for horizontal layering, gradient gives the best resolution, and wenner tolerates noise the best (Solberg et al., 2010).

The electrode spacing is another important factor of the resistivity measurement. The depth and resolution of the resistivity measurement is decided by the electrode spacing. As will be explained in the next section, the depth and resolution greatly affect the interpretation of the resistivity measurement. Typical minimum electrode spacing is 1 m, 2 m and 5 m (Solberg et al., 2010). The depth of the wenner electrode configuration is about 0,176 times the total length of the resistivity measurement (Loke, 2004). Table 2.1 gives examples of the total length and depth of surveys with the use of four cables with all electrodes connected:

Table 2.1: Total length and depth of surveys when using all four cables.

Electrode spacing	Total length	Approximate depth of survey
1 m	80 m	14 m
2 m	160 m	28 m
5 m	400 m	70 m

Interpretation of resistivity values

As a rule, different sediments have different resistivity values (Loke, 2004). However, there are many factors influencing the resistivity values, so different sediments have resistivity values within a large range, and many types of sediment do overlap each other. The most important factor that affects the sediments' ability to conduct electricity is porosity (Loke, 2004). This is the primary factor when one interprets the resistivity value. Then, saturation and dissolved ions affect this primary factor, so there is a large range of resistivity values for the sediment according to its porosity, level of saturation, and moreover whether the water contains a large amount of dissolved ions or not (Loke, 2004).

Furthermore, there are factors that affect the interpretation of the resistivity values from an inversion of a resistivity measurement. Heterogeneous material gives in general a higher resistivity than homogeneous material (Solberg et al., 2010). When a layer of low resistivity lies above a layer of high resistivity, e.g. clay over bedrock, an effect called 3d-effect usually occur (Solberg et al., 2010). The 3d-effect happens because the current prefers the path of least resistance: Instead of passing through the clay layer straight down to the bedrock, the current continues in the clay moving sideways. Then the image will not show the correct depth to bedrock (Solberg et al., 2010). Another factor is the capillary rising of the water in fine sediments, which will give an incorrect depth to ground water level (Solberg et al., 2010). The inversion profile will have a resolution which is the same size as the electrode distance, thus not showing layers which are smaller than this.

If there is too high resistivity at the surface, the resistivity values may be affected by this, thus showing incorrect resistivity values (Solberg et al., 2010). To lower the resistivity at the surface, the electrodes may be saturated with electrolyte fluid (water with salt), or one can connect two electrodes at the same electrode point (Solberg et al., 2010). The

measurements may also be affected by the amount of current used, e.g. 5 mA instead of 200 mA.

Table 2.2: Different resistivity values. From Palacky (1987), Reynolds (2011), Solberg et al. (2011) and Jeppson (2012).

Sediment	Sub-sediment	Resistivity value, Ωm
Water	Salt	0,5-1
	Fresh	5-100
Landfill	Saturated	15-30
	Unsaturated	30-100
Clay	Marine Clay	1-10
	Quick Clay	10-80
	Dry clay crust	80-200
Till	Clay-rich	20-200
	Clay-poor	300-3000
Sand	Saturated	100-500
	Dry	< 800
Gravel	Saturated	100-500
	Dry	< 1400
Bedrock	Weathered	100-4000
	Unweathered	< 2000
Rocks	Massive sulphides	0,01-1
	Graphite	0,1-10
	Magmatic and metamorfic rocks	100-100 000
	Sedimentary rocks	7-100 000
	Eroded rocks	5-50 000

The different resistivity values for different sediments are seen in table 2.2. As mentioned earlier, the primary factor of the resistivity value, namely porosity of the sediments, makes it possible to distinguish the different sediments. The second factor of the resistivity value, namely saturation, is the cause of the large range of the resistivity value of each sediment. Then other factors such as ground water level, level of ions in the water, and other factors must be reflected upon when interpreting the resistivity values. The interpretation of the resistivity values will be based on the table 2.2 above. Due to the many factors influencing the resistivity value of the sediment, the geological attributes of each location must be included when interpreting the resistivity measurements. In addition to this table, there are

some types of sediment in Revdalen that need to be explained further in the following chapter:

Specific resistivity properties of Revdalen deposits

Glaciofluvial delta deposit.

A large part of the northern part of our study area is a glaciofluvial delta deposits (Klempe, 1988). The glaciofluvial delta deposit is very dry at the surface, and as much as 5-15 m below the surface, depending on the ground water level. As explained earlier, this will give it a higher resistivity value than expected, from what the table value of sand in table 2.2 on page 20 shows (Wightman et al., 2003). The resistivity value for sand in the glaciofluvial delta deposit may be further increased if there are small or large pebbles or boulders in the deposit, which are to be found in the top sets of the delta deposits.

Earlier research shows that the upper layer of the glaciofluvial delta deposit in Revdalen, at 0-7 m below the surface, consists of such pebbles and boulders (Klempe, 2001; Børresen et al. 1990; Jansen, 1983). Layers in the middle consist of mostly sand and silt, and the lower layers consist of sand, silt and gravel. The upper layer of the glaciofluvial delta deposit is also observed as dry, something which the vegetation indicates (Klempe, 2001; Børresen et al. 1990; Jansen, 1983).

End-moraine material.

At some parts of the area, there is moraine material above the bedrock (Klempe, 1988). The areas where the end-moraine material is found are below the marine limit of this area. When till material from an end-moraine is accumulated in the sea, there will be both sand and clay found in the till, due to push processes, in addition to the general presence in tills of gravel (Klempe, 1988). If there are enough clay particles, it may give a lower resistivity value than for till without clay particles. As seen in table 2.2, clay-rich till have a resistivity value of 20-200 Ωm, and clay-poor till 300-3000 Ωm.

Weaknesses

It must be emphasized that the resistivity method may give results that contain a great deal of uncertainty. This is mainly due to the interpretation of the resistivity values. As a result, the resistivity measurements should be accompanied by other geological or geophysical results, in order to enhance the certainty of the measurements.

Factors that may give incorrect results are many. Since there is no single resistivity value for a sediment, the interpretation of the resistivity results may be incorrect. The range of resistivity values varies for the sediments, with the most important factors being different levels of saturation, weathering and dissolved ions in the water. The resistivity results have resolutions that are linked to electrode spacing, so if there are layers that are smaller than the electrode spacing, the resolution of the result will not show such layers (Solberg et al., 2010). In addition, since heterogeneous material gives on a general basis a higher resistivity value than homogenous material, the resistivity result may be incorrectly interpreted if the resolution is in a way that it do not show such layers (Solberg et al., 2010). The 3D-effect that has been discussed earlier is also an important source of error. The resistivity inversion gives smooth transitions of layers with high and low resistivity, so in areas with these conditions, the result may be incorrect (Solberg et al., 2010). Wrong use of the resistivity equipment in the field will give incorrect results. Incorrect placing of the resistivity values at the map, may also give incorrect values.

It is therefore important to use the results from this geophysical instrument with caution. All these sources of error must be reflected upon when using the results. As such, the results of the resistivity measurements should be interpreted by geological competent people, and the results should be used with caution and be followed by other geological surveys.

Field work

There were different limiting factors for our study, which affected the placement of the resistivity profiles. A map of the profiles is found in figure 2.4 on page 25. Profiles 6-20 were situated at farmland, so the profiles had to be made when the soil was in a condition that was not affected by our intervention. In 2014, this was only in a period of two weeks in March and April.

Profiles 26, 27, 30, 32, 33, 34, 35, 36 37, 39 and 42 were surrounded by roads with heavy-duty traffic, which could potentially damage our equipment. We therefore tried to avoid crossing of roads with our profiles, which affected the orientation and length of these. Profile 32 crossed a road with high resistivity, so there had to be some electrode exclusions in this profile.

Profile 29 had limitations in geographical spacing, with hills on the one side and farmland on the other, so we had to exclude some electrodes (see table 2.4).

Equipment used was an ABEM Terrameter LS from Lund Instruments AB, 61 electrodes and cable connectors, two cable joints and two batteries of 15 Ah and 17 Ah. The configuration of the terrameter can be seen in table 4. The different electrode distances for each resistivity measurement can be seen in table 5. It must be noted that due to equipment limitations, the current output was set between 10 mA and 200 mA.

After attempting the two electrode configurations that were suited for our study, gradient and wenner, it seemed that the background noise in the area affected the gradient configuration too much. Therefore, the wenner electrode configuration was chosen for all the measurements.

Table 2.3: Resistivity measurements configuration.

Electrode configuration	Wenner
Electrode distance	See table 2.4
Minimum current	10 mA
Maximum current	200 mA
Max power	250W
Max output voltage	600 V
Electrode test	Focus one
Bad electrode	20 KOhm
Failed electrode	300 KOhm.
Electrode test current	20 mA

Table 2.4: The different resistivity profiles length, electrode spacing, and other information.

Profile	Length	Direction	Number of electrodes	Spacing	Electrode exclusions	Data points	Soil type	Date
6	120	N-S	51	2	5 first, 5 last	232	farmland	27.03.2014
7	160	N-S	61	2		345	farmland	27.03.2014
8	192	N-S	79	2		482	farmland	27.03.2014
9	200	SE-NW	81	2		506	farmland	27.03.2014
10	136	NW-SE	55	2	3 first, 3 last	274	farmland	28.03.2014
11	160	W-E	61	2		345	farmland	28.03.2014
12	148	W-E	58	2	1 first, 2 last	309	farmland	28.03.2014
13	400	W-E	61	5		343	farmland	31.03.2014
14	400	W-E	61	5		339	farmland	31.03.2014
15	330	W-E	54	5	3 first, 4 last	263	farmland	01.04.2014
16	380	W-E	59	5	1 first, 1 last	321	farmland	02.04.2014
17	160	W-E	61	2		345	farmland	02.04.2014
18	400	W-E	61	5		345	farmland	02.04.2014
19	160	W-E	61	2		345	farmland	03.04.2014
20	400	NE-SW	61	5		345	farmland	03.04.2014
26	400	NW-SE	61	5		345	forest	19.05.2014
27	400	W-E	61	5		345	forest	20.05.2014
28	80	NW-SE	61	1		345	forest	20.05.2014
29	120	NW-SE	51	2	5 first, 5 last	232	forest	20.05.2014
30	400	W-E	61	5		343	forest	21.05.2014
32	400	W-E	115	5		262	forest	21.05.2014
33	160	SW-NE	61	2		345	forest	22.05.2014
34	156	W-E	60	2	1 first	333	forest	22.05.2014
35	160	W-E	61	2		345	forest	26.05.2014
36	160	SW-NE	61	2		345	forest	26.05.2014
37	400	W-E	61	5		345	forest	27.05.2014
39	400	SW-NE	61	5		345	forest	27.05.2014
40	160	NW-SE	61	2		345	forest	28.05.2014
41	160	NW-SE	61	2		345	forest	28.05.2014
42	96	S-N	45	2	8 first, 8 last	179	forest	10.06.2014

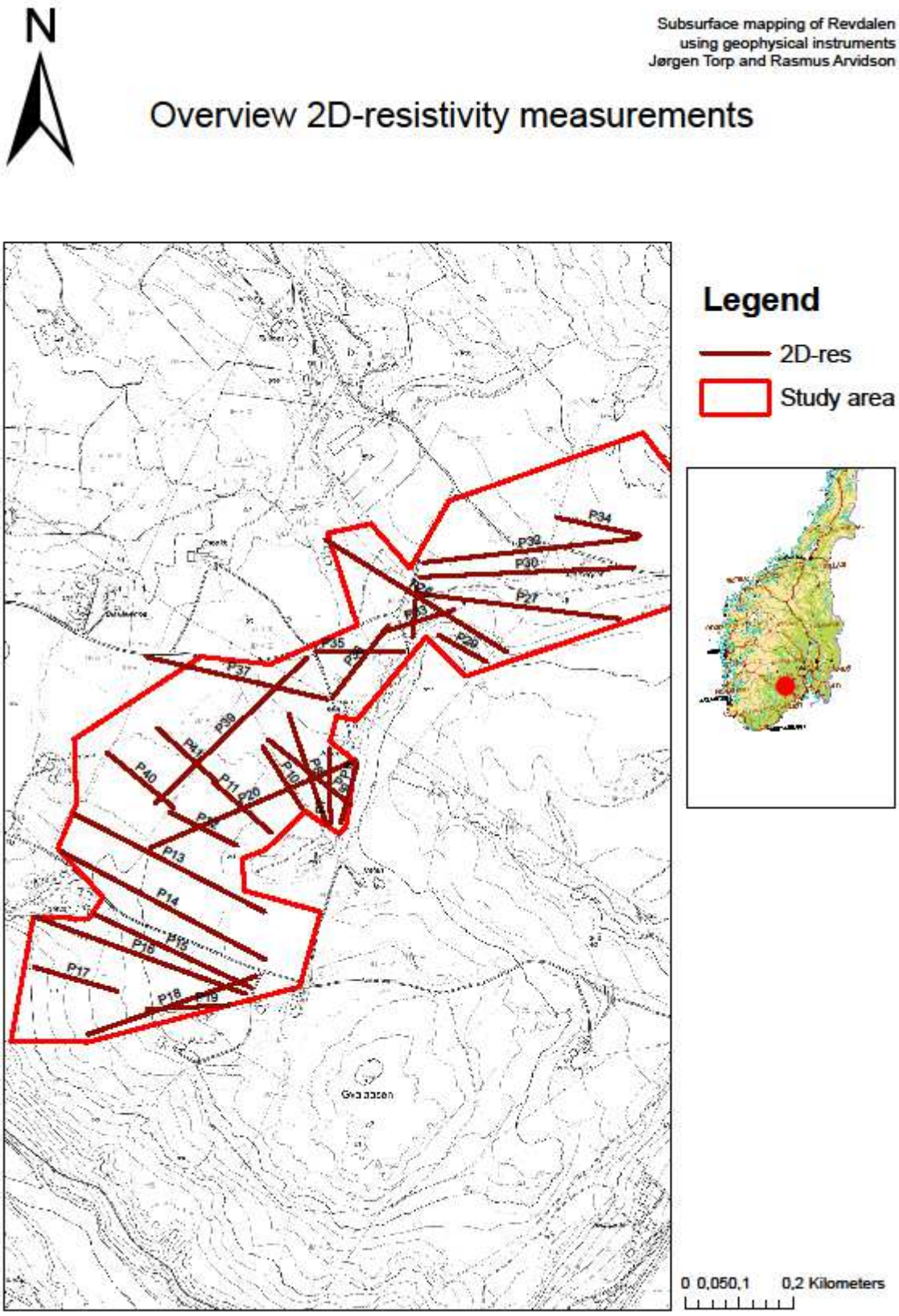

Figure 2.4: Map of the resistivity profiles.

Ground penetrating radar (GPR)

Choice of geophysical method

Our project has a main focus on the use of resistivity measurements to get an overview of the subsurface conditions in Revdalen. The use of GPR is to be considered only as a supplementation to the resistivity measurements. Therefore, the theory section for the GPR will be much less detailed than for the resistivity measurements.

In order to enhance the certainty of the interpretations of the resistivity measurements, GPR measurements were done at several locations. Since there was a limitation in time available for this study, all resistivity profiles could not be complemented by a GPR profile. Therefore, a number of locations were selected according to one of this study's aims: experimenting with resistivity and GPR measurements. Most of the GPR profiles were made with 50 MHz antennas in order to reach the bedrock if possible. As an experiment, two of the GPR profiles were done with 100 MHz antennas.

Theory

The GPR is today used in a great variety of areas for subsurface mapping purposes: survey of quaternary sediments, distance to bedrock, ground water surveys, environmental surveys and many others (Koziel et al., 1995). All these purposes enjoy the efficiency of the GPR.

The GPR emits electro-magnetic pulses via one antenna (Koziel et al., 1995). The signals are high frequent, short pulses at 10 MHz – 1000 MHz (Ibid). The subsurface material then reflects these signals, which are read by the receiver, the second antenna. The receiver transmits the signals to the computer, which displays the signals as an image of the subsurface (Koziel et al., 1995). Material with different dielectric attributes will create a reflection of the signals at the layer boundary, thus making it possible to distinguish them (Koziel et al., 1995). It is the dielectrical constant and the electrical conductivity that decides the signals reflection, where the former is the main factor for reflection (Koziel et al., 1995). The dielectrical constant is a function of water content, and the electrical conductivity is a function of ion content (Koziel et al., 1995).

Interpretation and weaknesses

A higher frequency gives a higher resolution, but lower penetration depth, and vice versa (Koziel et al., 1995). If there is material with high conductivity at the surface, e.g. clay and saltwater, the signals will be reduced (Koziel et al., 1995). The method will therefore be best suited for areas where there is coarse material, both dry and wet, at the higher level of the subsurface (Koziel et al., 1995).

Depth to a layer is calculated with the formula seen in figure 2.5 below (Annan, 2003):

$$d = \frac{(t * v)}{2}$$

Figure 2.5: Calculation of depth when using GPR.

Where d is distance, t is time and v is velocity. Values for velocity in different sediments are found in table 2.5 below.

Table 2.5: Values for velocity in different sediments when using GPR (Annan, 2003).

Material	V (m/ns)
Air	0,3
Distilled water	0,033
Dry sand	0,15
Saturated sand	0,06
Clays	0,06
Granite	0,13
Silts	0,07

The interpretation of the GPR results should be done by or together with experts with long experience in the field of GPR results, since the results may be somewhat ambiguous. The method contains several of such sources of error, and thus a certain degree of uncertainty. Therefore, the method should be complemented by other surveys in order to give a correct interpretation of the subsurface mapping.

Field days

The GPR profiles were done according to our planned schedule, with no encountered problems. A map of the profiles is seen in figure 2.5 on page 29. The equipment used was a Pulse Ekko Pro 1000 from Sensors and Software, Canada. The antennas used were 50 MHz and 100 MHz. The antennas used and length of the profile can be seen in table 2.6. The vertical speed of the profiles is seen in table 2.7. Five of GPR profiles were measured 10th and 11th of June 2014. One GPR profile was measured in April as a field work in a course taken at TUC.

Table 2.6: The GPR profiles' length, antennas used, and date.

Profile	Corresponding resistivity profile	Length	mHz	Date
GPR 07	Profile 29	55	100	11.04.2014
GPR 02	Profile 26	120	50	10.06.2014
GPR 05	Profile 27	100	50	11.06.2014
GPR 03	Profile 32	100	50	11.06.2014
GPR 04	Profile 32	100	50	11.06.2014
GPR 06	Profile 41	100	100	11.06.2014

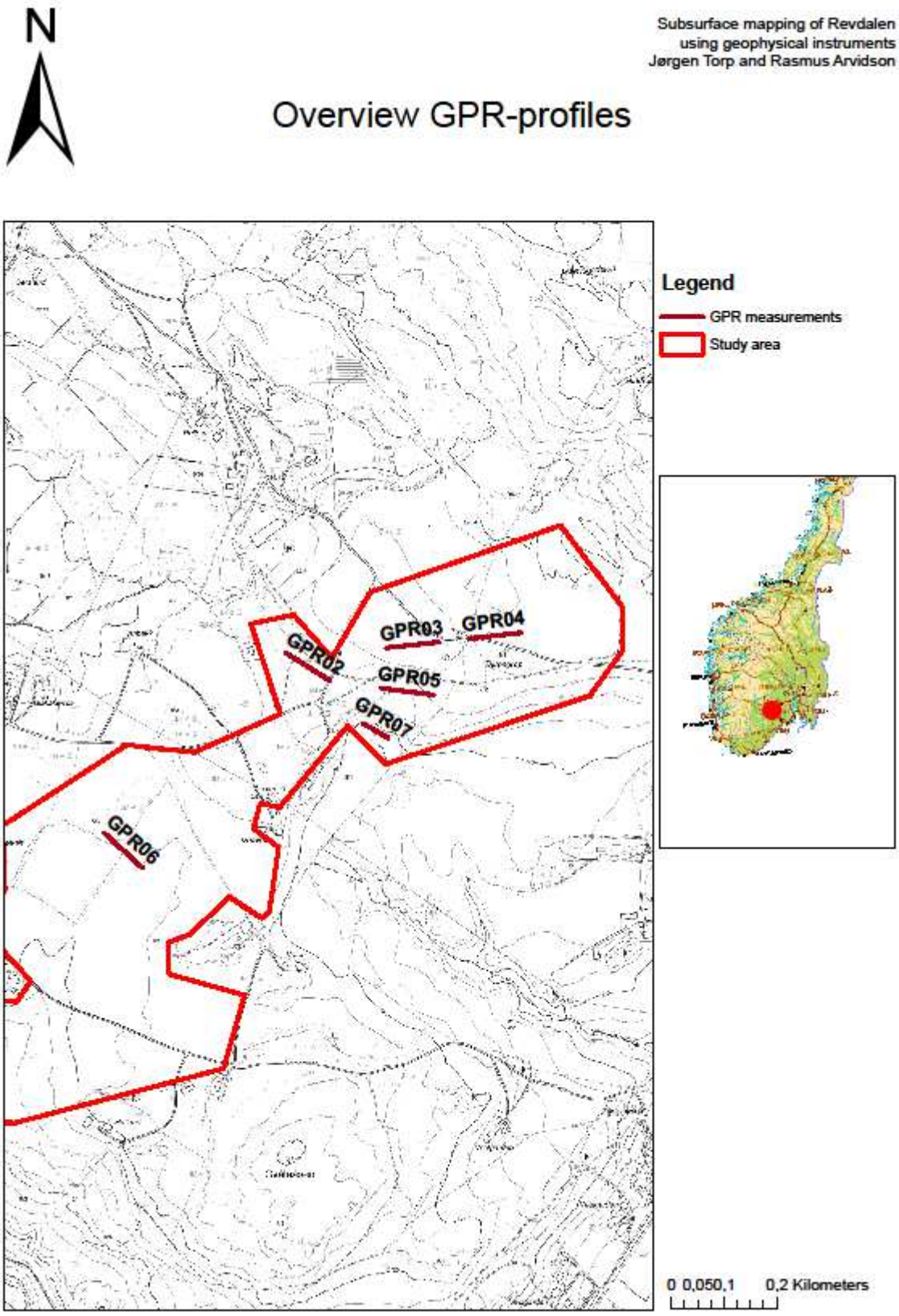

Figure 2.5: Map of the GPR profiles.

Table 2.7: The material and velocity of each GPR profile.

GPR profile	Corresponding resistivity profile	Material	V (m/ns)
GPR 02	Profile 26	Dry sand	0,15
GPR 05	Profile 27	Saturated sand	0,06
GPR 07	Profile 29	Saturated sand	0,06
GPR 03	Profile 32	Dry sand	0,15
GPR 04	Profile 32	Dry sand	0,15
GPR 06	Profile 41	Clay	0,06

GPS

The ABEM terrameter LS has an internal GPS. After the measurements, we did not manage to extract any information from the internal GPS. Therefore, we recorded the coordinates with a hand-hold Garmin Oregon 300 GPS that TUC possesses. At this time, it was no longer possible to walk on the farmland. Therefore, we were unable to record the coordinates for those of the resistivity profiles that had been located at farmland, see table 2.4. However, since we used landmarks when placing the resistivity profiles, all the profiles have been correctly placed on the map in GIS.

Software methods

Inversion and interpretation of the resistivity measurements.

The inversions of the data from the resistivity measurements were made in the program res2Dinv. The inversion type was least-square method, since this gives the most plausible geological inversion. Topography was included in all the profiles. All inversions used a horizontal/vertical filter ratio of 0.5. This made the inversion program emphasize the horizontal changes, which was beneficial for the interpretations of the profiles.

In this study we have done a qualitative and subjective interpretation of the inversions. With the use of theory, data from earlier research mentioned in the next sections, and deducing from known information about the area, the inversions have been interpreted in a manner which is geologically plausible.

Database in Geographic Information Systems (GIS)

To create a database from the resistivity measurements is time consuming. However, a database gives certain advantages that are profitable, so this study has given the database work priority. Firstly, with the database one can merge data from many different studies. Secondly, there are many ways to use the database, and since this area is a study area for Telemark University College (TUC), the database may be usable for future studies. For instance, there has been studies concerning waste water flux in this area, and with a database containing information about the subsurface conditions, there may be some interesting correlations which can be studied further.

GIS is a program suited for 2D and 2,5D representations. So to create a 3D representation of the subsurface may be challenging. Klempe (2004) tried to solve this challenge by creating a database, and then performed queries. The database contained information about grain size and position in space. We will also create a database, but since our study mainly focus on depth to bedrock, we will represent this by adding a layer which represents the subsurface depth to bedrock. By doing this, we may calculate the unknown depth by interpolation, thus getting a continuous representation. The interpolation method used will be inversed distance weighing (IDW). (Burrough and McDonnell 1998) This method was chosen since the terrain is very undulating. The work process for the database is summarized in table 2.8.

From the qualitative interpretations of resistivity measurements, GPR measurements and drilling data, a database has been made. From the interpreted resistivity and GPR data, we have created a database of depth to bedrock for use in GIS. We included drillings and GPR measurements from earlier studies by Jansen (1983), Klempe (1992), Klempe (Unpublished material) and Børresen et al. (1990). We used point digitalizing to create the points that would be connected to the database. Since the data from resistivity and GPR are continuous, points on the survey line have been made in GIS in order to make the data discrete. A digital terrain model with 1 m intervals (DTM) of Revdalen was used to get z-values of the surface for the points. Then, an interpolation between all the data points has been made. Now a continuous bedrock surface has been made out of the data available. The work process in GIS is summarized in table 2.9.

Table 2.8: Work process for the database.

Working order database:
1) Invert collected data.
2) Interpret the inverted data.
3) Create subsurface database from interpreted data.

Table 2.9: Work process in GIS.

Working order GIS:
1) Get background map.
2) Create survey lines.
3) Create points from survey lines.
4) Get x and y data to points.
5) Get surface m.a.s.l. data to points from altitude data.
6) Match subsurface database and point features at survey lines in GIS.
7) Interpolate the subsurface database.

Results and discussion

Results of resistivity measurements

Outline

In the following each profile measured in the field has been inverted and studied with regards to understanding the image, and given estimates of approximately depth to bedrock and subsurface sedimentology.

Each profile is described with a depth indication with regards to sediment type, and depth to bedrock along a longitudinal axis, with starting point at the starting point of the measurement, which means from left to right on the shown images. In the inversions, the depth to bedrock is indicated with a black line.

At the end of each profile description a short conclusion, with the main points observed in the modelled profile and connection to the surrounding areas quaternary geology and additional info available. It will also give an evaluation of the strength of the profile, and the modelled resistivity data.

Area description

For profiles 6 to 22, the area where measurements were taken mainly consists of relatively plane farmland. Skewness in profile horizontal direction was minimal due to good oversight of the study area. For profiles 26-42, many of the profiles were placed at dry glaciofluvial material. When this material has affected the results in any matter, there has been given a comment on this in the discussion of the relevant profile.

The inversion of the profiles has been made using the same resistivity value scale, see figure 3.1. The choice of using the same scale was given priority so that the representation of the results is consequent and perhaps more intuitive to understand. However, the resistivity values at the profiles where the dry glaciofluvial material is present were often extremely high, due to reasons discussed in the method section. For these profiles, the inversion with a different and higher resistivity value scale is to be found in the appendix, and the resistivity value from these inversions is often presented with a range of values, since the exact value is

hard to estimate. For many of the profiles 6-42, the 3d-effect has been present. This effect has been thoroughly commented on in the discussion of the relevant profile.

Table 3.1: Resistivity value scale used for inversions in results and discussion.

Resistivity value, Ωm	Colour	Colour	Typical sediment
<50	Very very dark blue		Wet clay
50	Very dark blue		Quick Clay
100	dark blue		Clay/wet sand
200	Blue		Dry clay/wet sand
300	Light blue		Wet sand/wet gravel
400	Very light blue		Wet sand/wet gravel
500	Tourquis		Sand/wet gravel
700	Neon green		Sand/gravel
1000	dark green		Gravel
1500	light dark green		Gravel
2000	yellow		Clay-rich till/gravel
3000	brown		Clay-rich till/gravel
4000	orange		Clay-poor till/gravel
5000	Red		Fractured bedrock
7500	Dark red		Somewhat fractured bedrock
10000	Purple		Bedrock
>10000	Dark purple		Bedrock

The numbers of the profiles are given according to the project at the Terrameter ABEM LS. In order to avoid any mishandling of the projects, we consequently have used the number of the project in the Terrameter ABEM LS, instead of giving them number starting from 1.

For some profiles different settings were used when measuring data, but in the handling of data the same settings were used in the Res2dinv-program. The vertical-to-horizontal flatness filter ratio was set to 0.5. Where large resistivity variations are observed near the surface a model refinement has been applied, using cell sizes with width of half the unit spacing in the model.

Profile 6

Profile 6 is situated along a hill as seen on figure 2.4 on page 25. The profile is 120 m long, with a minimum electrode spacing of 2 m, due to the terrain and a nearby domestic garden the length of the array was shortened by excluding electrodes in each end of the array. The general direction, from start to stop, of the profile is from North to South. The inversion of the profile is seen in figure 3.1 on page 36.

The RMS is 2.3 %. At the surface, which is a field of farmland, farmed with seasonal crops, the soil was open, at the time of measurements, due to agricultural purposes, and shows a clay surface with features of sand and small rocks. There was no obvious change in soil type along the length of the array.

At the starting point of the profile which is seen in *table 1*, and forward along the longitudinal axis, as far as 40 m, a clear image of a sediment which is shown in a depth from 0-5 m. The model shows resistivity values from 0-400 Ωm. This indicates clay with inserts of sand, silt and gravel. In the center of the area from 0-40 m where the resistivity values are from 0-200 Ωm, this indicates saturated clay.

At 20 m the depth to bedrock is approximately 5 m based on modelled resistivity values of 1500-10000 Ωm. At 40 m the depth to bedrock declines to approximately 7 m. And the layer from surface to bedrock has resistivity values from 700-1500 Ωm. This indicates a mix of different soils but mainly unsaturated sand and gravel, this could indicate that the area is part of a moraine build-up, that is situated almost perpendicular to the longitudinal axis of the profile.

In the center of the profile at 60 m, depth to bedrock has inclined to approximately 6 m and for the rest of the profile it declines to 6.5 m before inclining up to 5 m in the last 20 m of the profile longitudinal axis.

The interlaying layers from surface to bedrock from 60-120 m shows a mix of different soils due to resistivity values modeled from 700-7500 Ωm. This indicates a diamict of unsaturated soils, clay rich-till, and is most likely a part of a moraine.

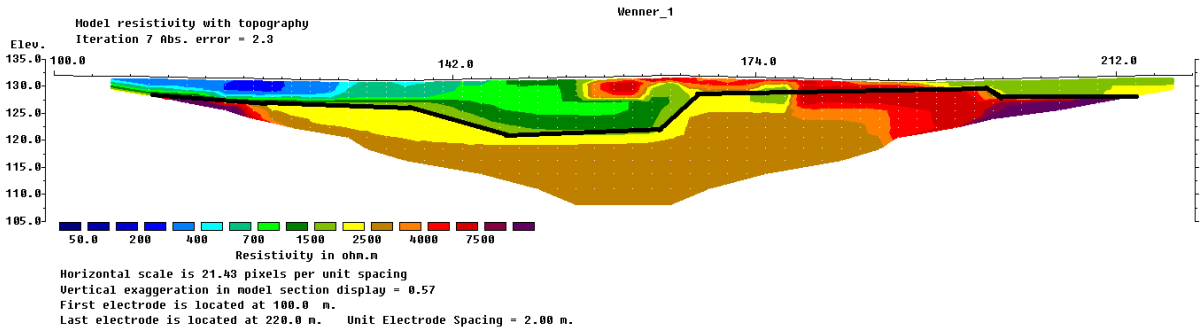

Figure 3.1: Inversion of profile 6.

Profile 6 summary

This profile shows a distinct layering in the sedimentology, at the first half of the profile. The validity of the modelled data is considered good, as it corresponds well with what was observed in the field.

The depth to bedrock visualization however is considered uncertain, as the overlying layers of sediment create a 3D effect in the modelled resistivity data.

Profile 7

Profile 7 is situated approximately 40 m west of profile 6 as shown on figure 2.4 on page 25. It is 160 m long and the minimum electrode spacing is 2 m. The general direction, from start to stop, of the profile is from North to South. The inversion of the profile is seen in figure 3.2 on page 37.

RMS IS 1.9 %. The surface shows the same type of soil conditions as profile 6, at the time of measurement, there was however a wet patch visible from approximately 10-40 m in the profile longitudinal direction.

At the starting point of the profile and forward to approximately 70 m along the longitudinal axis there is a distinct layering visible. It has a depth of 4-5 m along the stretch and the resistivity values are 100-250 Ωm. This indicates a saturated material, most likely clay and sand.

Underlying this layer there is layer of material with resistivity values from 250-2500 Ωm. This indicates a layer with mixed material, possibly unsaturated sand or gravel, and could be an indication of an underlying clay-rich moraine, placed on top of the bedrock.

The bedrock is possibly visible at 20 m along the longitudinal axis and is situated at 8.5 m depth. The profile does not show a clear image of the bedrock before at approximately 90 m along the longitudinal axis.

From 70-110 m along the longitudinal axis, there is a layer with resistivity values from 0-250 Ωm, the layer is deep and goes down to the bottom of the profile image, which is over 25 deep. This indicates that the layer has either been build up in between the fractured bedrock or between two moraines.

At 90 m along the longitudinal axis, there is indication of bedrock visible on the image; it is situated at approximately 25 depth. Throughout the remainder of the profile the bedrock is visible and inclines up to 13 m depth at 110 m, and inclines further up to 6 m depth at 130 m before stabilizing at that depth throughout the profile.

There is however a small block visible from 112-120 m in the longitudinal axis, with high resistivity values from 1500-5000 Ωm, and situated at a depth of 0-5 m. These resistivity values would normally correspond with the indications of bedrock, and it is possible that it is in fact bedrock visible very near and almost breaching the surface. Observations in the field did however not show the bedrock visible at the surface, but it could none the less still be possible that the bedrock is situated right under the surface, and not at approximately 9 m depth as earlier implied. Another possible explanation is that the mentioned block from 112-120 m is part of a moraine overlapping the bedrock. The layer overlying the bedrock from 90-160 m length has resistivity values from 500-2000 Ωm and indicates unsaturated material most likely sand and gravel, as part of a clay-rich moraine overlapping the bedrock.

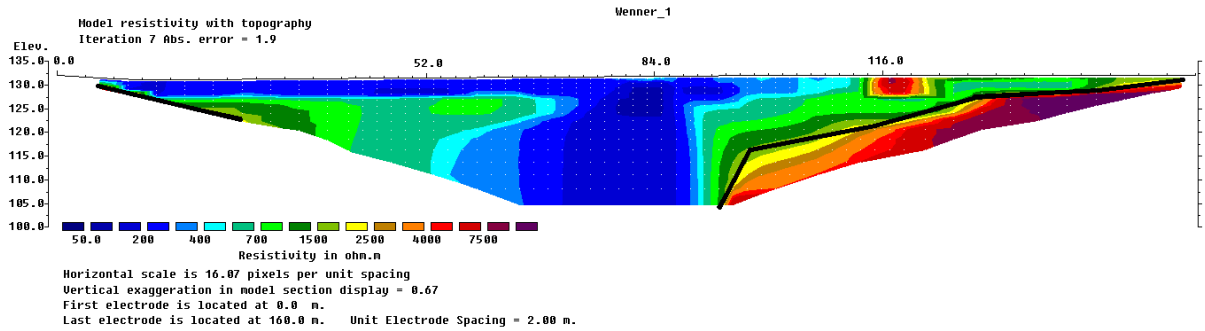

Figure 3.2: Inversion of profile 7.

Profile 7 summary.

As profile 6 did, so does profile 7 also show a distinct layering in the profiled image. There is also a good correspondence between the two profiles with regards to profiled sedimentology. However the very visible crack in the middle of profile 7, with low resistivity values, is not visible on profile 6. This indicates that the hill along profile 6 could work as a barrier for subsurface water movement.

With regards to showing the bedrock, there is a correlation between bedrock imaged in profile 6 and profile 7, but with the bedrock situated a little deeper under the surface in profile 7 than in profile 6.

Profile 8

Profile 8 is situated approximately 50 m west of profile 7 as shown on figure 2.4 on page 25. It is 192 m long, and the minimum electrode spacing is 2 meters. The measurement at profile 8 was taken using the roll-along technique. The general direction, from start to stop, of the profile is from North to South. The inversion of the profile is seen in figure 3.3 on page 39.

At the profile surface, the soil has the same conditions as profile 6 and 7, with the top soil plowed for agricultural purposes.

RMS IS 2.8 %. At the starting point of the profile from 0-45 m along the longitudinal axis there is a layer with high resistivity values, from 400-10000 Ωm, in depths from 0-15 m. This layer appears to be bedrock due to the high resistivity values. However there was no immediate bedrock observed in the field. The layer could however be part of a clay-poor moraine that stretches out in the near lying forested area. The reason for the high resistivity values, could be, that the moraine consists of unsaturated material, with very high resistivity values, as observed on other resistivity profiles in the area, and the 3D effect affects the measurement in that way.

From approximately 50-150 m in the longitudinal axis, and in a depth of 0-8 m there is a layer visible on the profile with resistivity values from 0-400 Ωm. This layer consists of saturated material, most likely clay and sand. This layer corresponds well with the similar layers observed in profile 6 and in particular profile 7.

It appears that this layer is present throughout the entire field, where profiles 6, 7, 8 and 9 were measured.

Underneath the before mentioned layer, at depths from 8-25 m, there is a layer with consistent resistivity values from 700-1500 Ωm. This layer most likely consists of mixed unsaturated material, mainly sand and gravel.

From approximately 110 m in the longitudinal axis at 25 m depth, the bedrock is visible, estimated due to resistivity values 1500-10000 Ωm. The bedrock layer inclines along the remainder of the profile, to the depth 11 m at 132 m along the longitudinal axis, and ending at approximately 4 m depth at the end of the profile.

Near the start of this profile, Klempe (unpublished material) has a drilling which indicates that depth to bedrock is at 23 m. This matches our interpreted depth to bedrock.

This also corresponds well with the bedrock layer observed in profiles 6 and 7.

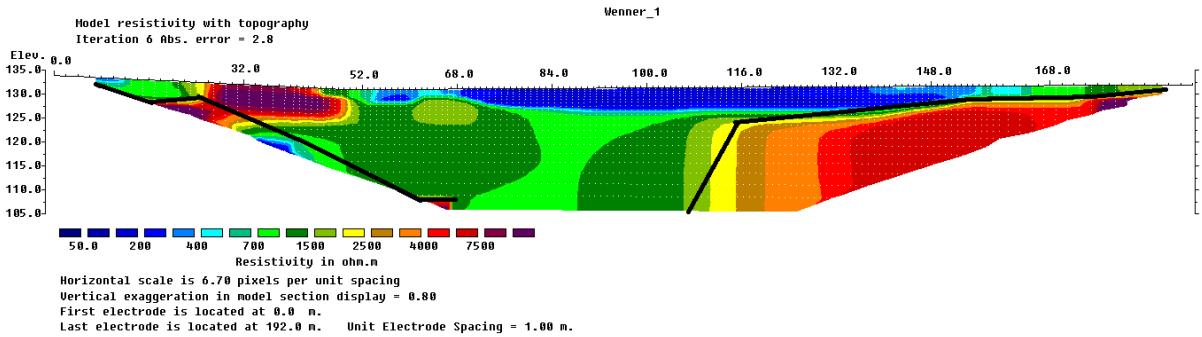

Figure 3.3: Inversion of profile 8.

Profile 8 summary

In connection with profiles 6 and 7, profile 8 shows a distinct layering in the sedimentology. However the large deep middle section, with material showing low resistivity values, observed in profile 7, is not visible in profile 8. This could be due to, that the layer observed in depths 8-25 m at 50-150 m along the longitudinal axis, forms an impermeable layer that restricts water from saturating further down subsurface.

The bedrock layer observed in profile 8 corresponds well with the surrounding profiles.

Profile 9

Profile 9 is situated at the same field as profiles 6, 7 and 8 as shown on figure 2.4 on page 25. It stretches across the mentioned profiles, and gives support to the validity of these profiles. The inversion of the profile is seen in figure 3.4 on page 42.

RMS IS 2.0 %. It is 200 m long, and the minimum electrode spacing is 2 meters. The measurement at profile 9 was taken using the roll-along technique. The general direction, from start to stop, of the profile is from South-East to North-West.

The surface soil at profile 9 has the same conditions as profiles 6, 7 and 8.

At the crossing points, where profile 9 crosses profiles 6, 7 and 8, a detailed analysis and comparison of profile points will be given.

At the starting point of profile 9, and up until 30 m along the longitudinal axis, ranging from depths 8m to 5 m, there is a layer with resistivity values from 250-1000 Ωm. This layer is most likely a mix of unsaturated clay and sand.

From 30 m along the longitudinal axis and for the full stretch of the profile, there is a layer visible on the profile image with resistivity values from 0-250 Ωm. This layer is most likely a layer of saturated material, consisting of clay and sand. Over the length of the layer visible, the depth of the layer varies from 0 to approximately 10 m depth.

Towards the end of the profile, it appears that the layer with saturated sand and clay is situated right on top of an underlying layer of bedrock. But from 45-95 m along the longitudinal axis, ranging from depths 5-16 m, there is a layer with resistivity values from 250-750 Ωm. This layer appears to consist of unsaturated material of sand and gravel.

The bedrock can be seen in profile 9 almost throughout the profile. The depth of the bedrock varies from 5 m in the beginning of the profile and declines down to 15 m at 50 m distance along the longitudinal axis. It inclines up to approximately 5 m depth throughout the next 100 m before becoming invisible towards the end of the profile.

Cross-points

There is 3 points along profile 9, where it crosses other profiles.

Profile 9 and 6

The first cross-point between profile 9 and profile 6 is situated at 10 m length in profile 9 and at 70 m length in profile 6. Due to the fact, that this cross-point is situated at the very start of profile 9, the correspondence between the two profiles and the resistivity values observed, is limited.

At this point there is a good correspondence between the resistivity values imaged. In profile 9 a layer with resistivity values of approximately 700 Ωm is observed, and in the corresponding point on profile 6 resistivity values of 700-1500 Ωm was observed.

The depth to bedrock in profile 9 at the point is at roughly 8 m depth, and in the corresponding point on profile 6 it is situated at about 8-9 m depth. This shows that there is a good correspondence between resistivity values observed at the cross-point between profile 9 and profile 6.

Profile 9 and 7

The cross-point between profile 9 and profile 7 is situated at 48 m length in profile 9 and 75 m length in profile 7. This cross point is situated fairly centered on both profiles, and should show a good correspondence between the profiles.

At this point there is a good correspondence between resistivity values observed in the top-layer and down to about 13 m depth. The resistivity values observed in this layer are 0-400 Ωm in both profiles.

At 75 m length in profile 7 the bedrock is not visible, there is instead a layer visible that goes from the surface to the bottom of the profile, which is at 25 m depth, with resistivity values from 0-400 Ωm. This layer most likely consists of saturated sand and clay. At 48 m in profile 9 the bedrock is visible at 13 m depth. This means that for the bottom part of the cross-point between the two profiles there is no correspondence.

An explanation for this could be that profile 7 is only 160 m long, and there has a strong signal at the top and center of the profile, but low strength in the bottom of the profile. And with a saturated layer placed at the top of the profile with low resistivity values, the imaged bottom part of the profile has become blurred.

Profile 9 and 8

The cross-point between profile 9 and profile 8 is situated at 100 m length in profile 9 and 115 m length in profile 8. This cross-point is also situated approximately at the center of both profiles.

This cross-point shows very good correspondence between the two profiles, and even helps the understanding of the resistivity values observed in profile 8. At the cross-point of the profiles a layer of resistivity values 0-400 Ωm is observed in both profiles. The depth of this layer is approximately 8 m observed in both profiles, and situated directly under this layer is the bedrock observed.

In profile 8 there was some confusion as to where the bedrock would be situated towards the end of the profile. Comparing profiles 8 and 9 has given some evidence to the fact that the bedrock is in fact situated at the point earlier described.

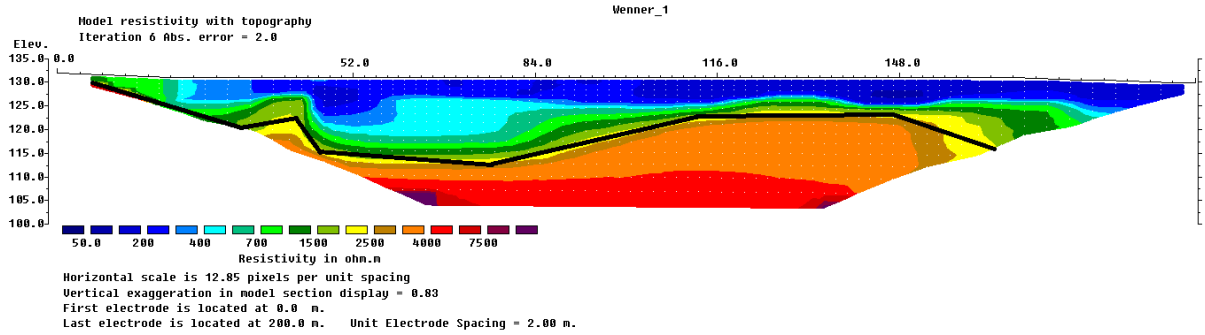

Figure 3.4: Inversion of profile 9.

Profile 9 summary

In connection with profiles 6, 7, and 8, profile 9 shows a very distinct layering in the sedimentology. The sedimentology pattern is very similar to profile 8. As profile 9 was done as a cross-section of profiles 6, 7 and 8 this profile offers a good oversight and validation of the layering in these profiles.

The bedrock layer observed in profile 9 corresponds well with the surrounding profiles. As the profile was done using the roll-along technique the profile is 200 m long with minimum electrode spacing of two meters, this offers a more detailed imaging of the bedrock, which can be observed clearly throughout the profile.

The cross-sections between each individual profile also offer a detailed point based depth to the bedrock at each cross-point, and in general the correspondence between each profile in these cross-points were good.

Profile 10

Profile 10 is situated 40 m west of profile 9 in and adjoining field, as seen on figure 2.4 on page 25. It is 136 m long and the minimum electrode distance is 2 m. This profile has been shortened by excluding profile-end electrodes, due to the terrain in which measurements were taken. The general direction of the electrode is north to south. The inversion of the profile is seen in figure 3.5 on page 44.

RMS IS 0.9 %. The top soil conditions are the same as the conditions in the field were profiles 6-7-8-9 were taken, opened soil, plowed for agricultural purposes.

At the starting point of the profile and forward to approximately 100 m along the longitudinal axis along the profile, starting at a depth of 8 m and inkling up to 5 m depth below the surface, a layer with resistivity values of 0-250 Ωm is visible. This layer is most likely a layer of saturated clay and sand. This layer resembles the one observed in profiles 6, 7, 8 and 9, and it is likely that it is a continuation of the layer visible in these other profiles.

Directly underneath this layer, starting at the depth 16 m and inclining up to 5 m below the surface, at 92 m along the longitudinal axis, a layer of material with higher resistivity values 250-1000 Ωm is visible. This material is most likely unsaturated sand and gravel.

The bedrock is visible from 58 m length, at the depth 16 m below the surface, inclining up to 5 m below the surface at 92 m length. The bedrock is visible throughout the remainder of the profile in depths varying from 3-5 m below the surface.

From the length of 100 m and throughout the profile and ranging down to the obvious layer of bedrock visible, e.g. 0-5 below the surface, a layer of material with resistivity values from 250-1500 Ωm, is observed. This layer is a continuation of the sand gravel layer and is likely a part of a clay-poor moraine placed in the edge of the research area, in the forested area south of the field.

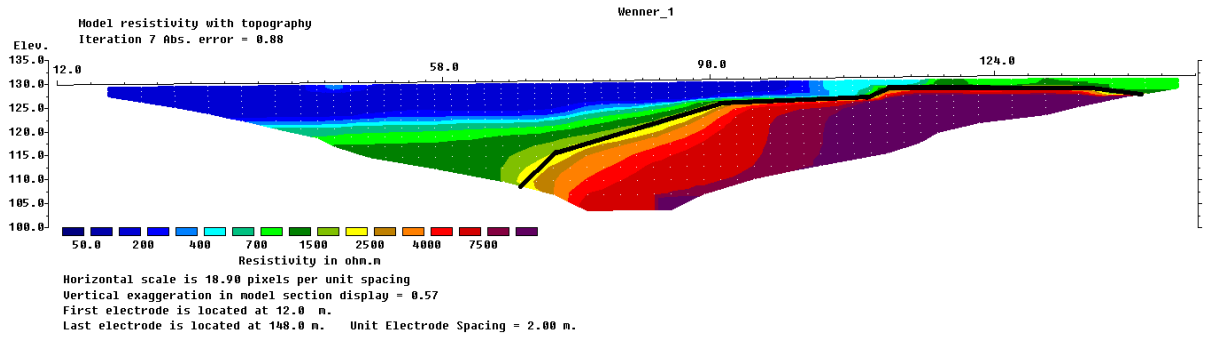

Figure 3.5: Inversion of profile 10.

Profile 10 summary

This profile shows similar patterns of resistivity values, as the ones observed in the adjoining field. The same layers of material can be observed, and the bedrock pattern is similar to the one observed in the previously described profiles.

It appears that the profiles validity is good, as the resistivity results observed correspond well with near lying profiles, and the conditions observed in the field. The profile could however have been longer, using a roll-along technique and extending the profile into the forested area north of the research area. This would have given a better image of the subsurface conditions, in particular the bedrock pattern in the starting point of the profile.

Profile 11

Profile 11 is situated approximately 90 m south-west of profile 10 as shown on figure 2.4 on page 25. It is 160 m long, and the minimum electrode spacing is 2 meters. The general direction, from start to stop, of the profile is from north-west to south-east.

RMS IS 1.4 %. Top soil conditions are the same as in profile 10. The inversion of the profile is seen in figure 3.6 on page 45.

At the starting point of the profile and up until 75 m length along the longitudinal axis, at depths 10 m below the surface and inclining up to 2 m depth, a layer with resistivity values from 0-250 Ωm is visible. This layer most likely consists of saturated sand and clay. This layer is likely a continuation of the layer observed in profile 10, with the same characteristics.

With a starting point of approximately 25 m length and in depths varying from 10-20 m up to 5 m depth at point 75 m length, placed underneath the sand-clay layer, a layer of material with resistivity values varying from 250-1000 Ωm is visible. Although the layer has a sharper inclination than the similar one observed in profile 10, this layer is likely a continuation of the layer described in profile 10, with the same characteristics, with regard to resistivity values and is most likely, based on resistivity values a layer of unsaturated sand and gravel. From 75 m length the layer inclines up to the surface until 108 m length, placed on top of an underlying layer of bedrock.

From the length 108 to 132 m and in the depth 0 to 4 m, a layer of material with resistivity values from 250-500 Ωm. This layer separates itself from layers observed in previously described profiles. It may be that this layer consists of saturated sand and gravel, and is a continuation of the previously described sand and gravel layer. But with lower resistivity values, due to the underlying bedrock creating a mini aquifer, and thus saturating the material placed on top of the bedrock.

The bedrock is visible in this profile from 52 m length, at the depth 20 m below the surface. From 52 m length the bedrock inclines sharply up to 5 m depth at 68 m length, and from there on throughout the profile undulating steadily in depths of 3-5 m below the surface. There is an indication on the profile that the bedrock, in the very last part of the profile, breaks the surface. This was however not observed directly in the field. Bedrock was however observed in the near lying forested area south the of the research area.

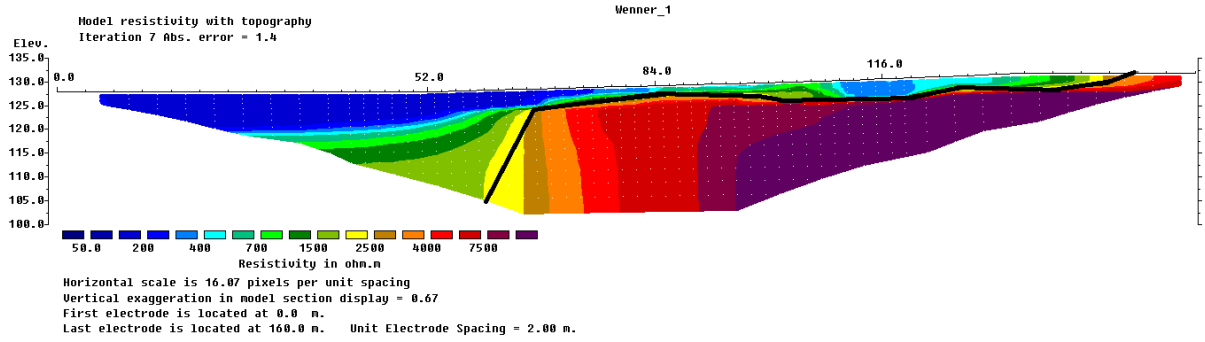

Figure 3.6: Inversion of profile 11.

Profile 11 summary

The correspondence with adjoining profiles in the area is strong as there is a distinct pattern visible between profiles 10 and 11. The same layers, based on resistivity values were observed in both profiles. There was however a stronger inclination on the sand-gravel layer and the bedrock layer which indicates a steeper fall in the bedrock, as was also observed in profiles 7 and 8.

This could be due to the unsaturated sand-gravel layer creating a 3D effect on the vertical imaging of the profile, but could also simply indicate that there is a distinct crack in the bedrock, centered approximately in the research area.

This profile can be assembled with the data obtained in profile 41. Profile 41 gives an imaging of the subsurface conditions north-west of profile 11.

Profile 12

Profile 12 is situated approximately 75 m south-west of profile 11 as shown on figure 2.4 on page 25. It is 148 m long, and the minimum electrode spacing is 2 meters, the profile has been shortened by excluding electrodes at each end. The general direction, from start to stop, of the profile is from north-west to south-east. The inversion of the profile is seen in figure 3.7 on page 47.

RMS IS 2.1 %. Top soil conditions are the same as in profile 10 and 11. The bedrock was however visible in the bottom of south-east corner of the profile.

Throughout the profile, from the starting point and to approximately 132 m length, with depth ranging from 10 m and slowly and gradually inclining up to the surface, a layer with resistivity values of 0-250 Ωm. This layer most likely consists of saturated sand and clay, and is a continuation of the sand-clay layer observed in profiles 10 and 11.

There is apparently a layer of material with resistivity values of 400-1500 Ωm situated directly beneath the sand-clay layer, and on top of the bedrock layer which is visible throughout the profile. This is most likely unsaturated sand and gravel. This also corresponds well with the layer observed in profiles 10 and 11. It is however much thinner than the previously observed layer, and is approximately 1 m deep.

The bedrock is visible almost throughout the entire profile, starting at 28 m along the longitudinal axis, at the depth of 10 m, and gradually inclining up to the surface.

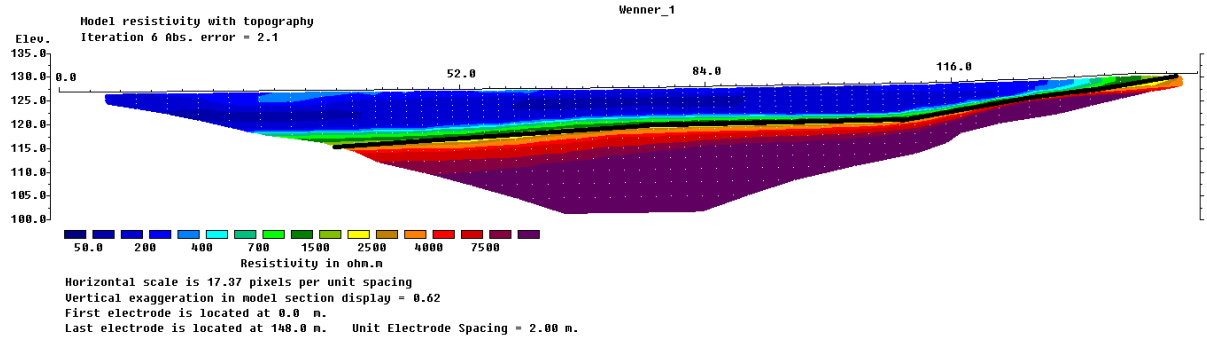

Figure 3.7: Inversion of profile 12.

Profile 12 summary

This profile, with regards to layering, corresponds well with the previously observed profiles in the research area. The bedrock however does not show a sudden drop in depth below the surface as profile 11 showed. This could be due to the proposed crack in the bedrock, observed in profile 11, shifting further north in terrain, and therefore out of the imaging shown in profile 12.

It would probably have been prudent to have the profile extended further north-west, to have a better image of the subsurface conditions in that area.

This profile can be assembled with the data obtained in profile 40. Profile 40 gives an imaging of the subsurface conditions north-west of profile 12.

Profile 13

Profile 13 is situated approximately 85 m south-west of profile 12 as shown on figure 2.4 on page 25. It is 400 m long, and the minimum electrode spacing is 5 meters. The general direction, from start to stop, of the profile is from north-west to south-east. The inversion of the profile is seen in figure 3.8 on page 48.

RMS IS 15.5 %. This indicates that the calculated and the theoretical inversion do not fully match. This may be due to the low resistivity values found in the center of the profile, which

will be discussed. Top soil conditions are the same as in profile 12 and 11. The terrain is undulating, shifting from 128 m.a.s.l at the starting point, descending to 125 m.a.s.l at the center of the profile, before ascending to 132 m.a.s.l at the end of the profile.

At the starting point of the profile, and present almost throughout the profile, a layer with resistivity values of 0-200 Ωm is visible. This layer most likely consists of saturated sand and clay. It ranges in depths from 5 to 15 m below the surface, and it present as far as to 320 m along the longitudinal axis, where it is replaced by a layer of material with resistivity values of 400-1500 Ωm.

This layer is most likely a layer of unsaturated mixed material of sand and gravel. The layering in the profile, is not very distinct, and it is likely that this layer is part of a clay-rich moraine placed at the end of the profile.

The bedrock is seen throughout the entire profile. It is apparently situated directly below the sand-clay layer. There is a drop in the bedrock approximately at the center of the profile, which forms a u-shape on the profiled image. In this center, the resistivity values are lower than in the surrounding bedrock. At the starting point of the profile and up to 110 m length, the depth to bedrock is approximately 10 m. From 120 to 170 the depth to bedrock varies between 5-7 m, before dropping down to 25 m depth at 190 m length. From 190 m length, the depth to bedrock goes up to 5 m depth at 210 m length. From there it drops down to 10 m depth at 250 m length, and is stable at this depth up until 340 m length where it gradually moves up to 4 m depth and is stabile there throughout the profile.

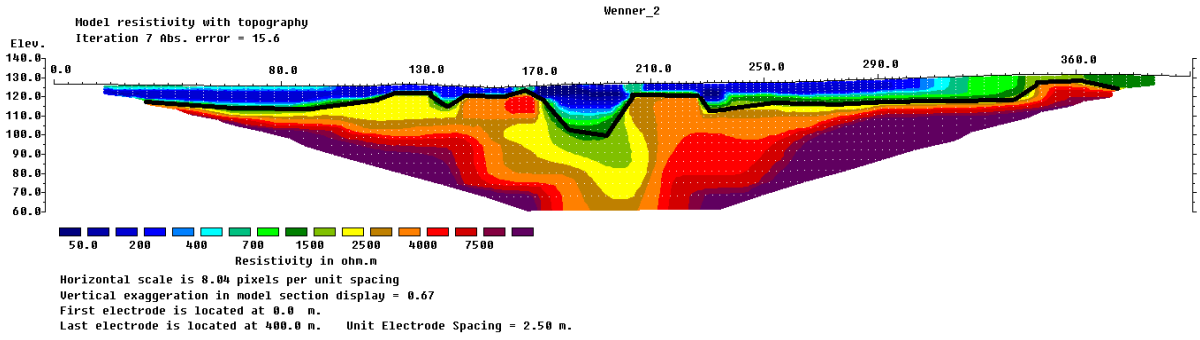

Figure 3.8: Inversion of profile 13.

Profile 13 summary

This profile is a 400 m long profile, with minimum electrode spacing of 5 m. As opposed to a shorter profile, this type of array gives a better imaging of the bedrock over a longer area. It is however more difficult to distinguish the layering in the top part of the profile.

The sand-clay layer observed in this profile, corresponds well with the layer observed in profiles 12 and 11, and should be seen as a continuation of this layer.

But the most interesting part of this profile is the center part with the distinct drop of the bedrock. Indications of this drop were also seen in previously described profiles, in particular profile 11.

Profile 14

Profile 14 is situated approximately 75 m south-west of profile 13 as shown on figure 2.4 on page 25. It is 400 m long, and the minimum electrode spacing is 5 meters. The general direction, from start to stop, of the profile is from north-west to south-east. This profile was taken precisely parallel to profile 13. The inversion of the profile is seen in figure 3.9 on page 50.

RMS IS 5.7 %. Top soil conditions are also the same as in profile 13. The terrain is very undulating, shifting from 128 m.a.s.l. at the starting point, descending to 123 m.a.s.l. at the center of the profile, before ascending to 131 m.a.s.l. at the end of the profile.

At the starting point of the profile and continuing to approximately 288 m along the longitudinal axis, a layer with resistivity values of 0-200 Ωm is observed. This layer consists of saturated sand and clay. The depth of this layer varies from 5-15 m, and is thickest in the beginning of the profile. The depth of the sand-clay layer is thinnest approximately at the center of the profile.

The sand-clay layer is replaced by a layer with higher resistivity values from approximately 288 length and throughout the profile. This layer has resistivity values of 700-1500 Ωm, and is likely a continuation of the similar layer observed in profile 13. This layer has he characteristics of a clay-rich moraine, with a mixture of unsaturated sand and gravel.

The bedrock is visible throughout this profile. It appears to be situated directly underneath the sand-clay and sand-gravel layer. It has an undulating profile, without any extreme vertical changes or fractures observed in the imaged profile. At the starting point of the profile, the depth to bedrock is at 6 m depth. It is stable at this depth up until 140 m, where the depth to bedrock ascends to 3 m depth at 170 m length. From that point, it gradually descends to 5 m depth, and is stable up until 250 length. From point 250 m length the bedrock descends to approx. 14 m up until 360 length where it ascends to 7 m depth at the end of the profile.

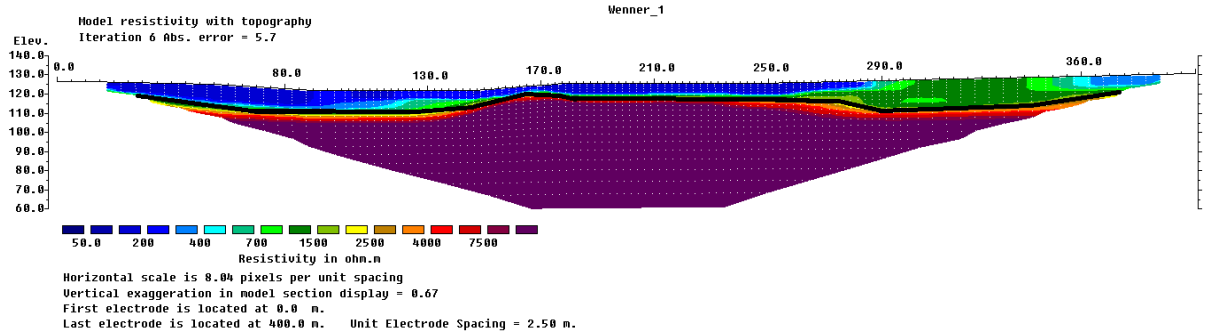

Figure 3.9: Inversion of profile 14.

Profile 14 summary

This profile shows a different picture of the subsurface conditions than profile 13. The distinct drop in the bedrock is gone, and instead there is relatively flat bedrock layer visible.

The sand-clay layer still has good correspondence with the surrounding profiles, and shows a similar pattern as seen in profile 13. The sand-gravel layer visible in this profile also corresponds well with the one seen in profile 13. It appears that for these loose material layers there is a distinct pattern throughout the research area.

Profile 15

Profile 15 is situated across the road Ågetveitveg, approximately 70 m south-west of profile 14 as shown on figure 2.4 on page 25. It is 330 m long, and the minimum electrode spacing is 5 meters. The general direction, from start to stop, of the profile is from north-west to south-east. This profile was taken precisely parallel to profile 13. Due to the terrain conditions, with a near lying domestic garden, limiting the research area, the profile was

shortened by excluding 5 electrodes in the beginning of the profile, and 1 in the end of the profile. The inversion of the profile is seen in figure 3.10 on page 52.

RMS IS 4.1 %. The terrain is very cragged, with large differences in the surface placement above sea level. The profile starts at 119 m.a.s.l. and descends to 116 m.a.s.l. at 30 m length, before ascending to 132 m.a.s.l. at the end of profile. The profile was placed to give a good image of the cleft in terrain.

Also this research area has different soil conditions at the surface. The surface along the cleft had a lot of rocks and appeared dryer than the soil observed at profiles 13 and 14. From approximately 200 m length the soil conditions changed as the terrain flattens out. From this point the top soil looked similar to what was observed at profiles 13 and 14.

At the starting point of the profile, and continuing to approximately 120 m length, there is layer visible with material with resistivity values of 400-1500 Ωm this appears to be a layer of unsaturated sand and gravel.

The imaged profile is challenging to analyze, since there is a segment of the profile from 120 length to 180 length, ranging from the surface down to a depth of 10-15 m, with resistivity values that indicates that this segment is bedrock. This is however highly unlikely, since no bedrock was observe din the surface or near the line of the profile. Our interpretation is that this layer is part of a clay-poor moraine, with very dry mixed material. This also corresponds with the moraine layer observed in profile 14 across the road.

From 180 m length and throughout the profile, a layer with resistivity values of 200-1500 Ωm is visible. This layer has a depth of 5-8 m below the surface. This layer appears to be a layer of saturated material, most likely sand and gravel.

The bedrock is visible throughout the profile, but there is some uncertainty as for the precise placement of it along the longitudinal axis. From the starting point of the profile, and to the point 120 length, what appears to be bedrock has very low resistivity values of 1000-2000 Ωm. From the point 120 length and throughout the profile, the bedrock has values of 2000-10000 Ωm and can be more certainly classified as bedrock. From point 70 m length, the bedrock is at 7 m depth. It ascends to 3 m depth at point 135 m length. From there it gradually descends to 11 m at point 190 m length. From there it ascends to 4 m depth at

point 235 m length. From this point, the bedrock descends to 5 m depth, where it stabilizes throughout the profile; with a slight ascend towards the very end of the profile.

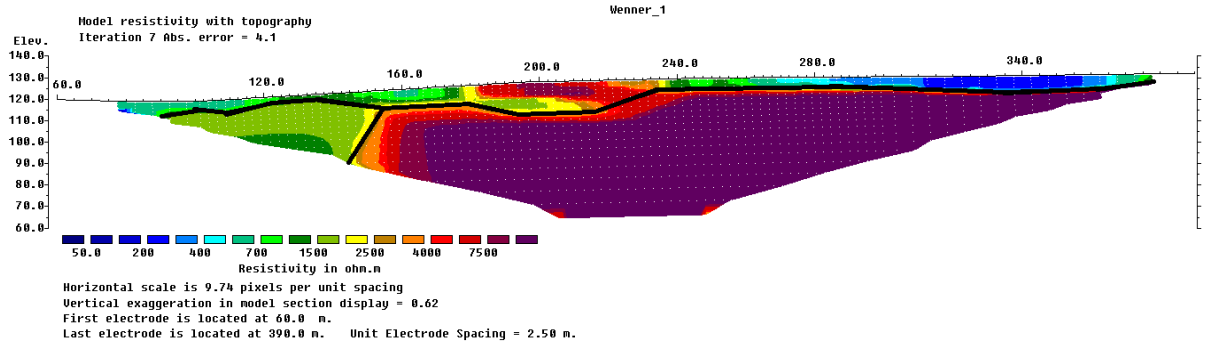

Figure 3.10: Inversion of profile 15.

Profile 15 summary

Profile 15 shows a few differences from the previously described profiles. The sand-clay layer that has been present in all the previously described profiles, appears to be gone, and replaced by what seems to be a layer of mixed material with higher resistivity values.

The bedrock has resemblances with the pattern that has been observed in other profiles. The bedrock with low resistivity values observed in the beginning of the profile indicates that water is seeping in to the bedrock, thus saturating it. This zone of weakness resembles what was seen in profile 13, although profile 15 does not give the full image, due to terrain obstacles.

Profile 16

Profile 16 is situated 40 m south-west of profile 15 as shown on figure 2.4 on page 25. It is 380 m long, and the minimum electrode spacing is 5 meters. The general direction, from start to stop, of the profile is from north-west to south-east. This profile was taken precisely parallel to profile 15. The profile has been shortened by excluding 2 electrodes in the beginning of the profile. The inversion of the profile is seen in figure 3.11 on page 54.

RMS IS 1.6 %. The top soil conditions are the same as in profile 15, with a dry rock-covered top soil in the beginning of the profile, along the cleft in the terrain, and a smoother and wetter top soil towards the end of the profile.

The terrain has a big difference in surface altitude, beginning at 111 m.a.s.l., gradually ascending up to 115 m.a.s.l., and after that ascending more sharply up to 128 m.a.s.l., and after that flattening out ending at 132 m.a.s.l..

At the start of the profile and going as far as 200 m length, with depths varying between 5-10 m below the surface, a layer with resistivity values of 250-1500 Ωm is visible. This layer most likely consists of unsaturated sand and gravel. Along the center of the cleft in the terrain, which this profile travels perpendicular to, the resistivity values seems to be lower than along the sides of the cleft.

From approximately 200 and forward to 300 m length with a depth of 0-10 m a segment of the profile shows very high resistivity values <7500 Ωm. These values correspond with bedrock, but no bedrock was observed in the field at this point. This is interpreted to be a layer of coarse material, probably consisting of gravel and pebbles.

From 300 m length and throughout the profile, in the depth of 0-10 m below the surface a layer with resistivity values 400-1500 Ωm can be seen. This layer is also most likely unsaturated sand and gravel, and corresponds well with the layer observed in the end part of profile 15.

The bedrock is visible almost throughout the profile. It is however apparent that the bedrock in the beginning of the profile, has significantly lower resistivity values than the bedrock in the rest of profile. This corresponds well with what was observed in profile 15. The bedrock becomes visible from approx. 65 m length at 15 m depth. From there it ascends gradually to 8 m depth at point 135 m length. From there it ascends rapidly from 8 m depth to 3 m depth between point 135 m length and point 145 m length. From this point, it remains at 3 m depth up until 190 m length. At point 190, length the bedrock descends to 10 m depth where it stabilizes at this depth throughout the profile.

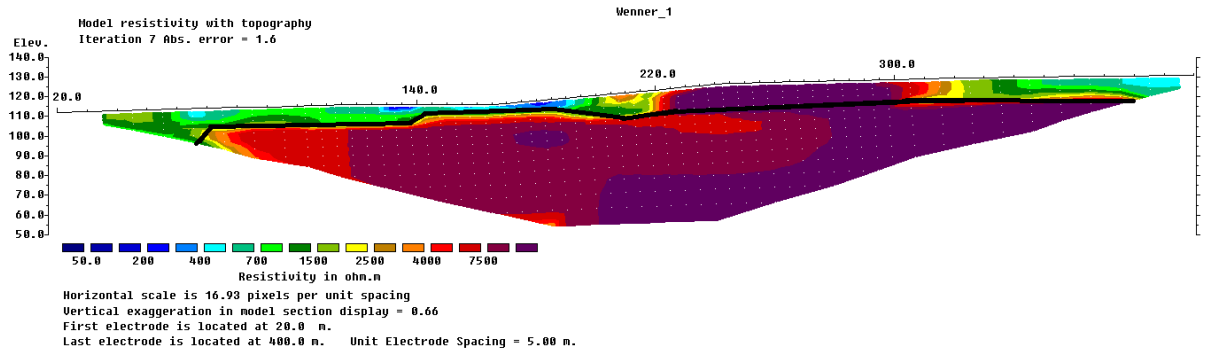

Figure 3.11: Inversion of profile 16.

Profile 16 summary

This profile shows many of the same patterns, with regards to resistivity values and layering as what was observed in profile 15. It appears that there is a weak zone in the bedrock, situated approximately at the center of the cleft in the terrain. This weak zone is characterized by having bedrock with relatively high resistivity values (1500-4000 Ωm).

The layering in the top part of profile, directly below the surface, is somewhat unclear due to the top part imaging being weaker in long profiles, as opposed to shorter profiles. A distinct layering is hard to determine, and could also be influenced by dry soil conditions and an abundance of rocks in the top soil, as is often observed in for an example a moraine.

Profile 17

Profile 17 is situated 80 m south-west of profile 16 as shown on figure 2.4 on page 25. It is 160 m long, and the minimum electrode spacing is 2 meters. The general direction, from start to stop, of the profile is from north-west to south-east. This profile was taken parallel to profile 16, but was shortened to a 160 m array, with a 2 m minimum electrode distance. This was done due to the terrain limiting the possibility of doing a 400 m array, but also to give a better resolution of the top part of the profile. The inversion of the profile is seen in figure 3.12 on page 55.

RMS IS 4.8 %. The top soil conditions are the same as in profile 16. And the profile was placed perpendicular to the cleft in the terrain.

The layering of the sedimentology in this profile is more distinct than what was observed in profiles 15 and 16. From the starting point of the profile and to approximately 65 m length, and in the depth of 5-6 m, a layer with resistivity values of 0-400 Ωm is visible. This is most

likely a layer of saturated sand and gravel. The depth of the layer is fairly stable, and it appears that the layer is placed directly above a layer of bedrock.

From 70 m length, and throughout the profile, ranging in depths of 3-7 m below the surface a layer with resistivity values of 400-1500 Ωm is seen. This layer is most likely unsaturated sand and gravel. The resistivity values seem to drop towards the end of the profile, as the terrain flattens out.

The bedrock is visible throughout the profile. It can be seen in the imaged profile. It appears that there is segment of the bedrock layer with significantly lower resistivity values. This layer can be seen in the imaged profile from the lengths of 50-100 m along the longitudinal axis and approximately 10-30 m depths below the surface. From the starting point, the bedrock is situated approx. 10 m below the surface. It remains at this depth up until point 52 m length where it gradually descends to 12 m depth at point 75 m length. From here, the bedrock ascends to 4 m depth at point 78 m length, and it remains at this depth up until 106 m length, where it descends rapidly to 13 m depth. From point 106 m length the bedrock gradually ascends from 13 to 5 m depth throughout the profile.

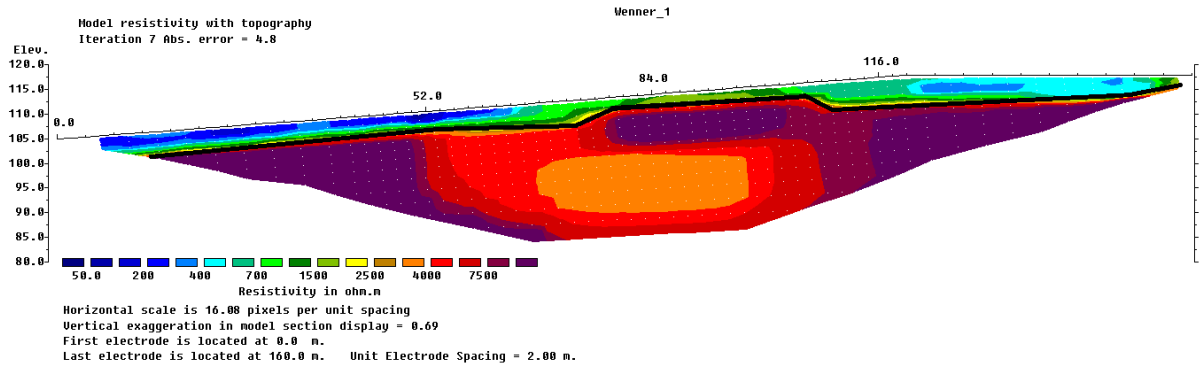

Figure 3.12: Inversion of profile 17.

Profile 17 summary

This profile shows the same patterns with regards to resistivity values as profile 16. Due to the shortened minimum electrode distance, the resolution in the top part of the profile is strengthened. The bedrock however seems to be situated fairly high, 3-7 m below the surface, as opposed to profile 15 and 16 were the bedrock was situated 10-15 m below the subsurface in average.

The apparent weak zone in the bedrock, which was also observed in profiles 15 and 16, is also seen in this profile. This strengthens the idea of a weak zone in the bedrock present throughout the research area, from Undermo to Ågetveit, as it has been observed in nearly every profily analyzed.

Profile 18

Profile 18 is situated in the bottom south-east area of the study area approximately 50 east of profile 17. The general direction of the profile is from south-west to north-east. It is 400 m long and the minimum electrode spacing is 5 m. No electrodes were excluded in the profile. The inversion of the profile is seen in figure 3.13 on page 57.

RMS IS 4.9 %. The soil conditions at this profile was open soils, but with a lot of smaller rocks visible in the field. The profile was along the edge of the field that makes up for the boundary of the study area.

It appears that a layer of material with resistivity values of 700-1500 Ωm is visible below the surface from the starting point of the profile and up to 170 m along the longitudinal axis. The depth of this layer determines the dept to bedrock as the bedrock is visible throughout the profile, and it is varying from 2-5 m subsurface.

From 170 m length to 250 m length there is a layer with above 4000 Ωm visible. This suggests that the bedrock is situated almost directly under the surface. However the bedrock was not observed in the field at this location.

From 250 m length and to 300 m length a layer with resistivity values from 400-1000 Ωm is visible. This layer indicates a mix of unsaturated material, probably sand or gravel. This layer is approximately 5m deep and is also situated on top of what appears to be bedrock.

From 300 m and throughout the profile a layer of material with resistivity values of 50-400 Ωm is visible. This layer resembles what was observed in the end of profiles 15 and 16. It is most likely a layer of saturated sand and clay. The depth of this layer varies from 5-8 m and is likely aituated on top of the bedrock.

The bedrock is visible throughout the profile. It has a steady depth of approximately 5 m up until the centre of the profile, where it appears to be situated almost directly under the

surface. From the centre of the profile and throughout it, it gradually descend to approximately 8 m allthough keeping a fairly steady depth beneath the surface.

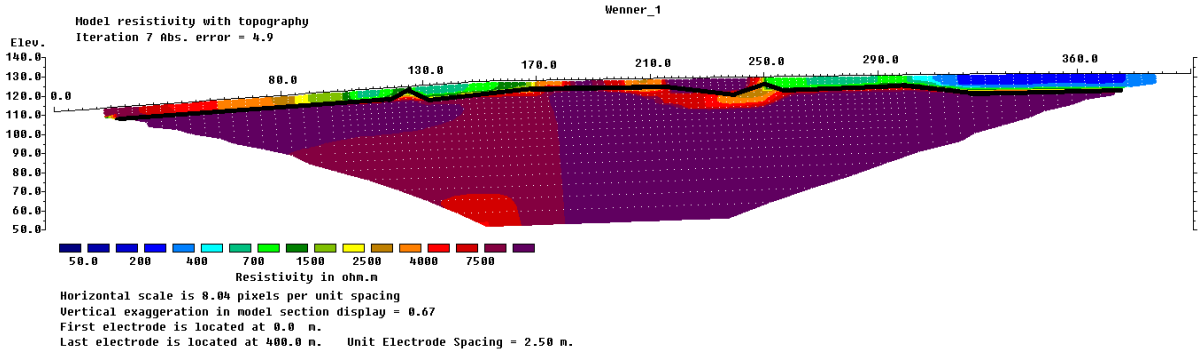

Figure 3.13: Inversion of profile 18.

Profile 18 summary

This profile shows some of the same tendencies as what was observed in profiles 15, 16 and 17. Although it appears that the depth to bedrock is quite low, it was not observed in the field. The bedrock does not show any sign of a weakness zone in this part of the study area, and this indicates that the weakness zone is situated further west of this profile.

The layering in the end of the profile, corresponds very well with what was observed in especially profile 15 and even profile 14 across Ågetveitvegen. That leads to conclusion that this layering is predominant throughut the study area.

Profile 19

Profile 19 is also situated in the south-east bottom part of the study area, approximately at the same position as profile 18. It is however only 160 long with a minimum electrode spacing of 2 m. The general direction of this profile is also south-west to north-east. No electrodes were excluded in this profile. The inversion of the profile is seen in figure 3.14 on page 59.

This profile was placed to give a more thorough look on the centre part of profile 18, as profile 18 did not show a very distinct layering at the centre part.

RMS IS 3.7 %. The soil conditions at this site were the same as for profile 18.

At the starting point of the profile and up until 32 m length, it appears that there is a layer of material with resistivity values of 1000-1500 Ωm. This layer has a depth of approx 5 m and could be mixed material of unsaturated gravel or sand. However the bedrock is dominant in this profile and it could simply be a very thin top layer on top of the bedrock, with the 3D effect blurring the image.

From 30 m length to 120 length the bedrock becomes visible almost in the top of the profile, with small pockets of material visible at the points 60 m length and 85-100 m length. The material in these pockets shows resistivity values of 400-1500 Ωm and is likely unsaturated sand and gravel which appears to be lying on top of the bedrock

From 120 m length the layering that was also observed in profile 18 becomes visible. A layer with resistivity values of below 400 Ωm, most likely saturated sand and clay. This layer has depths of 5-7 m from surface to bedrock However the continuation of this layer was only observed towards the end of the profile.

The bedrock is observed throughout the profile. From the starting point of the profile of the profile the bedrock is situated at 4 m depth. It remains at this depth up until point 60 m length, where the depth to bedrock ascends to 3 m depth. The bedrock remains at this depth up until point 100 m length where it ascends further to 2 m depth, and remains there from point 104 m length to point 118 m length. From point 118 m length the bedrock descends down to 6 m depth where the depth to bedrock remains throughout the profile.

Cross-point 18 and 19

The cross-point between these two profiles is at 215 m length on profile 18 and 30 m length on profile 19. On profile 18 the cross-point is situated fairly centered on the profile but on profile 19 it is situated in the beginning of the profile. This was doe due to terrain obstacles in the surrounding area.

At point 215 m length on profile 18, the bedrock is situated almost at the surface. The point does not show any distinct layering at this point. On point 30 m length on profile 19 the bedrock is situated at approximately 2 m below the surface with a thin layer of material on top. This should not be seen as a negative correspondence, although there is a difference in the imaged values at the cross-point. It simply offers a conclusion to the fact that for a 400 m

long 5 m electrode spacing profile which profile 18 is, there is a poor imaging of the top part of the profile.

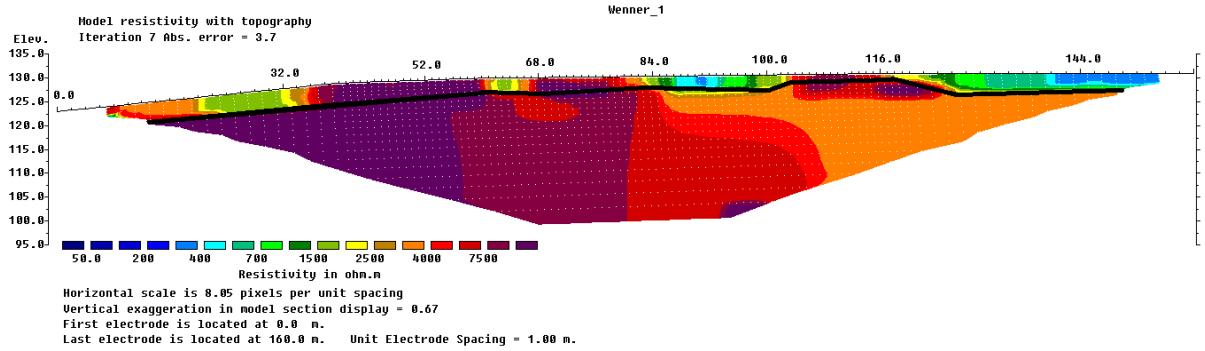

Figure 3.14: Inversion of profile 19.

Profile 19 summary

Although the reason for the placement of this profile was to give a better visualization of the top layer, that poorly visualized in profile 18, this was not the case. It appears that the bedrock is in fact placed directly beneath the surface in depths of 2-7 m. This shows good correspondence between profiles 18 and 19.

With regards to layering, there was no immediate layering visible in the first part of the profile, only a thin layer directly between the bedrock and the surface. For the end of the profile a more distinct layering was visible. This layer shows good correspondence between profiles 18 and 19 as the layering observed had the same tendencies with regard to resistivity values.

Profile 20

This profile is 400 m long and has a minimum electrode distance of 5 m. It was placed across profiles 7, 8, 9, 10, 11 and 12, to strengthen the interpretation of these profiles. It travels from the farm Undermo and in a south-west direction towards the farm Ågetveit. The inversion of the profile is seen in figure 3.15 on page 62.

RMS IS 2.2 %. The top soil conditions were the same, as for the respective additional profiles as earlier mentioned.

From the starting point of the profile, and forward to the length of 130 m, with a depth of 20 m gradually ascending to 5 m below the surface, a layer with resistivity values of 0-400 Ωm is visible. This is most likely saturated sand and clay. The layer might in fact be 2 layers, with the top part being sand and clay, and the bottom part being sand and/or gravel. But the limited resolution in the profile makes it hard to distinguish the two layer and separate them from each other.

The middle part of the profiles top layer, from approx 130 m to 240 m length, with a fairly stable depth of 5 m, the layering becomes hard to isolate. But it appears that, there is a layer of sand and gravel based on resistivity values varying from 250-700 Ωm.

From 240 m length and throughout the profile, with a depth of 10 m, a layer of saturated sand and clay, is visible. This is based on resistivity values varying of 0-200 Ωm.

The bedrock is visible throughout the profile, but with varying depths. The low point is at 50 m length where the depth is 20 m. After that the bedrock depth ascends gradually up to 5 m at 130 m length. The depth is fairly stable at 5 m forward to 240 m before it descends to 10 m and stabilizes there throughout the profile. The bedrock has a segment with relatively low resistivity values between 130 m and 240 m length, in depths ranging from 20 to 50 m. This zone corresponds with the proposed weak zone that was observed in profiles 9, 10 and 11, and again in profile 13, 15 and 16.

Cross-point 7 and 20

The cross-point of these two profiles is at 50 m length on profile 20 and 43 m length on profile 7. This cross-point is situated at the beginning of each profile, and might not give a distinct image of correspondence between these two profiles.

At point 50 m length on profile 20, the bedrock is situated at 22 m depth. On point 43 m length on profile 7 the bedrock is not visible. This should not be seen as a negative correspondence, as profile 7 has a limited resolution in the bottom part of the profile, and the depth 20 m is not even visible on profile 7.

Above the bedrock layer on profile 20 at point 50 m length, there is a layer of material with resistivity values of 200-400 Ωm, which goes all the way up to the surface.

This corresponds well with the layer visible at point 43 m length in profile 7. This layer also has resistivity values of 200-400 Ωm. But there is a segment of the layer at point 43 length, with a higher resistivity value, 400-700 Ωm from depths 5-15 m. An explanation for the difference between the two profiles at this point could be the problem with resolution in the top part of the profile in profile 20.

Overall, the comparison between the two profiles appears to validate the proposed layering and bedrock conditions.

Cross-point 9 and 20

The cross-point of these two profiles is at 80 m length on profile 20 and 82 m length on profile 9. This cross-point is situated at the beginning of profile 20 but fairly centered on profile 9 and should give a distinct image of correspondence between these two profiles.

At point 80 m length on profile 20 the bedrock is situated approximately at 15 m depth. On point 82 m length on profile 9, the bedrock is situated at 13-14 m depth. This means that there is a good correspondence between the two profiles with regard to bedrock depth.

Above the bedrock at point 80 length on profile 20, there is a 5 m thick layer of material with resistivity values of 250-700 Ωm. This is most likely unsaturated sand and gravel, and corresponds very well with what is observed at point 82 m on profile 9. Here the layer seems to be 5-7 m thick, but has the same characteristics as what is observed in profile 20.

Above this layer, there is on both profiles, a layer of material with resistivity values of 0-200 Ωm. This layer appears to be saturated sand and clay.

Overall there seems to be very good correspondence between, the resistivity values observed in these two profiles. This gives strength to the fact that the subsurface conditions is in fact as they appear in both profiles.

Cross-point 8 and 20

The cross-point of these two profiles is at 90 m length on profile 20 and 130 m length on profile 8. This cross-point is situated at the beginning of profile 20 but fairly centered on profile 8 and should give a distinct image of correspondence between these two profiles.

At point 90 m length on profile 20 the bedrock is situated at 15 m depth. On point 130 m length on profile 8, the bedrock is somewhat unclear but is approximately situated at the depth 10-15 m. This shows a relatively good correspondence between the two profiles, and supports the proposed depth to bedrock in profile 8.

Above the bedrock at point 90 m in profile 20, the layering is approximately the same as it was in the cross-point between profile 20 and 9. At point 130 m length in profile 8, he layering is somewhat unclear. But there is a distinct layering at depth 0-7 m below the surface. The same layering can be seen in profile 20 at point 90 m length. And it is most likely a continuation of the layering that was previously observed.

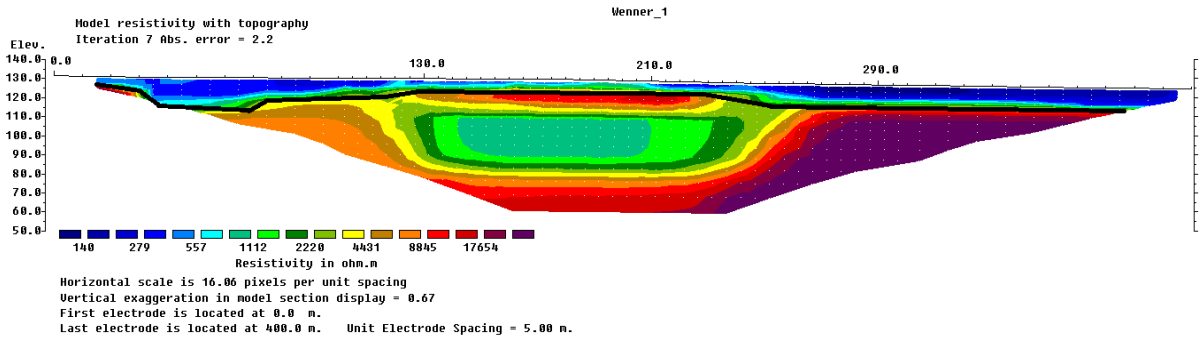

Figure 3.15: Inversion of profile 20.

Profile 20 summary

Profile 20 shows a good imaging of the layering throughout the profile. As the profile offers cross-sections of several other profiles, this profile will also offer good validation points in these cross-sections for interpretation of the other profiles.

The bedrock was observed throughout the profile in varying depths. The minimum electrode spacing of 5 meters gave a good imaging of the profile, and therefore the bedrock was clearly illustrated in the imaging of the profile.

Profile 20 was important for validating depths to bedrock across the profiles in study area 1.The cross-sections between each individual profile offered a good understanding and validation of the bedrock conditions in the area.

Profile 26

Profile 26 is situated in a forest area, north of profile 33, as seen on figure 2.4 on page 25. The profile is 400 m long, with a minimum electrode spacing of 5 m. At 200 m the profile crosses a road. We chose to have a 400 m long profile with 5 m electrode spacing in order to reach great depth, even though this meant that we had to stop traffic. The general direction of the profile is north-west to south-east from start to stop. The profile crosses profile 42 at 210 m and profile 33 at about 300 m, but these cross-points will be analyzed in the interpretations of profile 33 and 42. The profile was placed in the forest, but the surface conditions were heavily influenced by the glaciofluvial delta deposit material. The soil at the surface was both dry and consisted of coarse material. This may affect the resistivity results, rendering very high resistivity values, higher than normal resistivity values for sand and gravel. The inversion of the profile is seen in figure 3.16 on page 65, and with a logarithmic scale in figure 4.1 on page 114 in the appendix.

In some parts of the profile, because sources of error such as 3D-effects, the resistivity values at the depth of interpreted bedrock does not correspond with typical resistivity values for bedrock < 5 000 Ωm. The electricity will follow the till layer just above the bedrock, instead of following the direct path down and into the bedrock. This layer may also be saturated, so it is difficult to distinguish the sediment at this point. Whether the layer is clast-poor till or saturated sand, gravel and stones from the delta deposit is therefore difficult to determine from the resistivity values alone. However, the layer above the bedrock is because of the high resistivity values, for the most of the area interpreted to be a layer of dry glaciofluvial material.

RMS is 2,7 %. The depth to bedrock is not possible to estimate from the inverted image before 65 m since the depth of the inversion up until this point is less than the bedrock depth. At 65 m distance the depth to bedrock is 22 m. Our GPR profile 02 results also support such a depth to bedrock. From 65-112 m it is increasing from 22-26, something which also our GPR profile 02 results support. At 112-230 it is at 26 m. At 230-300 it is decreasing 22 m, mostly due to surface height changes. At 300-325 it is decreasing to 15 m depth.

Table 3.2: Depth to bedrock from earlier research near profile 26.

Author	Length	Deviation from line	Depth to bedrock	Method	Survey name
Jansen	85	30 SW	22	Drilling	A16
Klempe	264	12 NE	20	Drilling	Unpublished
Klempe	309	20 NE	6	GPR	Unpublished
Klempe	325	21 NE	14	GPR	Unpublished
Klempe	339	22 NE	28	GPR	Unpublished
Klempe	359	18 SE	13	GPR	Unpublished
Klempe	374	13 SE	15	GPR	Unpublished
Klempe	390	24 NE	30	GPR	Unpublished
Klempe	400	25 NE	19	GPR	Unpublished
Klempe	400	28 NE	10	GPR	Unpublished

As seen in 3.2, from the earlier research the depth of the bedrock is indicated to be more undulating than the resistivity measurements indicates. However, the interpreted depth to bedrock does match several of the data from earlier research.

At 10-150 m the layer above bedrock has very high resistivity values, from about 9 000-60 000 Ωm. This is interpreted to be dry glaciofluvial material. The resistivity is very high, and this may be due to very little to no saturation, and very high resistivity values at the surface. This layer indicates the highest resistivity values in the middle, at 60 000 Ωm, the lowest resistivity values just above the bedrock, at 9 000-12 000 Ωm, and a layer on top of this and at the surface with resistivity values of 25 000-40 000 Ωm. The differences in the resistivity values may be due to different content of larger particles such as pebbles.

From 150-190 m the layer of resistivity values at 9 000-12 000 Ωm continues. This is interpreted to be dry glaciofluvial material. Above this layer is first a layer of about 25 000 Ωm which is dominating, which after 180 m is replaced by a layer of 18 000 Ωm. This is interpreted to also be dry glaciofluvial material. At 180-200 m the layer shows a larger depth to bedrock, but this is believed to be caused by 3D-effect, possibly from a higher level of saturation around this point.

From 190-200 m, the layer above the bedrock at 19 m depth has a resistivity value of 19 000 Ωm. This layer is interpreted to be dry glaciofluvial material connected to the same layer at

170-190 m. From 200-210 m there is a layer of low resistivity values, 3 000 Ωm. This is interpreted to be saturated glaciofluvial material. This may also be clast-poor till material.

From 210-290 m, the top layer has very high resistivity, of 80 000 Ωm, and this is interpreted to be dry, coarse glaciofluvial material. Below there is a layer of low resistivity, less than 1 000 Ωm. This is saturated gravel and sand connected to the aquifer which is situated here. This layer continues to the surface from 300-380 m. The layer just above the bedrock has a resistivity value of 2500 Ωm, and this is interpreted to be clast-poor till.

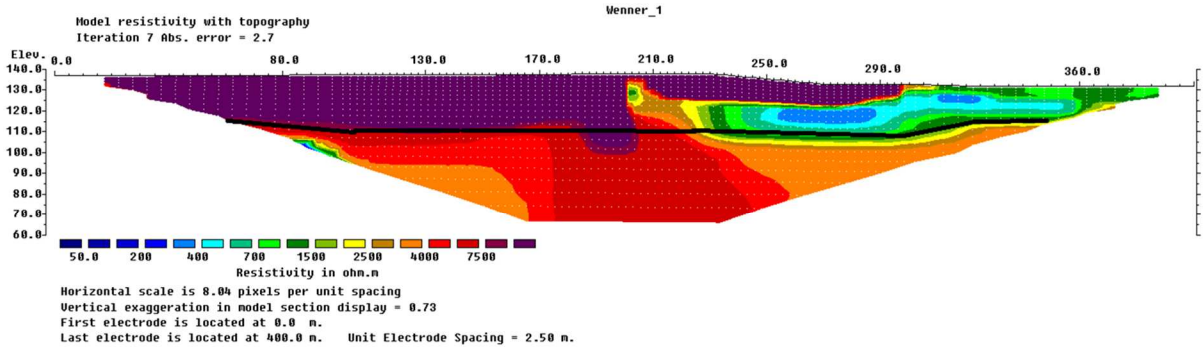

Figure 3.16: Inversion of profile 26.

Profile 26 summary

Both the depth to bedrock and the layering of the profile is hard to estimate in a precise way for this profile. The depth to bedrock is hard to estimate since the typical resistivity values for bedrock is not present, mainly due to 3D-effects. This may give an estimation of depth to bedrock that is too large. The earlier research indicates that the bedrock is more undulating than what the resistivity measurements does. This may be due to the low resolution that a minimum electrode spacing of 5 m gives, thus not showing these variations. The layering of the profile indicates that there are two separate areas on each side of the gravel road at 200 m. In the western area there is dry glaciofluvial material, and this has very high resistivity. In the eastern area there is saturated glaciofluvial material.

Profile 27

Profile 27 is situated east of profile 26 as shown on figure 2.4 on page 25. The start of profile 27 is situated 60 m east of the center of profile 26. It is 400 m long, and the minimum

electrode spacing is 5 m. The general direction is from west to east. The profile was placed in the forest, but the surface conditions were heavily influenced by material from the glaciofluvial delta deposit. The inversion of the profile is seen in figure 3.17 on page 67, and with a logarithmic scale in figure 4.2 on page 114 in the appendix.

The RMS is 3,0 %. For the whole profile, the resistivity value does not correspond with typical resistivity values for bedrock due to 3D-effects, as explained earlier. At 40-200 m, the resistivity value is as low as 1500 Ωm. The 3D-effect makes it very difficult to estimate the depth to bedrock, but the layer from the delta deposit at 220-300 m and a layer with resistivity values of 2000 Ωm at 105-140 m, give an indication of where the bedrock may be. At 65-125 m, the interpreted depth to bedrock is increasing from 16 m to 28 m. Our GPR profile 05 results support an increase in depth to bedrock, but the depth indicated is not that large. At 125-150 m, the depth to bedrock is stable at 28 m. At 150-160 m it is decreasing from 28 m to 23 m. At 160-225 it is increasing from 23 m to 28 m. At 225-270 it increases from 28 m to 35 m. At 270-320 it decreases from 35 to 29 m. As seen in table 3.3, depth to bedrock is more undulating than what the resistivity measurement shows. However, the interpreted depth to bedrock does match several of the data from the earlier research.

Table 3.3: Depth to bedrock from earlier research near profile 27.

Author	Length	Deviation from line	Depth to bedrock	Method	Survey name
Klempe	140	5 NE	29	GPR	Unpublished
Klempe	190	21 S	31	GPR	Unpublished
Klempe	190	21 N	28	Drilling	Unpublished
Børresen et al.	205	15 SE	17	Drilling	S3
Klempe	205	18 S	20	Drilling	Unpublished
Klempe	210	4 NW	27	GPR	Unpublished
Klempe	235	18 SW	16	GPR	Unpublished
Klempe	253	18 S	26	Drilling	Unpublished
Børresen et al.	263	7 N	13	Drilling	S2
Klempe	285	7 N	26	Drilling	Unpublished
Børresen et al.	300	25 N	24	Drilling	S1

The upper layer from 10 m to 230 m, plus 280 m to 320 m, has a value of 18 300-100 000 Ωm, both with the highest resistivity value in the center. This is interpreted to be dry, coarse

glaciofluvial material. From 120 m to 140 m is situated a kettle hole. Below this layer at 70-220 m the resistivity value is lower, 200-2 000 Ωm, and this is probably due to higher degree of saturation, due to water content from the kettle. At 260-280 m, at the surface and from 340-400 m below the upper layer, there is an area of lower resistivity value, 1 500-3 000 Ωm. This is interpreted to be another material, sand and gravel, which probably is saturated. The upper layer at 280-320 m is the esker which is visible in the field.

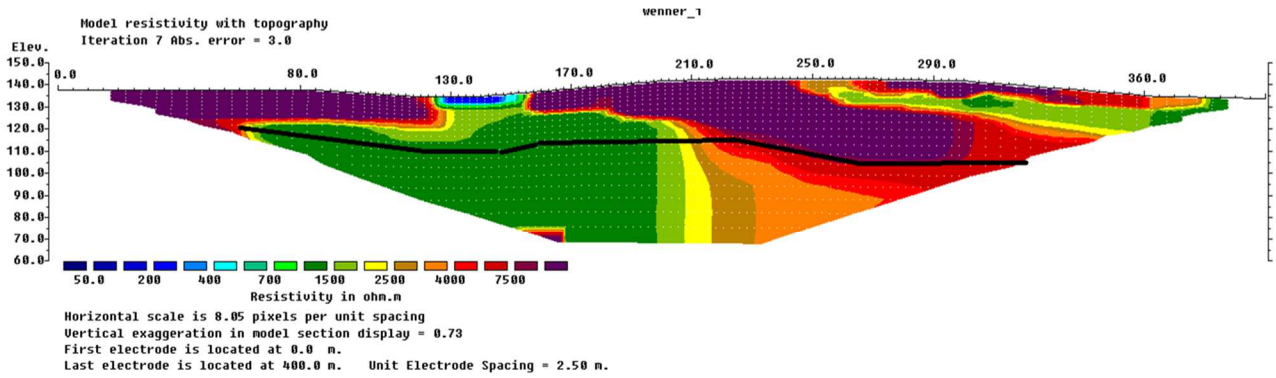

Figure 3.17: Inversion of profile 27.

Profile 27 summary

The eastern part of profile 26 seems to correspond well with the western part of profile 27. Depth to bedrock for this profile is difficult to estimate due to 3D-effects. The earlier research indicates that the bedrock is more undulating than what the resistivity measurements does. This may be due to the low resolution that a minimum electrode spacing of 5 m gives, thus not showing these variations. The layering of the profile seems to indicate that there are two different areas which are saturated. It is believed that there is a bedrock ridge creating a water divide at about 220 m (Børresen et al., 1990). This may be one explanation of the existence of two saturated areas. The relatively low resistivity values for the area 340-400 m is believed to be connected to the landfill of 1989 located at Djupegrop.

Profile 29

Profile 29 is situated approximately 90 m south of profile 27 as shown on figure 2.4 on page 25. It is 120 m long, and the minimum electrode spacing is 2 m. Due to limitations in the area, we had to exclude 5 electrodes in each direction, in total 10 electrode exclusions. The general direction is from north-west to south-east. The profile was placed near farmland, on a grass field. The inversion of the profile is seen in figure 3.18 on page 69.

RMS is 1,66 %. For the whole profile, the resistivity value does not correspond with typical resistivity values for bedrock due to 3D-effects, as explained earlier. For the whole profile, the resistivity value is as below 3000 Ωm. The 3D-effect makes it very difficult to estimate the depth to bedrock, but the indicated layering from the resistivity results gives an indication of where the bedrock may be. From 34-100 m the bedrock is interpreted to be steadily decreasing from 13 m to 8 m. Our GPR line 07 result supports this interpretation. As seen in table 3.4, earlier research also supports our interpretations. The resistivity value of 2000 Ωm is lower than typical values for bedrock, but this may be due to 3D-effects.

Table 3.4: Depth to bedrock from earlier research near profile 29.

Author	Length	Deviation from line	Depth to bedrock	Method	Survey name
Klempe	0	7 NW	0	GPR	Unpublished
Klempe	7	11 S	17	Drilling	Unpublished
Klempe	16	3 NE	13	GPR	Unpublished
Klempe	32	3 SW	15	Drilling	Unpublished
Klempe	32	7 NE	15	Drilling	Unpublished
Klempe	37	8 NW	12	Drilling	Klempe 4
Klempe	47	11 NE	13	Drilling	Unpublished
Klempe	47	8 NE	13	Drilling	Unpublished
Børresen et al.	57	10 NE	9	Drilling	S11
Klempe	92	18 SW	7	Drilling	Unpublished

Above the bedrock at 34-78 m there is a layer with low resistivity, 300-700 Ωm. This is interpreted to be saturated sand. This area is connected to the aquifer. At the surface, the layer has a higher resistivity, 1000 Ωm. This is interpreted to be the saturated sand. From 78-100 m, there is a layer at the surface and above the bedrock with resistivity value of 1500

Ωm. Both of these layers are interpreted to be sand and gravel. In the middle of these layers is a layer with resistivity value of 1000 Ωm. This is interpreted to be saturated sand and gravel. At 94- 114 m, there is a layer at the surface with resistivity value between 3 000-5 000 Ωm. This is interpreted to be saturated glaciofluvial material. From 86-100 m there is a layer below the surface with resistivity value of 300-400 Ωm. This is interpreted to be saturated sand.

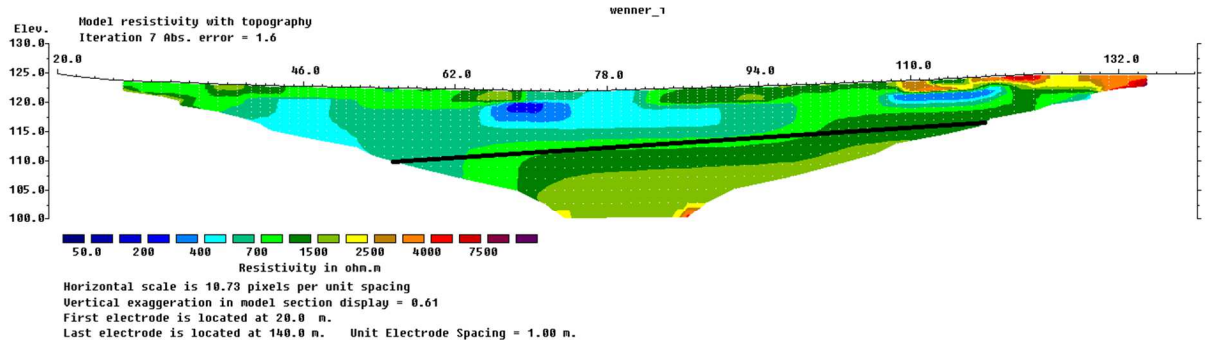

Figure 3.18: Inversion of profile 29.

Profile 29 summary

The profile's depth to bedrock is hard to estimate accurately, due to 3D-effects. The earlier research indicates that the bedrock is located at the same depth as our interpretations of the resistivity measurements. The resistivity measurements show the same sediments as earlier research (Jansen, 1983). The area consists of an aquifer. We can clearly see how the aquifer affects the resistivity values.

Profile 30

Profile 30 is situated approximately 55 m north of profile 27 as shown on figure 2.4 on page 25. It is 400 m long, and the minimum electrode spacing is 5 m. The general direction is from south-west to north-east. The profile was placed in the forest, but the surface conditions were heavily influenced by material of the glaciofluvial delta deposit. The soil at the surface was both dry and consisted of coarse material. This may affect the resistivity results, rendering very high resistivity values, higher than normal resistivity values for sand and gravel. The profile crosses the landfill from 1958-1974, Djupegrop. The inversion of the

profile is seen in figure 3.19 on page 71, and with a logarithmic scale in figure 4.3 on page 115 in the appendix.

RMS is 2,2 %. At 65-210 it is increasing from 20 m to 25 m. At 210-220 m there is a sudden increase in depth to bedrock, from 25 m to 32 m, and this depth continues to 265 m. From 265-275 m, the depth decreases from 32 m to 29 m. At 275-300 m, the depth is stable at 29 m, and this depth continues to 325 m. From the earlier research seen in table 3.5, the depth of the bedrock is indicated to be more undulating than the resistivity measurements indicates. However, the interpreted depth to bedrock does match several of the data from the earlier research.

Table 3.5: Depth to bedrock from earlier research near profile 30.

Author	Length	Deviation from line	Depth to bedrock	Method	Survey name
Klempe	80	7 NW	33	Drilling	Unpublished
Klempe	85	14 SW	7	GPR	Unpublished
Klempe	90	18 SW	17	GPR	Unpublished
Klempe	145	4 N	31	GPR	Unpublished
Klempe	155	9 SE	24	GPR	Unpublished
Klempe	270	18 S	24	Drilling	Unpublished
Klempe	290	15 N	26	Drilling	Unpublished
Klempe	310	20 N	18	Drilling	Unpublished
Børresen et al.	350	5 N	18	Drilling	S7
Jansen	395	23 S	25	Drilling	A4

The resistivity value is lower at the depth of bedrock than at the layer above, but we still interpret the bedrock to at this depth. The lowering in the resistivity value may be due to a higher level of saturation, which then creates a 3D-effect. The lower resistivity values may also be due to another type of sediment, such as clast-poor till. We do however not interpret this layer to be clast-poor till, but saturated glaciofluvial deposits. There should be moraine material at this depth, but it may be that the layer is too small to be seen because of our inversion's resolution. From the earlier research the depth of the bedrock is indicated to be more undulating than the resistivity measurements indicates. However, the interpreted depth to bedrock does match several of the data from the earlier research.

From 20-210 m and from 280-380 m, only interrupted by the area from 240-280 m, the situation is the same. The layer at the surface has a very high resistivity of 40 000-100 000 Ωm. This is interpreted to be dry, coarse glaciofluvial material. Below this layer, the resistivity is the highest in the center of these layers, and the center is believed to be very dry glaciofluvial material. At the bottom, it is a layer interpreted to be saturated sand and gravel from the glaciofluvial deposit.

From 210-280 m, the layer above the bedrock has a resistivity of 26 000 – 40 000 Ωm. This is interpreted to be dry glaciofluvial material. Above this layer, which stretches to the surface, there is a layer with low resistivity of 300-4000 Ωm. This is the landfill.

At 220-280, the landfill from 1958-1974, Djupegrop, is situated. Under this layer at 220-280 m, earlier research indicates that there may be a cleft. This may explain the lowering of depth to bedrock. In reality, this lowering should be steeper, but the resolution of the inversion is not able to represent this.

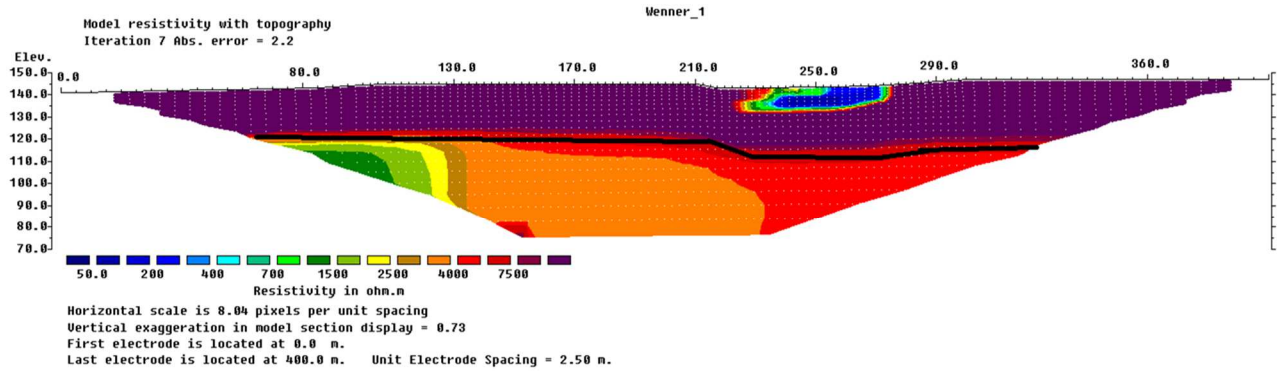

Figure 3.19: Inversion of profile 30.

Profile 30 summary

The depth to bedrock is difficult to estimate accurately. The high surface resistivity may have reduced the quality of the resistivity results. Earlier research has indicated that the bedrock is undulating, but the fluctuations may be too small for our profile's resolution. The earlier research indicates that the bedrock is more undulating than what the resistivity measurements does. This may be due to the low resolution that an electrode spacing of 5 m gives, thus not showing these variations. The layering seems to give two separate areas of dry glaciofluvial material, just as for profile 27.

Profile 32

Profile 32 is situated approximately 35 m north of profile 30 as shown on figure 2.4 on page 25. It is 400 m long, and the minimum electrode spacing is 5 m. The general direction is from south-west to north-east. The profile was placed in the forest, but the surface conditions were heavily influenced by material of the glaciofluvial delta deposit. The soil at the surface was both dry and consisted of coarse material. This may affect the resistivity results, rendering very high resistivity values, higher than normal resistivity values for sand and gravel. The profile crosses a gravel road at 200-220 m, and we had to exclude four electrodes at this area. Here there was also a very high surface resistivity. The profile is placed in a manner that at 220-240 m, it is just north of the landfill from 1958-1974, Djupegrop. The inversion of the profile is seen in figure 3.20 on page 73, and with a logarithmic scale in figure 4.4 on page 116 in the appendix.

RMS is 2,9 %. From 80-230, the depth to bedrock is interpreted to be stable at 27 m depth. Our GPR profile 03 results support a large depth, and depth to bedrock is indicated to be at about 30 m. From 225-230 m, it increases from 27 m to 30 m depth, and it continues at this depth to 320 m. Our GPR line 04 results support this. From the earlier research seen in table 3.6, the depth of the bedrock is indicated to be more undulating than the resistivity measurements indicates. However, the interpreted depth to bedrock does match several of the data from the earlier research.

Table 3.6: Depth to bedrock from earlier research near profile 32

Author	Length	Deviation from line	Depth to bedrock	Method	Survey name
Klempe	85	8 N	32	Drilling	Unpublished
Klempe	120	12 SE	28	GPR	Unpublished
Klempe	180	6 N	31	Drilling	Unpublished
Klempe	185	22 N	32	GPR	Unpublished
Børresen et al.	215	5 S	31	Drilling	S8
Klempe	225	3 N	30	GPR	Unpublished
Klempe	225	2 NE	30	Drilling	Unpublished
Børresen et al.	260	7 S	30	Drilling	S10
Klempe	260	12 S	32	GPR	Unpublished
Klempe	260	16 SE	24	GPR	Unpublished
Klempe	270	12 NW	28	Drilling	Klempe 2

Klempe	280	22 S	22	GPR	Unpublished
Klempe	305	5 N	20	Drilling	Unpublished
Klempe	315	16 N	23	Drilling	Unpublished

From 60-200 m the layer just above the bedrock has resistivity values of 4000-5000 Ωm, and is interpreted to be poor saturated glaciofluvial deposit. This may also be clast-poor till material. Above this layer there is a layer of very high resistivity at 30 000-100 000 Ωm. The resistivity is highest in the center. This is interpreted to also be dry glaciofluvial material, in connection with profile 30. The center is believed to be very dry material. From 200-250, there is a layer above bedrock with resistivity value of 18 000 Ωm. This is interpreted to be dry glaciofluvial deposits. The road is situated at 200-220 m, where we had to exclude four electrodes. At 200-220 m, the layer at the surface is the road, and it has a high resistivity of about 60 000 Ωm at the surface. Between 225 m and 250 m there is the cleft that is connected to Djupegrop, which contains material with lower resistivity values. From 250-390 m, there is a layer with high resistivity of about 50 000 Ωm above the bedrock. This is interpreted to be dry glaciofluvial material. At the surface, the resistivity is somewhat lower at 13 000-28 000 Ωm. This is interpreted to be dry, coarse glaciofluvial material, perhaps more saturated than the layer below.

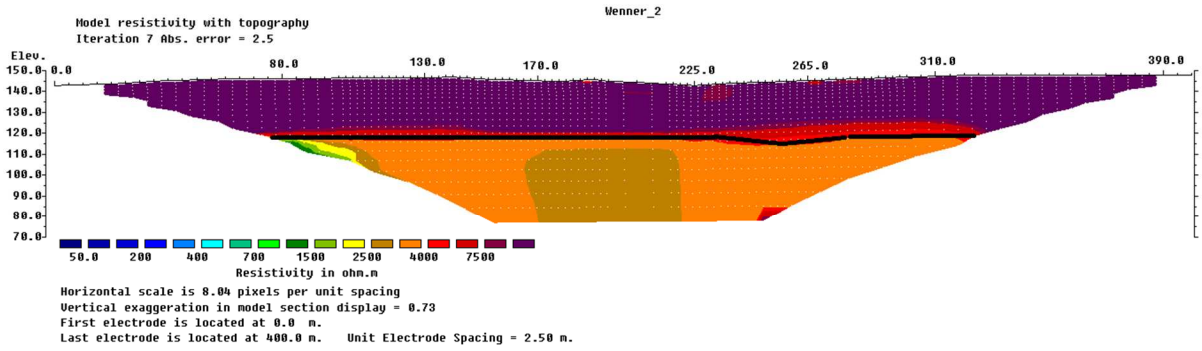

Figure 3.20: Inversion of profile 32.

Profile 32 summary

The profile shows similar results for depth to bedrock and layering as profile 30. The high surface resistivity may have reduced the quality of the resistivity results. Just as what is the

case with many of the profiles in this area, depth to bedrock is difficult to estimate accurately due to the 3D-effect. The earlier research indicates that the bedrock is more undulating than what the resistivity measurements does. This may be due to the low resolution that a minimum electrode spacing of 5 m gives, thus not showing these variations. The glaciofluvial material has very high resistivity values. The dry glaciofluvial material seems to have two separate entities, just as profile 30. So in profile 27, profile 30 and profile 32 there are the same tendencies regarding the two separate entities in the glaciofluvial material.

Profile 33

Profile 33 is situated south of profile 26 as shown on figure 2.4 on page 25. It is 160 m long, and the minimum electrode spacing is 2 m. At 40 m the profile crosses a gravel road, but we managed to place the electrodes so that we avoided any electrode exclusions. The general direction is from south-west to north-east. The profile was placed in the forest, but for the last 60 m the soil was influenced by the glaciofluvial material, giving the surface a high resistivity value. The profile crosses profile 26 at 140 m and profile 42 at 70 m. The inversion of the profile is seen in figure 3.21 on page 76, and with a logarithmic scale in figure 4.5 on page 116 in the appendix.

RMS is 1,66 %. At 30-116 m the depth bedrock is interpreted to be steadily increasing from 12 m to 19 m. The resistivity values do not at all reflect this interpretation, but we believe this to be caused by 3D-effects. As seen in table 3.7, earlier research supports our interpretations. There is a drilling point on the profile line, and this indicates a depth to bedrock of about 21 m, something which supports the interpretation of the profile.

Table 3.7: Depth to bedrock from earlier research near profile 33.

Author	Length	Deviation from line	Depth to bedrock	Method	Survey name
Jansen	33	9 SE	13	Drilling	A12
Jansen	50	3 NW	8	Drilling	A13
Klempe	120	7 SE	20	Drilling	Unpublished
Klempe	127	4 SE	4	GPR	Unpublished
Klempe	131	On the profile line	21	Drilling	Unpublished

At 28-76 m, the layer above bedrock has a resistivity value of about 2000 Ωm. This material is interpreted to be saturated clast-poor till. However, it may also be saturated sand and gravel. The layer above this material, which continues to the surface, has a resistivity value of 1500 Ωm, and this is believed to be due to high content of water. This is interpreted to be saturated sand and gravel. In the same area in the field, there was a wet area, which strengthens this interpretation. At 76-114 m the layer above bedrock has a resistivity value of 2500 Ωm. This is interpreted to be clast-poor till. The layer above this material, which continues to the surface, has a resistivity value of 15 000-80 000 Ωm. This is interpreted to be the same dry glaciofluvial material as seen in profile 26.

Cross-point.

At 100 m for profile 33, and at 249 m for profile 26, the two profiles intersect. At this point the depth to bedrock is not the same for the two profiles. It is interpreted to be about 17 m depth in profile 33, and at 25 m depth at profile 26. This difference can be due to errors in interpretation and/or have other sources. However, they both show a depth to bedrock which is 17 m or more. Thus, we can estimate the depth to bedrock to be between 17-25 m. The layer at the surface shows the same resistivity value of 15 000-80 000 Ωm. The thickness of this layer is the same for both profiles, at about 12 m. The layer below shows the same resistivity value of 2000-2500 Ωm. The thickness of the upper section of this layer is the same for both profiles. However, below this layer the two profiles do not match concerning the layering. This may have several causes. The resolution of the two profiles is not the same, and 3D-effects may also affect the results.

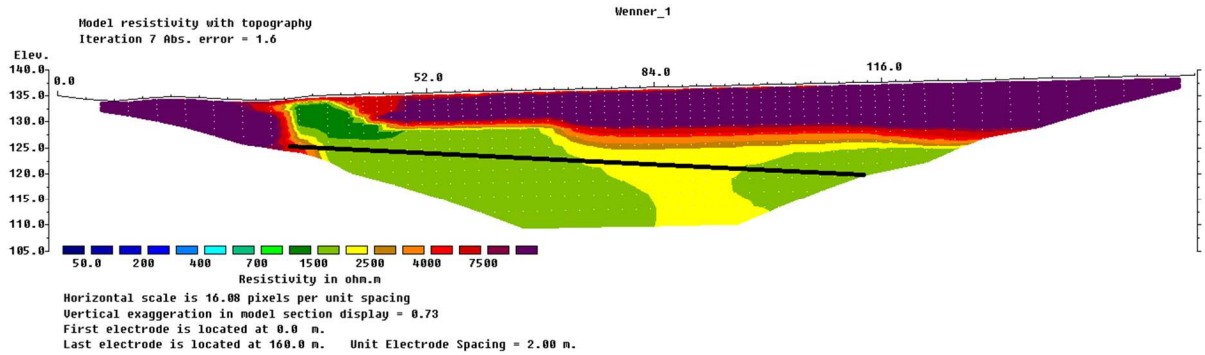

Figure 3.21: Inversion of profile 33.

Profile 33 summary

The profile shows the same tendencies for depth to bedrock and layering as the profiles around. Profile 33 has a smaller electrode distance than profile 26, something which gives a better resolution, but this does not give any new results.

Profile 34

Profile 34 is the most northern profile, situated approximately 35 m north of profile 32 as shown on figure 2.4 on page 25. It is 156 m long, and the minimum electrode spacing is 2 m. At the start there was a gravel road, so we had to exclude one electrode. The general direction is from south-west to north-east. The profile was placed in the forest, but for the whole profile the soil was heavily influenced by the glaciofluvial material, giving the surface a high resistivity value. The soil at the surface was both dry and consisted of coarse material. This may affect the resistivity results, rendering very high resistivity values, higher than normal resistivity values for sand and gravel. The inversion of the profile is seen in figure 3.22 on page 77, and with a logarithmic scale in figure 4.6 on page 116 in the appendix.

RMS is 1,9 %. The gravel pit is situated where the profile started, so we could see the bedrock 20 m west of the profile. This gives us strong indications for the depth to bedrock at our profile. From 50-118 m, the depth to bedrock is interpreted to be steadily decreasing from 21 m to 19 m depth. As seen in 3.8, earlier research supports our interpretations of depth to bedrock.

Table 3.8: Depth to bedrock from earlier research near profile 34.

Author	Length	Deviation from line	Depth to bedrock	Method	Survey name
Klempe	0	16 W	19	Drilling	Unpublished
Klempe	0	6 S	21	Drilling	Unpublished
Klempe	12	7 S	22	Drilling	Unpublished
Klempe	25	8 S	19	Drilling	Unpublished
Klempe	25	9 SW	20	Drilling	Klempe1
Klempe	46	11 S	21	Drilling	Unpublished
Klempe	65	18 S	23	Drilling	Unpublished
Klempe	75	3 N	24	Drilling	Unpublished
Børresen et al.	100	8 S	20	Drilling	S5

For the whole profile, it seems to be one continuing layer which increases in resistivity value at 70-125 m, with resistivity values from 33 000-100 000 Ωm. This is interpreted to be dry glaciofluvial material, in connection with profile 32. Just below this layer there is a layer with lower resistivity of 10 000-33 000 Ωm. This is interpreted to be dry glaciofluvial material. From 48-100 m there is an ice kettle hole, making this material even more compact. The resistivity values are much lower at the upper one meter than for the rest. The cause for this is believed to be that the ground was very moist here, since the forest here recently had been cut, thus leaving much moist from precipitation. The whole area consists of material with very high resistivity.

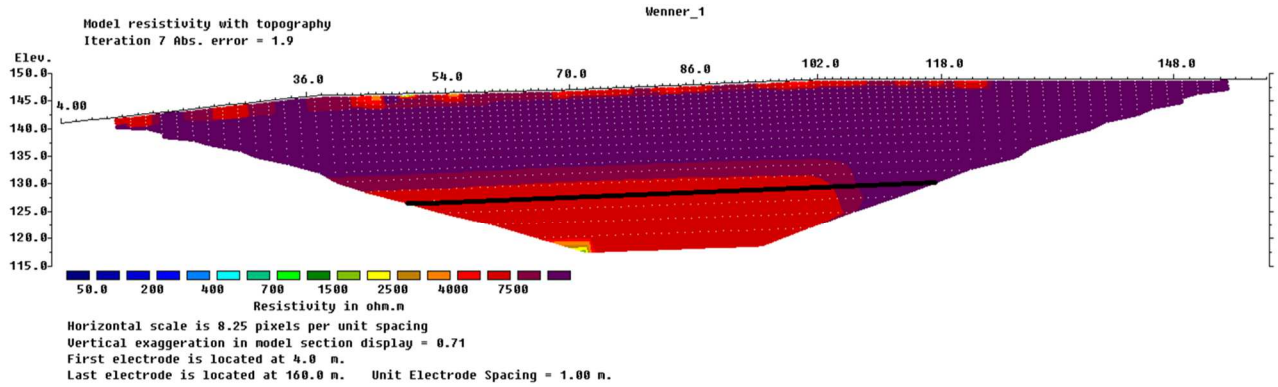

Figure 3.22: Inversion of profile 34.

Profile 34 summary

Profile 34 has the same challenges for estimation of depth to bedrock and layering as nearby profiles. The high surface resistivity may have reduced the quality of the resistivity results.

However, since the bedrock was observed about 20 m west of the profile, there is a match between the observed bedrock and interpreted bedrock from the result.

Profile 35

Profile 35 is situated south-west of profile 33 as shown on figure 2.4 on page 25. It is 160 m long, and the minimum electrode spacing is 2 m. The general direction is from west to east. The profile was placed in the forest, but for the last part of the profile, the soil was influenced by the coarse material from the glaciofluvial deposits, giving the surface a high resistivity value. The profile crosses profile 36 at about 115 m. The inversion of the profile is seen in figure 3.23 on page 79, and with a logarithmic scale in figure 4.7 on page 117 in the appendix..

RMS is 1,9 %. It is believed that the lower resistivity values at the level where we find the bedrock is due to 3D-effects. From 34-90 m the depth to bedrock is interpreted to be stable around from 13 m. From 90-112 m it decreases from 13 m to 8 m. At 112-140 m it decreases from 8 m to 7 m. As seen in 3.9, earlier research supports our interpretations of depth to bedrock.

Table 3.9: Depth to bedrock from earlier research near profile 35.

Author	Length	Deviation from line	Depth to bedrock	Method	Survey name
Klempe	65	30 N	28	Drilling	Unpublished
Klempe	148	4 N	13	Drilling	Unpublished

From 4-110 m, the layer above has a high resistivity value of 40 000-100 000 Ωm. This is interpreted to be dry glaciofluvial material. From 110-148 m, the layer has a lower resistivity value of about 14 000-50 000 Ωm. This is also interpreted to be dry glaciofluvial material, but with a lower resistivity value.

The estimation of depth to bedrock is uncertain due to the 3D-effects. The interpretations of the two profiles show the same results as for bedrock depth and layering. A detailed analysis of the cross-points will be given in the interpretation of profile 36.

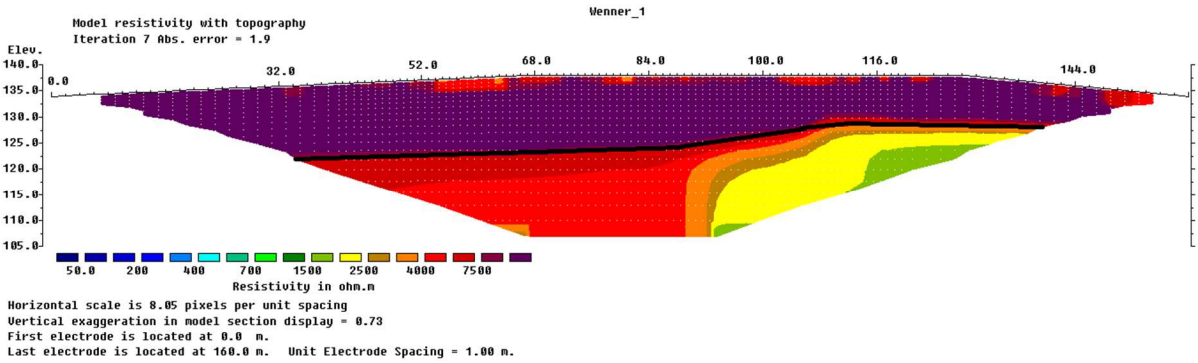

Figure 3.23: Inversion of profile 35.

Profile 35 summary

Profile 35 shows a smaller depth to bedrock than what is the case for profile 26, profile 27, profile 30 and profile 32. This was an unexpected result. The results match however the results for profile 36. The implication of this is a bedrock that has a ridge at this part. Then this ridge may be a barrier of water movement. Because of the 3D-effects, the accurate depth to bedrock is hard to estimate.

Profile 36

Profile 36 is situated east of profile 35, crossing profile 35 at about 115 m, as shown on figure 2.4 on page 25. It is 160 m long, and the minimum electrode spacing is 2 m. The general direction is from south-west to north-east. The profile was placed in the forest, but for the whole profile the soil was influenced by the glaciofluvial deposit, giving the surface a high resistivity value. The inversion of the profile is seen in figure 3.24 on page 80, and with a logarithmic scale in figure 4.8 on page 117 in the appendix.

The RMS is 6,2 %. At 26-36 m the depth to bedrock is increasing from 8 m to 9 m depth. At 36-68 m the depth to bedrock is increasing from 9 m to 10 m depth. At 68-100 m it is increasing from 10 m to 11 m. At 100-128 m it is increasing from 11 m to 13 m depth. As with profile 35, at the level where we have interpreted the bedrock to be, it is believed that the lower resistivity values is due to 3D-effects. This makes the interpretation of depth to bedrock more uncertain. As seen in 3.10, earlier research supports our interpretations of depth to bedrock.

Table 3.10: Depth to bedrock from earlier research near profile 36.

Author	Length	Deviation from line	Depth to bedrock	Method	Survey name
Klempe	26	20 NW	7	Drilling	Unpublished

The layer above the bedrock has a resistivity value of about 18 000-80 000 Ωm. This is believed to be dry glaciofluvial material, just as seen in profile 35. It seems that this layer consist of two different areas, each with the center of the area having the highest resistivity value. In the entire profile, above the layer of high resistivity, there is a small layer which has a lower resistivity value. This is believed to be saturated sand and/or gravel on which there is vegetation. At 24-48 m there is an ice kettle hole which makes the material more compact.

Cross-point profile 35 and profile 36.

At 98 m for profile 35, and at 107 m for profile 36, the two profiles intersect. At this point the depth to bedrock is the same for the two profiles, at 12 m. For both the profiles, the layer above bedrock has a resistivity value of 18 000-34 000 Ωm.

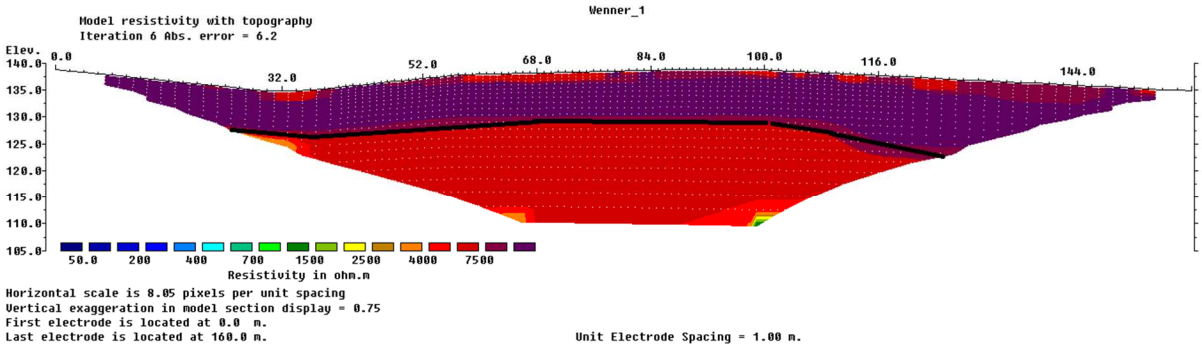

Figure 3.24: Inversion of profile 36.

Profile 36 summary

Profile 36 has similar values for depth to bedrock and layering as profile 35. This may give the results for profile 35 and profile 36 higher certainty. Both profiles show that the depth to bedrock is not so large, something that was not expected. The unexpected result for profile 35 may in fact seem to be correct, since both these profiles shows the same result.

Profile 37

Profile 37 is situated south of profile 35 and profile 36, as shown on figure 2.4 on page 25. It crosses profile 39 at about 320 m. It is 400 m long, and the minimum electrode spacing is 5 m. The general direction is from north-west to south-east. The profile was placed in the forest, but for most of the profile the soil was influenced by the glaciofluvial deposit, giving the surface a high resistivity value. The inversion of the profile is seen in figure 3.25 on page 81, and with a logarithmic scale in figure 4.9 on page 118 in the appendix.

RMS is 1,9 %. At 30-125 m the depth to bedrock is interpreted to be at about 12 m. At 125-145 m it increases to from 12 m to 24 m. At 145-225 m it increases from 24 m to 35 m. At 225-325 it decreases from 35 m to 25 m.

The layer above the bedrock from 20 m to 130 m has a resistivity value of 500-1500 Ωm, and it is interpreted to have a high content of water from 20 m to 60 m. This layer is interpreted to be saturated sand and gravel. The layer above the bedrock from 130 m to 180 m has a resistivity value of 40 000-60 000 Ωm. This is interpreted to be dry glaciofluvial material. At 180-230 m there is a layer with lower resistivity, 20 000-28 000 Ωm. This is interpreted to be dry glaciofluvial material. At 230-400 m there is a layer with resistivity value of 25000-100000 Ωm. This is believed to be the same glaciofluvial deposit, as found in profiles 35, 36 and 39. At 230-280 m this layer lies above the layer of dry glaciofluvial material.

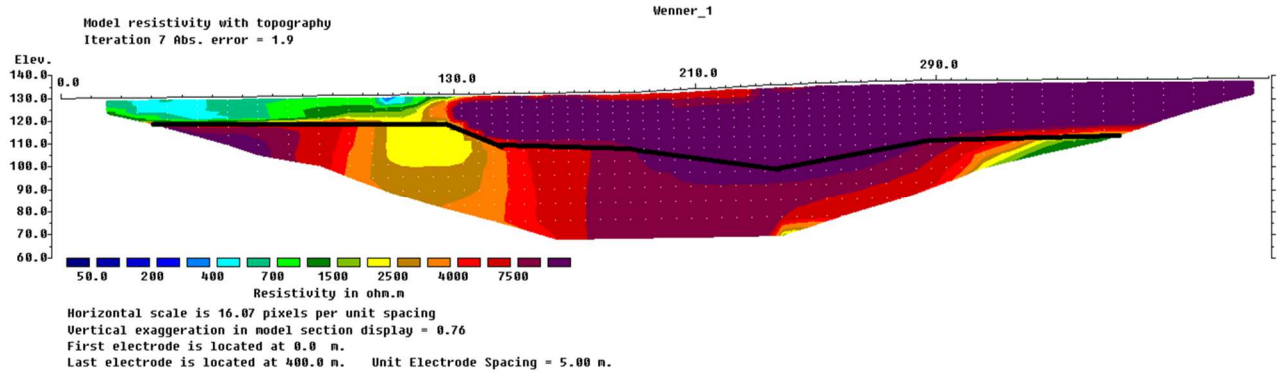

Figure 3.25: Inversion of profile 37.

Profile 37 summary

Profile 37 had some areas where the depth to bedrock was difficult to estimate. It may be that the depth to bedrock at 130-230 m is in fact located at a higher point. At the northern

part, the depth to bedrock and layering follow the same pattern as the profiles that are nearby, profile 35 and profile 36. So there seems to be a match here, even though these profiles are located about 100 m north of profile 37.

Profile 39

Profile 39 is situated south of profile 37, as shown on figure 2.4 on page 25. It crosses profile 37 at about 320 m. It also crosses profile 40 and profile 41, but these cross-points will be analyzed when profile 40 and 41 is examined. Profile 39 is 400 m long, and the minimum electrode spacing is 5 m. The general direction is from south-west to north-east. The profile was placed in the forest, but in great parts of the profile the soil was influenced by the glaciofluvial deposit, giving the surface a high resistivity value. The inversion of the profile is seen in figure 3.26 on page 83, and with a logarithmic scale in figure 4.10 on page 118 in the appendix.

RMS is 2,4 %. At 80-155 m the depth to bedrock is at 5 m. At 155-165 m, the depth to bedrock increases from 5 m to 15 m. At 165-255 m it is at 15 m depth. At 255-270 it increases from 15 m to 24 m depth. At 270-340 m it is stable at 24 m depth. This corresponds well with profile 37.

At 20-90 m, the layer above bedrock has a resistivity value of 200-1000 Ωm. This is interpreted to be saturated sand and perhaps some clay. At 110-140 m, the layer above bedrock has a resistivity value of 500-700 Ωm. This is interpreted to be saturated sand. At 160-230 m the layer above bedrock has a resistivity value of 7 000-12 000 Ωm, and this is interpreted to be dry glaciofluvial material. At 230-380 m the layer above bedrock has a resistivity value of 16 000-80 000 Ωm, and this is interpreted to be dry glaciofluvial material.

Cross-point.

At 313 m for profile 39, and at 250 m for profile 37, the two profiles intersect. At this point the depth to bedrock is not the same for the two profiles. For profile 37 the depth to bedrock is interpreted to be at about 30 m, whereas for profile 39 it is interpreted to be at about 24 m depth. This may be due to incorrect interpretations. Both profiles do however show a depth to bedrock of 24 m or more. The layer above bedrock is the same for the two profiles, with a resistivity value of 35 000- 80 000 Ωm.

This profile crosses profiles 37, 40 and 41, and the area from 230 m to 400 m consists of the same material as seen in profile 37. The cross point of profiles 37 and 39 matches well. The cross points with the other profiles will be discussed in the section of the relevant profile.

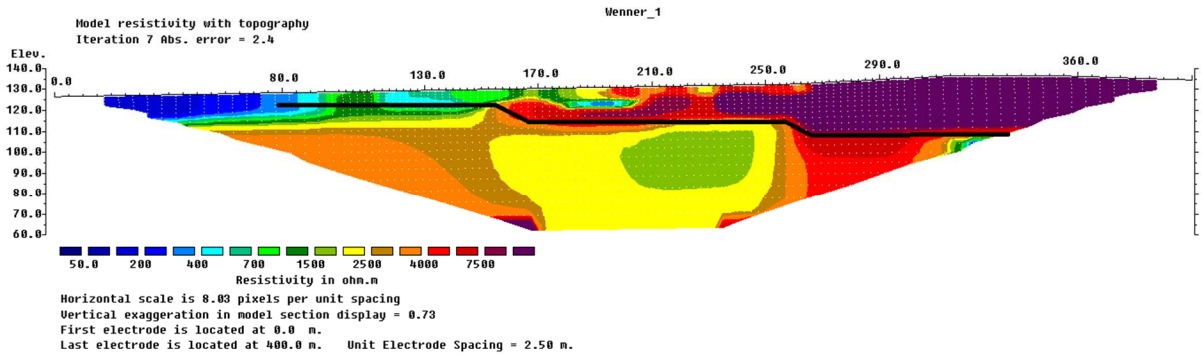

Figure 3.26: Inversion of profile 39.

Profile 39 summary

Profile 39 crosses three profiles. Only one of these cross-points is discussed here, the others will be discussed at the next profiles. However, it must be emphasized that at two of these cross-points, there is good correlation between the profiles, and at the cross point of profile 37 and 39 there is some correlation. This may give an indication that the interpretations are correct. The low resistivity below the upper layer at 290 m is also seen at profile 37. The low resistivity may be due to saturation, so that this is indicating that there is water in this area.

Profile 40

Profile 40 is situated approximately 230 m south of profile 37, as shown on figure 2.4 on page 25. It crosses profile 39 at about 120 m. This cross-point will be analyzed. Profile 40 is 160 m long, and the minimum electrode spacing is 2 m. The general direction is from north-west to south-east. The profile was placed in the forest. The inversion of the profile is seen in figure 3.27 on page 84, and with a small-value scale in figure 4.11 on page 119 in the appendix.

RMS is 2,9 %. At 32-120 m the depth to bedrock is steadily increasing from about 6 m to 13 m. Large parts of the profile consist of a layer with low resistivity, between 200-500 Ωm. This is interpreted to be fine sand that is saturated and clay. From 52 m to 116 m there are parts

at the surface which have a layer with higher resistivity, about 1000-1500 Ωm. This is interpreted to be dry sand and/or gravel. From 48-94 m and 100-148 m there are some layers with resistivity values 80-100 Ωm. This material has resistivity values that correspond with potential quick clay. The resistivity values depend on the different settings for the inversion, with the present values being the most conservative values. We also find such a layer in profile 12, which is the profile which continues directly from profile 40. We observed in the field that there was a great deal of water accumulation in this area. With two resistivity profiles indicating the same, with different inversion settings used, and with observations of water accumulation in this area, we conclude that this layer may very well be a layer of potential quick clay. There is also a low possibility that these values are too high because of high level of general saturation, since the level of precipitation was low at the time of measurement.

Cross-point

At 150 m for profile 40, and at 20 m for profile 39, the two profiles intersect. At profile 40, the depth to bedrock is 13 m. We cannot estimate the bedrock at this point in profile 39. The layer above bedrock has a resistivity value below 200 Ωm at this point in profile 40, while this layer has the same value 20 m north of this point in profile 39.

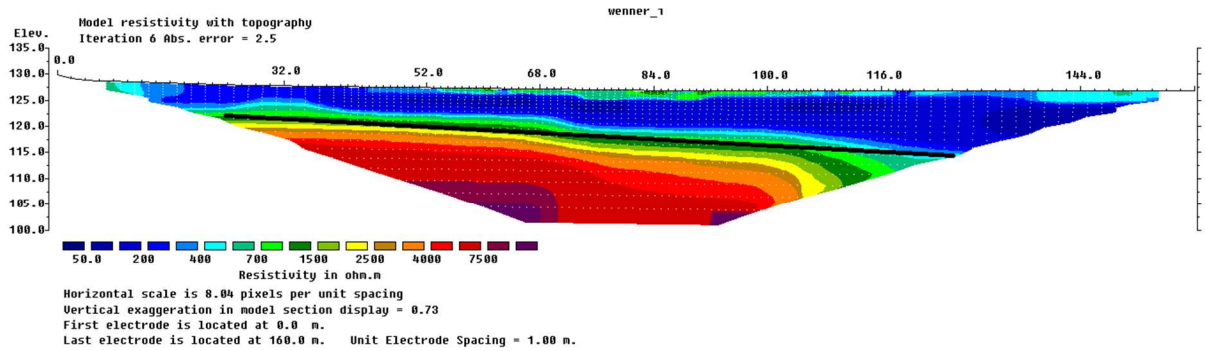

Figure 3.27: Inversion of profile 40.

Profile 40 summary

The depth to bedrock at profile 40 is somewhat difficult to estimate, and this is due to 3D-effects. It is interesting to see that the results of profile 40 match the results of profile 12, which is located east of this profile, as a continuation of profile 40. These two profiles were

placed in order to obtain this collective interpretation. The fact that these two profiles have the same result may increase the certainty of our interpretations.

Profile 41

Profile 41 is situated approximately 95 m north of profile 40, as shown on figure 2.4 on page 25. It crosses profile 39 at about 110 m. This cross-point will be analyzed. Profile 41 is 160 m long, and the minimum electrode spacing is 2 m. The general direction is from north-west to south-east. The profile was placed in the forest. The inversion of the profile is seen in figure 3.28 on page 85, and with a logarithmic scale in figure 4.12 on page 119 in the appendix.

RMS is 3,3 %. From 20 m to 96 m the depth to bedrock is very shallow, at about 3 m. At 96-98 m, it increases from 3 m to 5 m depth. From 98 m to 128 m the depth to bedrock increases sharply, from 5 m to 10 m. Our GPR results do not match this, and the cause for this may be that the two profiles do not overlap each other. From 20-105 m the layer near the surface have a resistivity between 2000-3000 Ωm. This is interpreted to be dry soil, sand and gravel. From 105-160 m there is a layer of low resistivity, from 130-290 Ωm. This is interpreted to be clay or fine sand which is saturated.

Cross-point

At 100 m for profile 41, and at 107 m for profile 39, the two profiles intersect. At this point the depth to bedrock for profile 41 is interpreted to be 5 m. At profile 39 the depth to bedrock is 5 m, so this is interpreted to be the depth to bedrock at this point. The layer above bedrock has the same resistivity value for both profiles, at 100-700 Ωm.

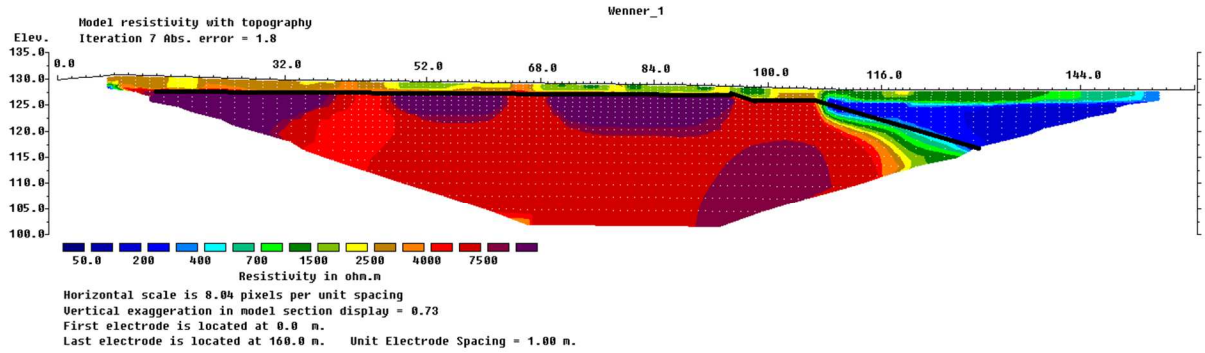

Figure 3.28: Inversion of profile 41.

Profile 41 summary

The depth to bedrock for this profile is hard to estimate accurately after 105 m. This is due to the 3D-effect, which may give an overestimation of depth to bedrock. However, this result matches the estimated depth to bedrock for profile 11, which is a continuation of profile 41. These two profiles were placed in order to obtain this effect, just as the case was with profile 40 and profile 12. Even though profile 40 and profile 41 are not situated far away from each other, they differ in terms of depth to bedrock and layering. Both profiles indicate that depth to bedrock decreases with distance from the farmland. When looking at profile 40, profile 41 and profiles 9-14, all this indicates that the depth to bedrock follows a weakly U-shaped form, and that this possibly is a weakness zone.

Profile 42

Profile 42 is situated south of profile 26, as shown on figure 2.4 on page 25. It crosses profile 33 at 90 m, and profile 26 at 15 m. This cross-point will be analyzed. Profile 42 is 96 m long, and the minimum electrode spacing is 2 m. There was a gravel road at both the northern and southern part of this area, which gave limitations concerning the length of the profile. We chose to exclude 8 electrodes in each end, in total 16 electrodes. The general direction is from north to south. The profile was placed in the forest. The inversion of the profile is seen in figure 3.29 on page 87, and with a logarithmic scale in figure 4.13 on page 120 in the appendix.

RMS is 2,8 %. Depth to bedrock is about 14 m throughout the whole profile. The layer above the bedrock has a resistivity value 2000-4000 Ωm, with the highest resistivity value in the center of this layer. This is interpreted to be clast-poor till, and the different values may be due to different levels of saturation. Above this layer, which continues to the surface, there is a layer with high resistivity of 16 000-60 000 Ωm. This layer is also present at profiles 26 and 33. This layer is believed to be dry glaciofluvial material, the same material which is mentioned for profiles 26 and 33.

Cross point profile 42 and 33.

At 47 m for profile 42, and at 68 m for profile 33, the two profiles intersect. At this point the depth to bedrock is the same for the two profiles. The upper layer has the same resistivity value for both profiles, at 22 000-80 000 Ωm. The depth of this layer is also the same for

both profiles, at about 7 m thick. The layer below has the same resistivity values of 3000-4000 Ωm. The layer is thicker in profile 42 than in profile 33. This may be due to 3D-effects.

Cross point profile 42 and 26

At about 16 m for profile 42, and at 216 m for profile 26, the two profiles intersect. At this point the resistivity value of the upper layer is the same for the two profiles, 22 000-80 000 Ωm. The depth of this layer is not the same, but this may be due to too few data points in profile 42, since this point is at the beginning of the data collection in profile 42.

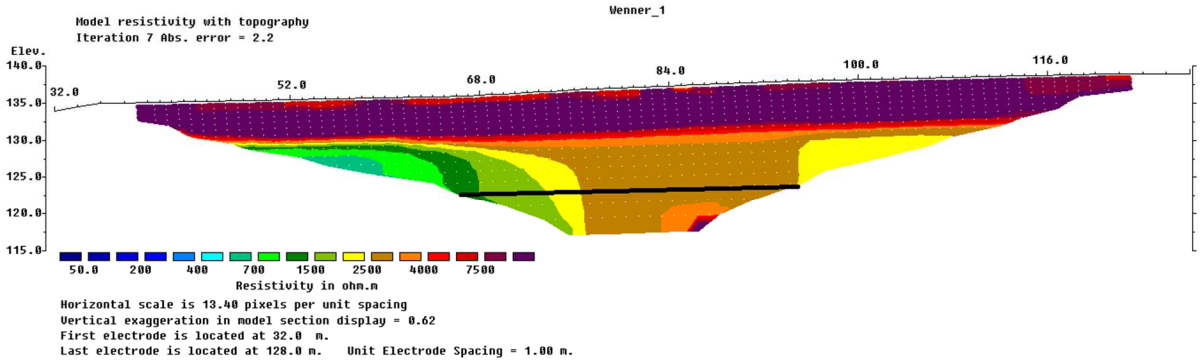

Figure 3.29: Inversion of profile 42.

Profile 42 summary

Profile 42 has the same results as profile 33 and profile 26 regarding layering and the same results concerning depth to bedrock as profile 33. The fact that all these three profiles have the same result may be an indication that our interpretations are correct. Profile 35 and profile 36 are placed south of these three profiles, and the results of these profiles show the same tendencies.

GPR measurements

GPR 02.

GPR profile 02 is situated at the same area as resistivity profile 26, as seen on figure 2.5 on page 29. The GPR profile 02 is 120 m long, whereas the resistivity profile 26 was 400 m long. GPR profile 02 starts at 200 m in resistivity profile 26. The direction of the GPR profile 02 is south-east north-west, so it is opposite of the direction of the resistivity profile 26. Hence,

GPR profile 02 stops at 80 m in resistivity profile 26. The antennas used were 2 m 50 MHz, and this was chosen in order to get a good penetration depth. From the resistivity profiles we knew that there were great depths here, so we used the large antennas in order to get a better estimation of depth to bedrock. We also wanted to compare the results from the GPR profile and resistivity profile from this area which were influenced by great depth to bedrock and a layering atop which was dry and compact. The result of the GPR measurement is seen in figure 3.30 on page 89.

The result shows GPR signals that are not so strong. This may be due to errors in the field work, or it may be due to the areas dry layering. The reflection of the signal is mostly at 300 ns, 350 ns and 450 ns. The material was dry sand, making the velocity of the signal at 0,15. The depth is then as seen in the table 3.11 below:

Table 3.11: Velocity and calculated depth of GPR profile 02.

Time	Velocity	Calculated depth
300	1,5	22,5
350	1,5	26,25
450	1,5	33,75

This is matches somewhat the resistivity result.

GPR 02 summary.

The signals from the GPR profile are somewhat weak. This may give an incorrect interpretation. The layer above bedrock is more detailed than what was detected with the resistivity measurement. The results from GPR profile 02 does correlate with the results from resistivity profile 26. The depth to bedrock is placed at the same level. With the GPR we can see that the bedrock is undulating, while this was not possible to detect with the resistivity measurement, due to the resolution. Even with a smaller electrode spacing, this would be difficult to detect. The GPR profile 02 does reflect the details in the layering. The resistivity profile shows fewer details in the layering, but gives perhaps a more intuitive result, and a result that perhaps gives a better overview.

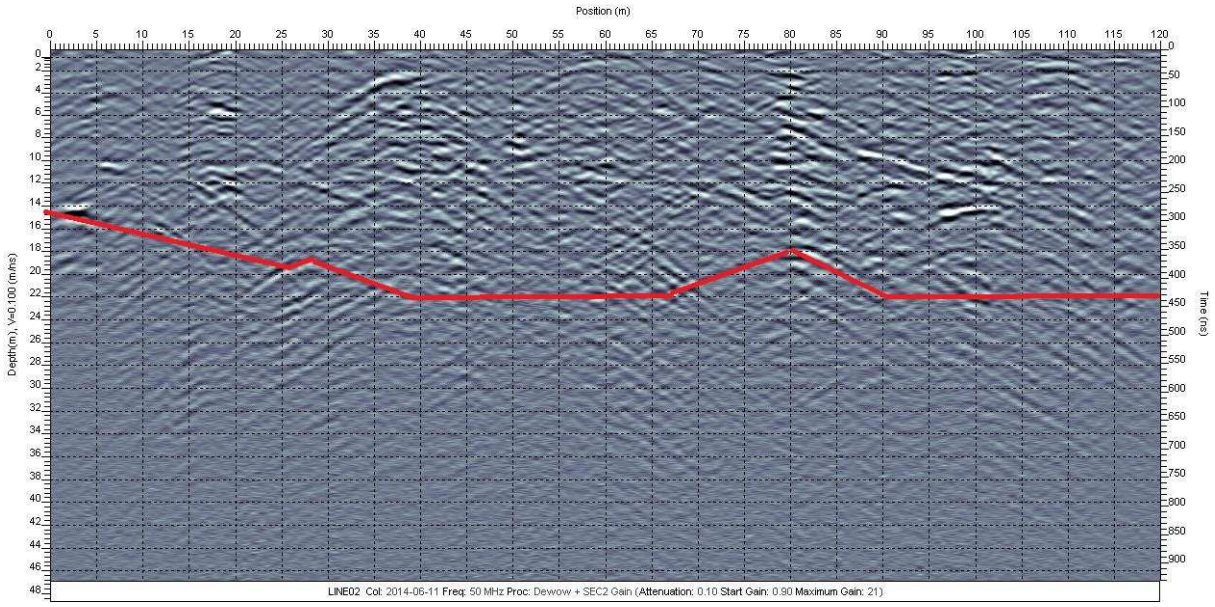

Figure 3.30: Result of GPR profile 02.

GPR 05.

GPR profile 05 is situated at the same area as resistivity profile 27, as seen on figure 2.5 on page 29. The GPR profile 05 is 100 m long, whereas the resistivity profile 27 was 400 m long. The direction of the GPR profile 05 is north-west to south-east, so it is the same direction as the resistivity profile 27. GPR profile 05 starts at 90 m in resistivity profile 27, and stops at 190 m in resistivity profile 27. The antennas used were 2 m 50 MHz, and this was chosen in order to get a good penetration depth. From the resistivity profiles we knew that there were great depths here, so we used the large antennas in order to get a better estimation of depth to bedrock. We also wanted to compare the results from the GPR profile and resistivity profile from this area which were influenced by great depth to bedrock and a layering atop which was saturated and consisted of sand, gravel and perhaps some clay. We also wanted to compare the results of the two instruments when crossing the water filled bog. The result of the GPR measurement is seen in figure 3.31 on page 90.

The profile does not give that great penetration depth. This may be due to errors in the field work, or it may be due to the conditions in the area.

The reflection of the signal is mostly at 200 ns, 300 ns and 500 ns. The material consisted of both dry sand and saturated sand, making the velocity of the signal changing. In each end of the profile, the signal velocity is 0,15. In the middle of the profile is situated the bog, making

the material saturated sand, and corresponding signal velocity at 0,06. The depth is then as seen in the table 3.12 below:

Table 3.12: Velocity and calculated depth of GPR profile 05.

Time	Material	Velocity	Calculated depth
200	Dry sand	0,15	15
300	Dry sand	0,15	22,5
500	Saturated sand	0,06	15

This matches the resistivity result somewhat.

GPR 05 summary.

The signals from the GPR profile do not give a great penetration depth. This makes the interpretation of depth to bedrock more uncertain. The layer above bedrock is more detailed than what was detected with the resistivity measurement. The results from GPR profile 05 does correlate with the results from resistivity profile 27. The depth to bedrock is placed at the same level. The GPR profile 02 does reflect the details in the layering, and the resistivity measurement does not show this in the same manner. The resistivity measurements show what is believed to be saturated sediments.

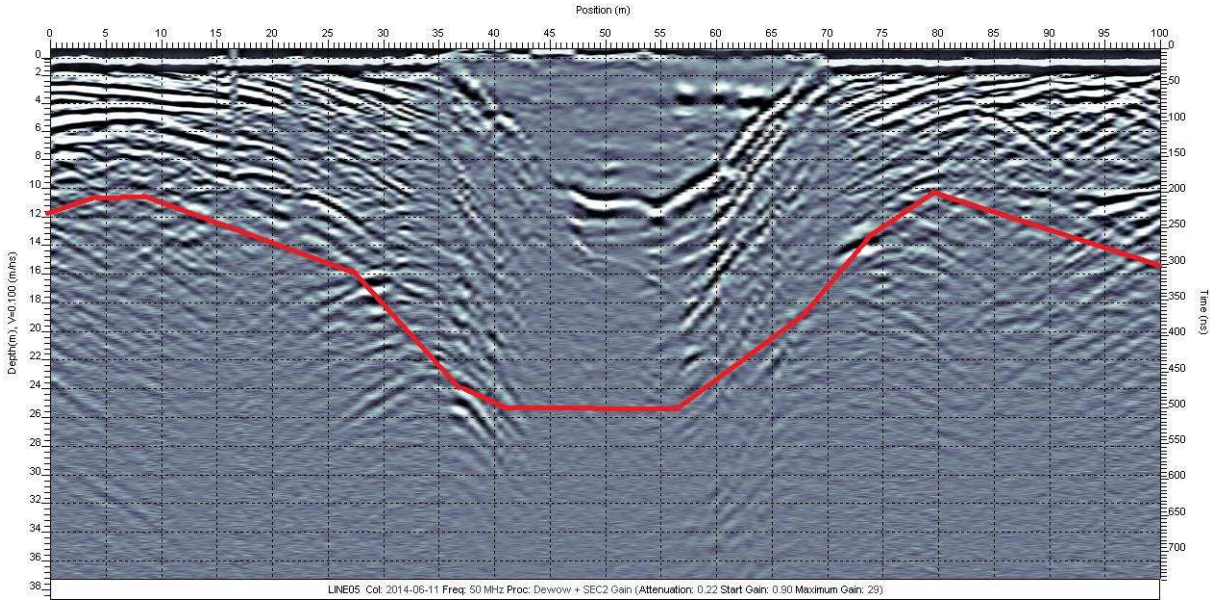

Figure 3.31: Result of GPR profile 05.

GPR 07.

GPR profile 07 is situated at the same area as resistivity profile 29, as seen on figure 2.5 on page 29. The GPR profile 07 is 55 m long, whereas the resistivity profile 29 was 120 m long. The direction of the GPR profile 07 is north-west to south-east, so it is the same direction as the resistivity profile 29 GPR profile 07 starts at 14 m in resistivity profile 29, and stops at 69 m in resistivity profile 29. The antennas used were 1 m 100 MHz. The result of the GPR measurement is seen in figure 3.32 on page 92.

The reflection of the signal is between 550 ns, 400 ns and 200 ns. The material was saturated sand, making the velocity of the signal at 0,06. The depth is then as seen in the table 3.13 below:

Table 3.13: Velocity and calculated depth of GPR profile 07.

Time	Material	Velocity	Calculated depth
550	Saturated sand	0,06	16,5
400	Saturated sand	0,06	12
200	Saturated sand	0,06	6

This is matches the resistivity result very well.

GPR 07 summary.

The strength of the GPR signals gives a good image of the subsurface conditions. This makes the interpretation of the layering more detailed than what was possible from the results of the resistivity measurements. The result from GPR 07 matches resistivity profile 29 very well. From the GPR result it is possible to get a good understanding of depth to bedrock, and it reveals that the interpretation of depth to bedrock from the resistivity measurement was correct.

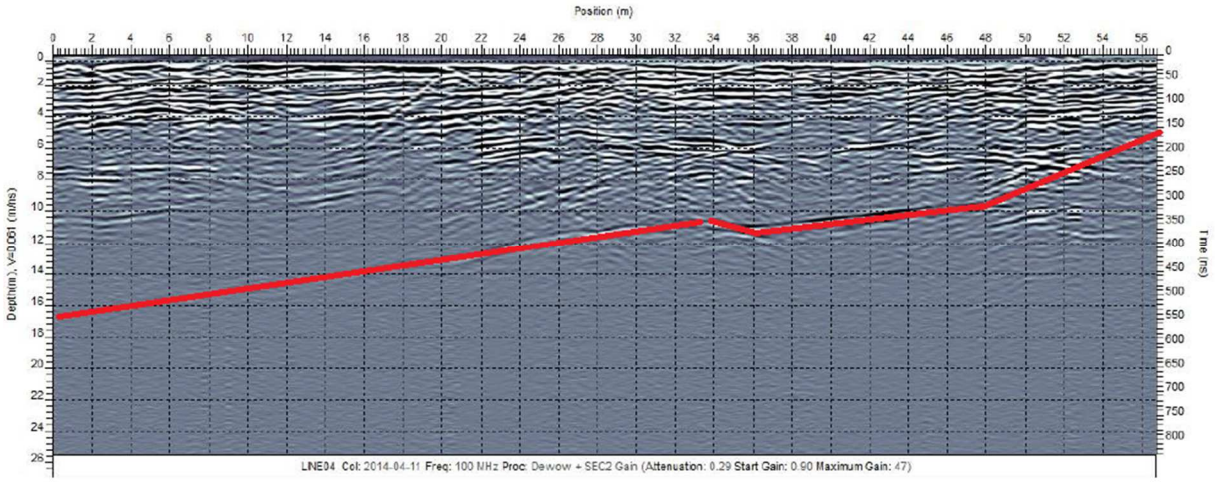

Figure 3.32: Result of GPR profile 07.

GPR 03 and 04.

The two GPR profiles 03 and 04 follow the resistivity profile 32, and the two GPR profiles are separated by only 20 m. We chose to have to profiles of about 100 m each, instead of having one long profile of 200 m. This choice was made in order to lower the possibility of errors in the field work, and thus possibly strengthen the data. GPR profile 03 is 100 m long. The direction of the GPR profile 03 is south-west to north-east, so it is the same direction as the resistivity profile 32. GPR profile 03 starts at 30 m in resistivity profile 32, and stops at 130 m in resistivity profile 32. The antennas used were 2 m 50 MHz, and this was chosen since the depth to bedrock was large, and since we wanted to get a good penetration depth. GPR profile 04 is 100 m long. The direction of the GPR profile 04 is south-west to north-east, so it is the same direction as the resistivity profile 32. GPR profile 04 starts at 170 m in resistivity profile 32, and stops at 270 m in resistivity profile 32. The antennas used were 2 m 50 MHz, and this was chosen since the depth to bedrock was large, and since we wanted to get a good penetration depth. The results of the GPR measurements are seen in figure 3.33 and figure 3.34 on page 94.

GPR profile 03 shows somewhat weak signals. The reflection of the signal is mostly at 400 ns. The material was dry sand, making the velocity of the signal at 0,15. The depth is then as seen in the table 3.14 below:

Table 3.14: Velocity and calculated depth of GPR profile 03.

Time	Material	Velocity	Calculated depth
400	Dry sand	0,15	30
400	Dry sand	0,15	30
400	Dry sand	0,15	30

This matches the resistivity result very well.

GPR profile 04 shows somewhat weak signals. The reflection of the signal is mostly at 400 ns and 500 ns. The material was dry sand, making the velocity of the signal at 0,15. The depth is then as seen in the table 3.15 below:

Table 3.15: Velocity and calculated depth of GPR profile 04.

Time	Material	Velocity	Calculated depth
400	Dry sand	0,15	30
400	Dry sand	0,15	30
500	Dry sand	0,15	37,5

The GPR profile is indicating a bedrock which is undulating. The resistivity result did not show this in the same manner. However, the GPR profile shows that the bedrock is undulating around 30 m, and this is the same depth as the resistivity result shows.

GPR 03 and 04 summary

The signals from the GPR profiles are at some points weak, and this may give an incorrect interpretation. The interpretation of the GPR profiles does match our resistivity results in many ways. The GPR profiles gives a more detailed image of the bedrock, than what the resistivity profiles does, since the resolution of the resistivity profiles was the lowest due to the large electrode spacing. The interpretation of the GPR profiles does also match earlier research.

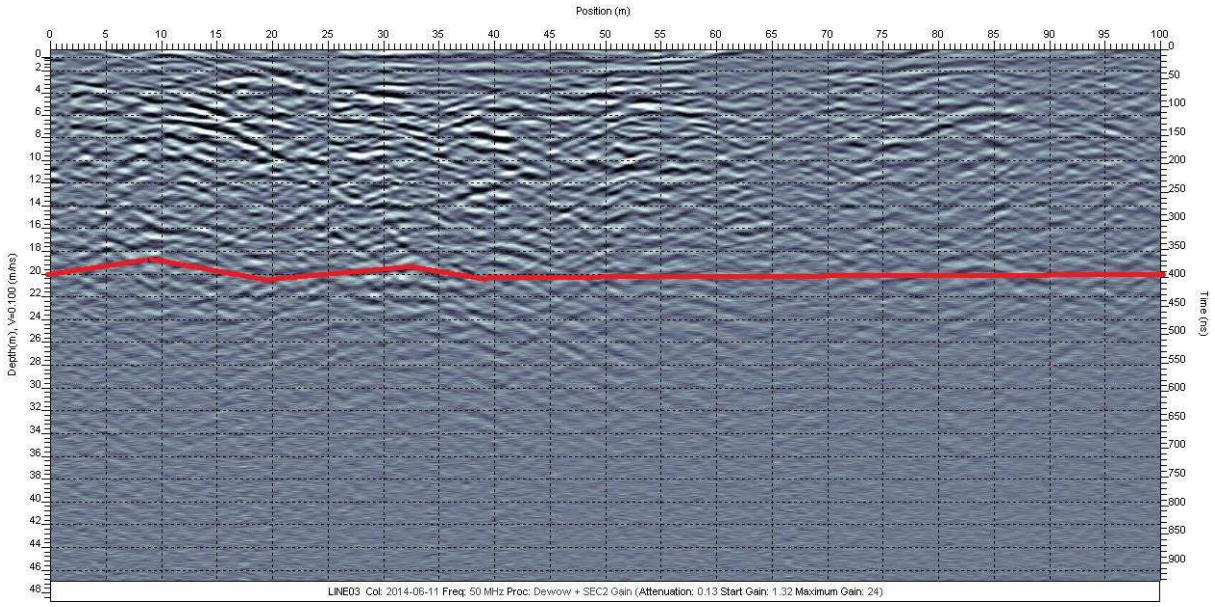

Figure 3.33: Result of GPR profile 03.

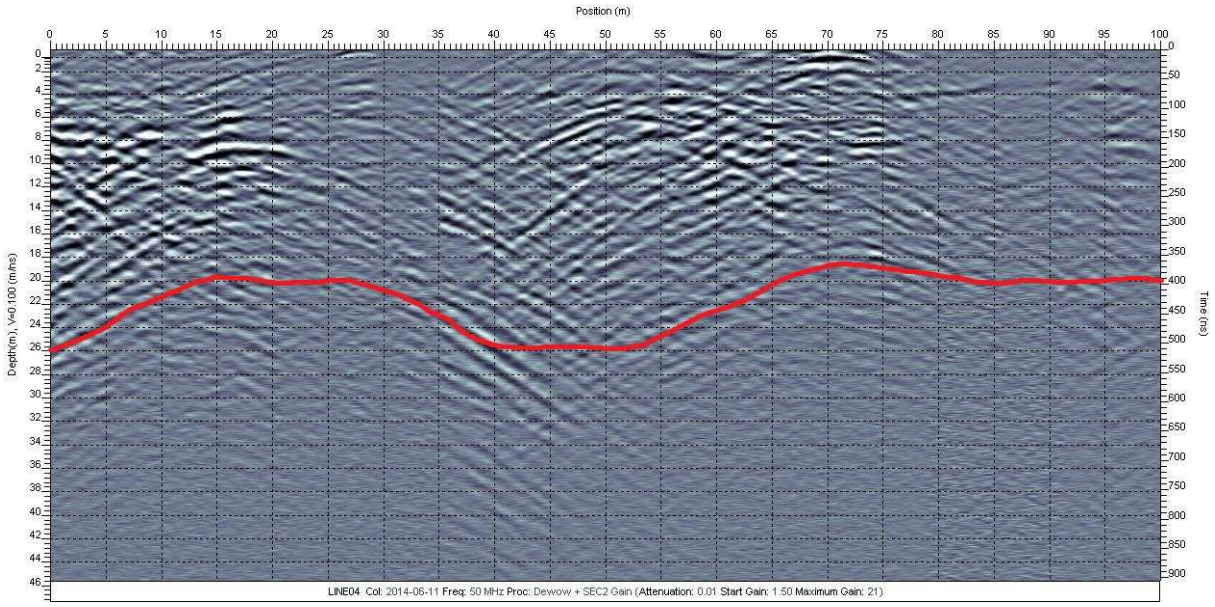

Figure 3.34: Result of GPR profile 04.

GPR 06.

As seen on figure 2.5 on page 29, GPR profile 06 is situated at the same area as resistivity profile 41, but not entirely at the same place, due to limitation in movement because of vegetation. The GPR profile 06 is 100 m long, whereas the resistivity profile 41 was 1260 m long. The direction of the GPR profile 07 is east to west, so it is the opposite direction of the resistivity profile 41. GPR profile 06 starts at 160 m in resistivity profile 41, and stops at 60 m in resistivity profile 41. The antennas used were 1 m 100 MHz, and this was chosen since the

depth to bedrock was not that large, and since we wanted to get a resolution of the layering. From the resistivity profiles we were unsure of the depth to bedrock for the first 40 m. We also wanted to compare the results from the GPR profile and resistivity profile from this area which were influenced by sediments such as clay and saturated sand at the surface. The result of the GPR measurement is seen in figure 3.35 on page 96.

The reflection of the signal is mostly at 250 ns. The material was clay, making the velocity of the signal at 0,06. The depth is then as seen in the table 3.16 below:

Table 3.16: Velocity and calculated depth of GPR profile 06.

Time	Material	Velocity	Calculated depth
250	Clay	0,06	7,5
250	Clay	0,06	7,5
250	Clay	0,06	7,5

From 0 m to 50 m the GPR shows a depth to bedrock at 4 m, whereas the resistivity indicates that the depth to bedrock is 15 m. This is due to the clay layer at the top, which effectively stops the GPR signals. From 50 m to 100 m the GPR shows a depth to bedrock at about 7,5 m, and this is more than the resistivity result indicated.

GPR 06 summary

Almost half of the GPR profile does not show the bedrock, due to the surface material. However, the resistivity profile does show the bedrock, so this clearly shows the different areas of use that is suitable for the two geophysical instruments. The GPR result of the last half of the profile does not match the result of the resistivity result entirely.

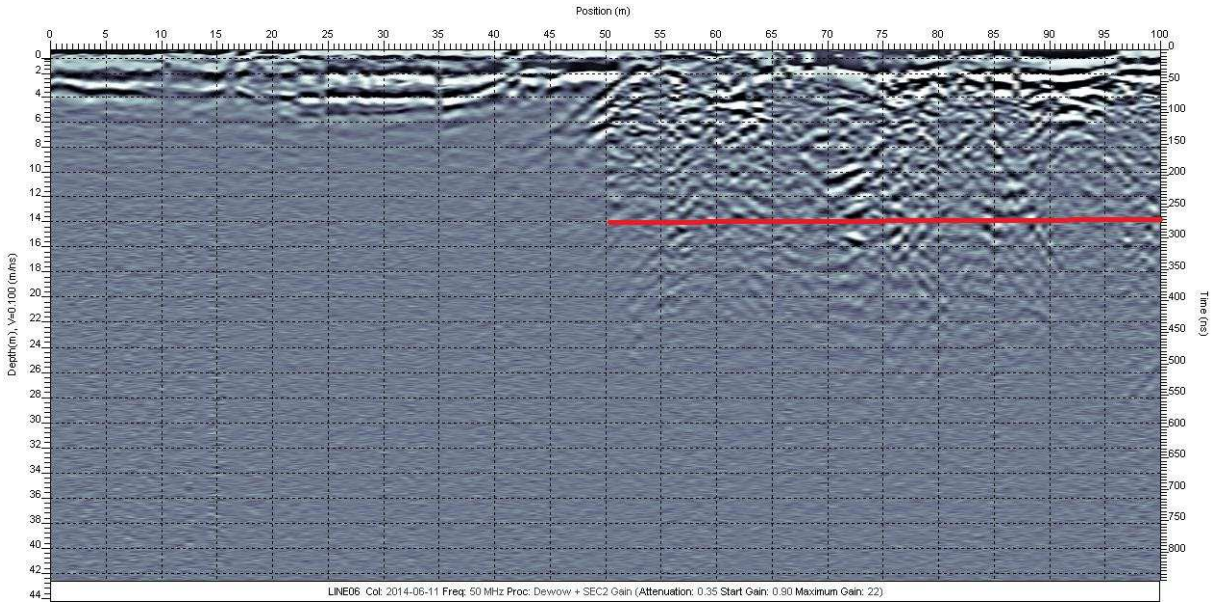

Figure 3.35: Result of GPR profile 06.

Summary and discussion of results

The results of this work were based on the study aims. The aims of study are shown in table 3.17:

Table 3.17: Overview of study aims.

Main study aim.	Partial study aim.
1) Subsurface mapping of Revdalen.	1-1) Using resistivity measurements to map the subsurface. Use other sources of information such as GPR and earlier data.
1) Subsurface mapping of Revdalen.	1-2) Creating a database from resistivity measurements readings and available data from TUC's geological and geophysical surveys.
2) Get experiences with the use of resistivity measurements by experimenting.	2-1) Get experiences with different subsurface conditions: resistivity profiles alone; combining TUC's two available geophysical instruments.

Below follows a summary of the results for each of these aims.

Study aim 1-1

With all the resistivity profiles and data from earlier research combined, the result of the study aim is seen in figure 3.36 below. A comment on the bedrock, sediments, general aspects and uncertainty of this summary of the results are followed below.

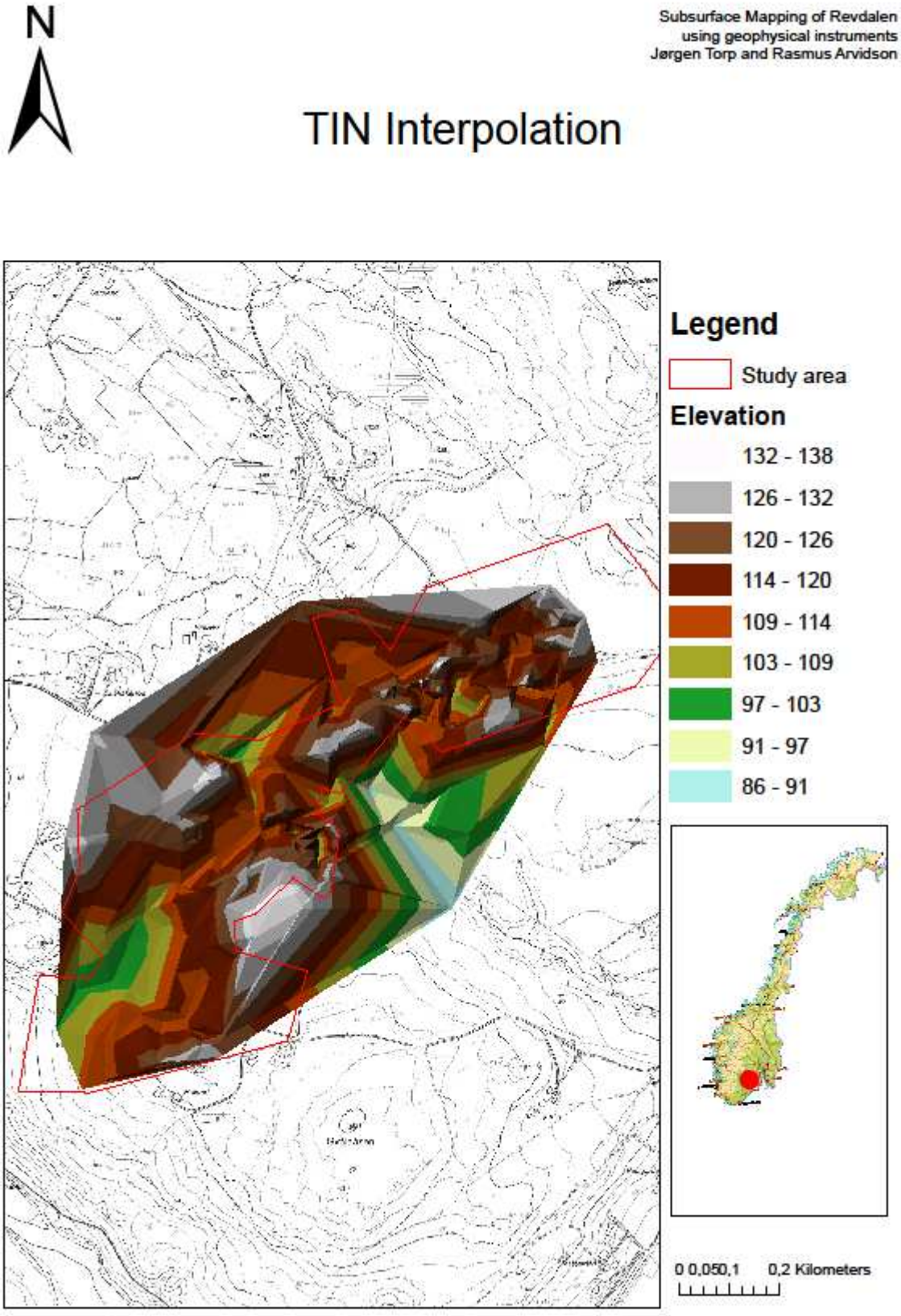

Figure 3.36: Interpolation of the data.

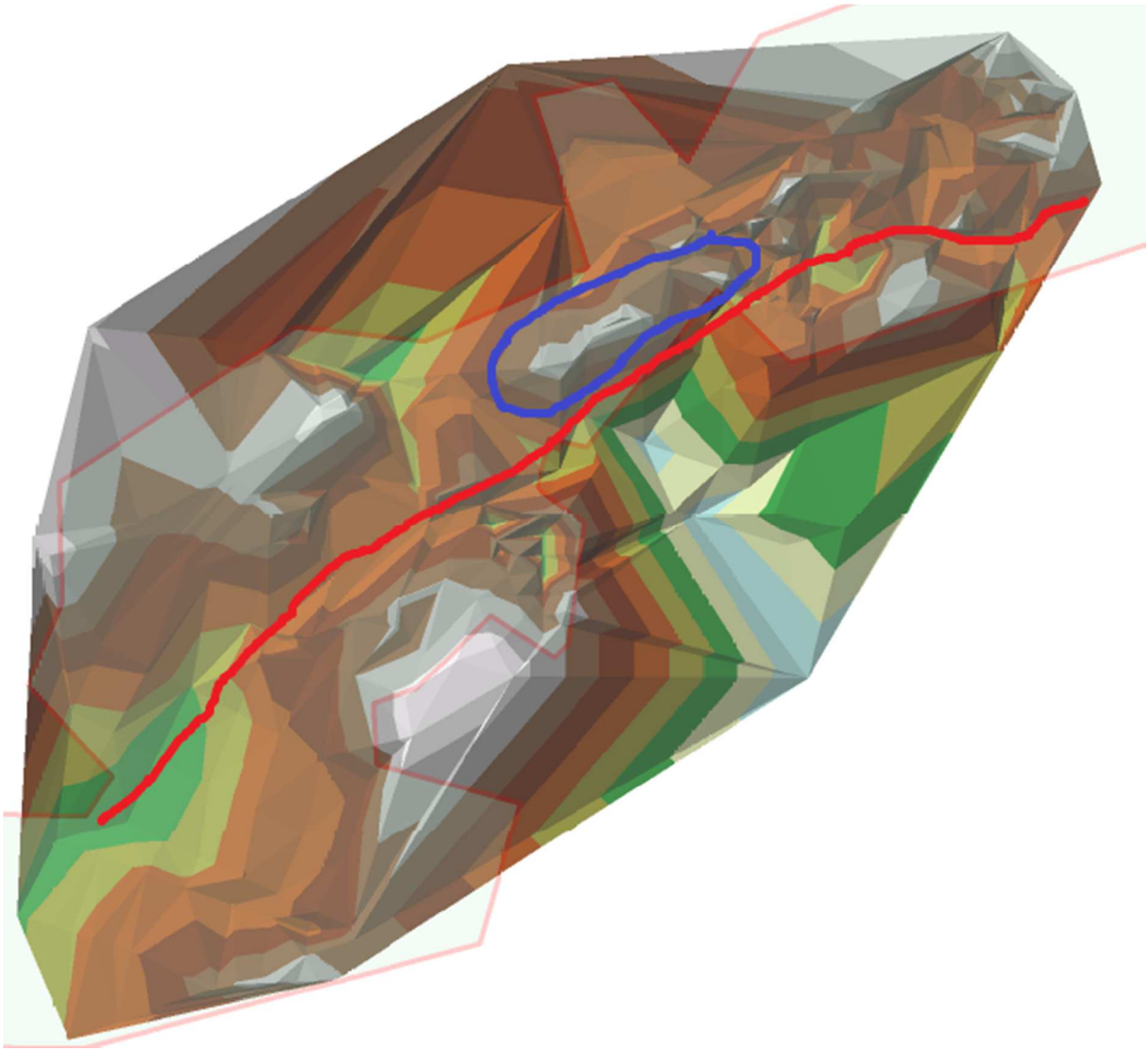

Figure 3.37: Indication of weakness zone (red line) and ridge (blue circle) in the copy of the interpolated map.

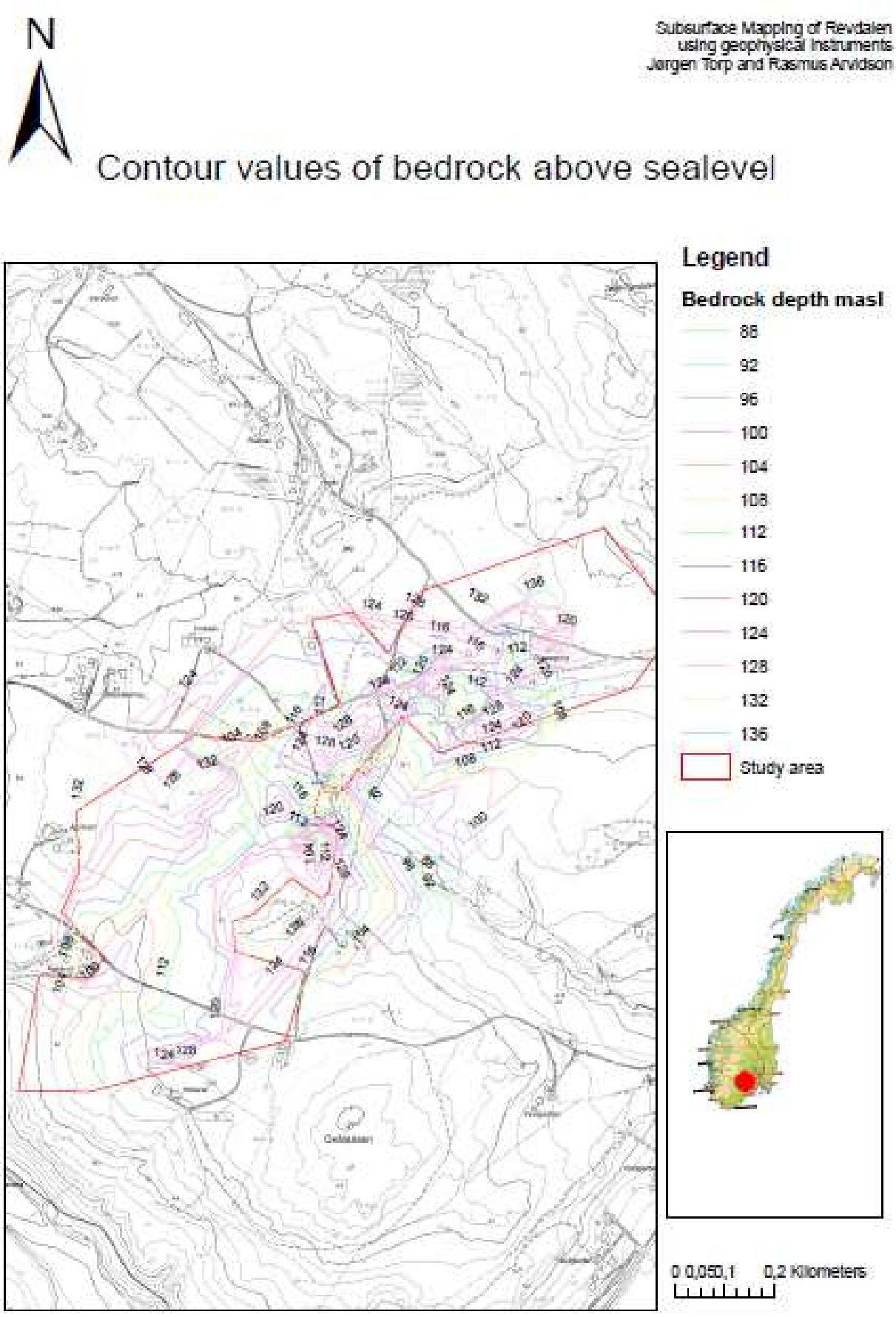

Figure 3.38: Contour lines of the interpolated data.

Bedrock

The bedrock in our area is complex, and in the southern part it is more complex than what has been estimated from earlier research. The general topography is downward sloping from north to south. The subsurface bedrock, naturally, follow this tendency, see figure 3.38 on page 100, but our results reveal what is believed to be both weakness-zones and a ridge below the surface, see figure 3.37 on page 99. The results also reflect earlier findings of a cleft below Djupegrop. All of these tendencies follow the general direction of the weakness-zones in the area (Jansen, 1982).

The weakness zone is interpreted to be fractured bedrock that is saturated. Since this weakness zone may be interpreted in many independent profiles, the certainty of the existence of this feature is strengthened. From what is seen in our results presented in GIS, figure 3.36 on page 98, this weakness zone may possibly be connected with the cleft at Djupegrop. The direction of the weakness zone in these two areas is the same, and they appear almost directly on line with each other. This weakness zone has evolved differently in the two areas, due to the later different geological influences. However, the result that there may be a long weakness zone in this area may strengthen the theory about the cleft below Djupegrop.

The existence of the interpreted bedrock ridge is not certain. It is based on only four resistivity profiles (profiles 35, 36, 37 and 39) and three drillings. However, the four resistivity profiles are two pairs of crossing profiles, and since the pairs match, there are no other ways to interpret the results. This ridge matches the resistivity results for both southern and northern parts. It has the same direction and the same geographical placement as southern and northern ridges. It seems that in the north and south of this ridge there has been glacial erosion, since this follows the glacier movement of the area, NW-SE.

The cleft at Djupegrop is not as detailed and visible as it is in the results from the drillings. Nevertheless it is still visible in the resistivity results. The cleft was found in the center of the resistivity inversion, and here the results are generally strong. The lowering in the bedrock at the cleft is not as steep as it is interpreted by drillings in earlier research, and this may be due to the resolution of the resistivity inversion and the following interpretation of what was visually observed on the resistivity profiles.

In the south-eastern part of our area, that is, in the western parts of resistivity profiles 13 and 14, there are some geological features that may give new information on water movement. In discussion with our student counselor, the relatively large depth to bedrock that is found here, may give new interpretations of ground water movement, and on the research on distribution of pollution from the Revdalen dump site.

Our findings deviate from earlier estimations of depth to bedrock in the southern part of our area, especially for the ridge, weakness-zone and P13-14. This area has not been subject to examination before, so earlier estimations relied on interpolation. In the northern area our results match well with earlier research. However, our results are much less detailed.

Sediments.

There is a great variety in the sediments in the study area, something earlier research reflects. In some area, our results add more information to what is already known about the sediments in the area, especially depth. In other areas, the limitations of the resistivity method make it difficult to add new information. In general, existing geological maps, such as Olsen and Jansen (1973), matches our results. However, in some profiles we found some new details.

We found moraine material just above the bedrock in the western parts of profiles 9, 10 and 11. This is somewhat indicated earlier (Olsen and Jansen, 1973). However, since the marine clay is found above the moraine material, it may add new information on the geological history at the area around these profiles.

At profile 41 there is found what may be potential quick clay. This is useful information regarding safety for movement at this area, especially for heavy duty machinery. This finding may also be useful in an academic aspect in the future, especially since the quick clay occurrence is so limited and somewhat isolated.

At profiles 30, 27 and 29 water was identified, and this is probably connected to the landfill at Djupegrop. Such contaminated water should have lower resistivity values than what was the case in our results. This deviation should be interesting to examine further in the future.

In several of the northern resistivity profiles, the surface material was very dry. This may possibly be one of the reasons for the extremely high resistivity values for much of the

subsurface material. This may in turn have given less detailed results of the resistivity measurements. Earlier research (Klempe, 2001) has indicated that the subsurface material below profiles 26, 27, 30, 32 and 34 should be more diverse than what our results reflect. The low detailing of our results may be the cause for this.

The southern profiles (6-20) shows a much more detailed, and visually better understanding of the sedimentology in the study area, than the northern profiles. Although exact layering, was somewhat difficult to measure precisely, due to resistivity profiles being estimated by examining them visually, there was some distinct trends that occurred throughout profiles 6-20.

For most of the profiles, a layer of saturated sand/clay was observed above a layer of unsaturated sand/gravel, with varying depths observed. Underneath these layers, the bedrock could be estimated precisely throughout the profile, for most of the profiles with some exceptions in profiles 6, 7, 18 and 19. In these profiles the bedrock was either not visible as a whole, or had some confusing parts that made estimation of depth to bedrock hard.

Moraine material was observed in profiles 6, 7, 8 and 9 in the north-western parts of these profiles. This shows a good correspondence with the moraine material observed in profiles 37 and 39.

In general the southern profiles offered an easier visual understanding of the subsurface sedimentology and bedrock presence.

In general

The results observed in these inversions are generated from 33 resistivity profiles totaling in 7798 m and 10973 resistivity data points. The maps in GIS are created from 239 digitalized points from resistivity and GPR interpretations, in addition to 129 points from earlier research. This is a lot of data material gathered into one result, and this possibly improves the certainty of the result. Something that may weaken the result is the fact that external data have been used both to interpret the resistivity inversions, and to generate the interpolation in GIS. In this way, the external data are given a much higher emphasis to the result in GIS than our own resistivity measurements. However, since the external data are

either drillings or geophysical data gathered by projects at TUC, the data should be emphasized due to their high degree of certainty.

This project has used different sources of data: the two geophysical methods of resistivity measurements and GPR, and the geological method of drilling. When combining all of these, the result is both an accurate understanding and good overview of the subsurface material and bedrock position below the surface. The weakness of each method is another method's strength. In this way, more data sources give higher certainty. The experiences of combining different methods are discussed in detail in sections below. These methods have on the other hand weaknesses when used alone. As for the resistivity method, it is clear that the resolution of the result does not permit accurate data like drilling or GPR.

Weaknesses

As mentioned in the theory chapter, there are many factors that influence the resistivity results and the accompanied interpretation. The relevant factors that may increase the uncertainty for our results have been many. The 3d-effect is present for most of the profiles. This makes the estimated depth of the layers or depth to bedrock much less certain. As mentioned earlier, the external data have been given a relatively high emphasis comparing to the resistivity results, and the 3d-effect present in the resistivity measurements is one of the reason for this. It must also be mentioned that drilling data is much more precise than subjective estimation of resistivity profiles images.

All sediments have a large range of resistivity values, and the values are affected by factors such as different levels of saturation, weathering and dissolved ions in the water. The interpretation of the results has therefore been greatly based on already existing information about the subsurface. Unfortunately, many of the profiles have high surface resistivity, which may have increased the uncertainty, due to the 3D-effect. For the southern profiles, there was a lower surface resistivity, but these profiles were still hard to estimate due to the above mentioned factors.

The type of inversion affects the result of the resistivity measurements. We used only one configuration for type of inversion, and we did this in order to be consistent in the data treatment. Such an approach may in general lead to loss of information due to imperfect type of inversion suited for some areas. However, since all of the profiles was suited for the

type of inversion chosen, we believe that the uncertainty of the inversion of our profiles have not been increased by an unsuitable inversion type.

The resolution of the inversion affects the interpretation. A positive feature of our resistivity results is that many of the profiles' focus area are in the middle and above in the inversion, which are the areas where the inversion give the highest certainty. This was no coincidence, since we had good estimations of depth to bedrock at each profiles, making it possible for us to choose suitable electrode spacing. Many of the resistivity profiles used relatively large electrode spacing. This increases the chances of small layers not being present in the inversion due to the low resolution caused by large electrode spacing.

Something that increases the certainty of the resistivity measurements is the fact that the interpretations are connected to drill data. In addition to this, few of the resistivity profiles have been interpreted alone. In contrary, most of the resistivity profiles have been interpreted simultaneously with nearby resistivity profiles. This may possibly increase the certainty of each resistivity profile interpretation. So several resistivity profiles interpreted simultaneously makes the whole greater than the sum of the parts. The more resistivity measurements, the easier it may be to interpret more correctly.

Another factor which may affect the certainty of the results is the uncertainty in GIS. The results have been point digitalized, which creates a chance of misplacement of the data. The flat 2d representation in GIS, where much of the data have been treated, is not completely equal to the actual 3d world in which we live. At small distances, this rarely have any relevant effect. But since our research area is quite large, and since many of our profiles are 400 m long, there is a possibility that there are some small errors in the data representation.

Study aim 1-2

Our experiences with creating a database from resistivity measurement readings are many. The negative side of this work is that it is time consuming. One should have a good reason to use so much time for this work. However, there are many positive effects of having such a database. Firstly, it is very useful to have the subsurface mapping in a GIS-database, since this is a good base for future hydrogeological research. The GIS tool computes enormous

amounts of data in a few seconds, which is a good advantage when dealing with geological or hydrogeological work in such a large area. Secondly, a GIS database makes it easier to include data with high amount of certainty, for instance a drilling. Thirdly, when there are many resistivity profiles in the area, it becomes increasingly difficult to have the overview of the geological data. With the GIS database, it is much easier to maintain this overview.

Another positive effect of having a GIS database, with profiles that crosses each other, we control the data plotting ourselves. It is therefore easier to match the two crossing profiles, since we now can interpret the results simultaneously. A very simplified example would be: We know that the depth to bedrock in a very small area is relatively homogeneous. If profile A has a strong 3d-effect and profile B and C does not, we can ignore this factor for profile A, emphasizing the depth to bedrock to profiles B and C. To remove such noise in the data when having much data to handle has been useful.

Study aim 2-1

Seen in table 3.18 is an overview of the different subsurface conditions we have examined:

Table 3.18: Overview of different subsurface conditions.

Label	resistivity profiles	GPR profiles	Surface and subsurface conditions
A	P6-P9	-	Area with clay at the surface, and till above bedrock.
B	P10-P19	(First part of Line 06)	Area with clay at the surface, and clay above bedrock.
C	P29	Line 01	Survey of an aquifer.
D	P27-P34	Line 03+04, Line 05	Area with delta deposit material, and/or land fill (leachate plume) and terrace.
E	P40-P41	Line 06	Area with forest soil at the surface.

Our experiences with surveys at the five different surface and subsurface conditions are as follows:

A: Area with clay at the surface, and till above bedrock.

Experiences from areas with clay at the surface are many. Profiles 6-9 were profiles where such surface and subsurface conditions were present. Since the electrodes get good conductivity in the clay at the surface, the flow of the current is better. Hence, the resistivity results are often better and much more detailed. However, the transition from low resistivity areas, the clay, to high resistivity areas, the till, may be harder to identify, just as Solberg et al. (2011) has experienced. It is hard to avoid an overestimation of depth to bedrock in such cases, especially without other geological information. However, our experience was that, as mentioned earlier, when there are many resistivity measurements in one area instead of a

single one, there may be easier to get a plausible geological interpretation. With many resistivity measurements there is more data to analyze, and often was the case that we could be more certain of the depth to bedrock, since the 3d-effect was not the same for many profiles.

The 3d-effect was smaller if there was clay above bedrock instead of till above bedrock. If the till did not have unusual high resistivity values, then the current was less reluctant to choose another path than into the till. This was not the case when the clay was above bedrock.

Since we were not able to do GPR surveys at the farmland when this was in use, we did not do any surveys at these surface and subsurface conditions.

B: Area with clay at the surface, and clay above bedrock.

As with label A, clay at the surface gives good conductivity for the electrodes. Profiles 10-19 were examples of such surface and subsurface conditions. However, as mentioned above, when there was clay above the bedrock, there were much higher chances of strong 3d-effects. This is due to the nature of the current flow, which, as mentioned in the method chapter, chooses the path of least resistance, making the current somewhat reluctant to penetrate the bedrock below the clay. In such surface and subsurface conditions, our experience was that the chances of an overestimation of depth to bedrock increased.

Since we were not able to do GPR surveys at the farmland when this was in use, we did not do any surveys at these surface and subsurface conditions. However, the placement of Line 06 did include about 50 meters of survey where the surface contained of grass above clay and clay above bedrock. Here, the GPR did not manage to penetrate the surface, while the resistivity measurement got good results. This demonstrated how effective it may be to combine the use of the two geophysical instruments that are available at TUC: the weaknesses of the GPR are the strengths of the resistivity measurement, and vice versa.

C: Survey of an aquifer.

These surface and subsurface conditions were met at profile 29. The resistivity result gave a very good image of the aquifer, and this greatly enhanced the understanding of the aquifer. This was particularly due to the possible identification of saturated areas, which was easily

detected in this area from the resistivity measurement. In some parts of the profile, there was gravel at the surface. Even though the electrodes were put directly in this layer, which normally gives high surface resistivity, the results were good. This was probably due to a high amount of saturation of the sediment at the surface. This is a condition which is not always met at an aquifer, so our experiences from this profile may be connected to this fact.

The GPR results at this profile were also very good. The penetration was not blocked by a layer of clay at the surface, and the image of the subsurface conditions was very detailed. The GPR result gave a much more detailed result concerning both layering and depth to bedrock than what the resistivity result did. The resistivity result gave a much better image of all the qualities of the aquifer than what the GPR result did. This profile was therefore a good example of how the use of these two methods together can give a really good understanding of the geological and hydrogeological attributes of an area.

D: Area with delta deposit material, and/or landfill (leachate plume) and terrace.
Areas with delta deposit were found at profile 26, 32-37 and 39. Areas with delta deposit material and land fill were found at profiles 27 and 30. Profiles 27 and 30 show that resistivity measurements are well suited for hydrogeological surveys. It was easy to detect areas with high level of saturation. However, concerning the results, the resistivity values did not stand out in the manner that we anticipated. The resistivity results did not exclusively show possible pollution. This may be due to too low pollution, too much water that makes this site contain lower amount of pollution (confer Klempe 1992), or errors in the field work.

Profiles 26, 32-37 and 39 however, show that identification of different mediums in very dry areas is difficult when using the resistivity method, especially when the surface conditions are dry. Our experiences were that the detailing of the resistivity result often was not adequate for a good geological understanding of the subsurface. In such areas we had great success with complementing the resistivity measurement with GPR measurements. The GPR result was in our cases more detailed than the resistivity measurement, both for estimating depth to bedrock and the subsurface layering.

Another experience from these profiles was that the nature of resistivity measurements is in a way that they lack information in each end, since the image of the subsurface is not rectangular, but has the shape of an inverted trapezoid. Our experience was that it may be

difficult to get this information, since the area had limitations in movement, topography, surface conditions suitable for resistivity measurements, and other factors. GPR may give additional information in such cases.

E: Area with forest at the surface.
This surface condition was met in profile 40 and 41. This was an ideal situation for resistivity measurements. The electrode connectivity was good, and therefore the image of the resistivity result was detailed.

In conclusion of the study aims, resistivity measurements are well suited for an overall description of the subsurface, especially when the subsurface sediments are known. Because of the overlapping range of the sediments, the interpretation may include high level of uncertainty if the subsurface sediments are unknown. When this is known, however, the overall description has a much higher degree of certainty.

Combining the use of the two geophysical instruments GPR and resistivity measurements was found to be useful in several cases.

Conclusion

The subsurface of Revdalen with main focus on depth to bedrock has been mapped with geophysical instruments, and earlier data from both geophysical instruments and drillings has been used. The depth to bedrock has been estimated for each resistivity profile. There is some uncertainty in the results, and this is connected to typical issues with the geophysical instruments used. However, the result of the mapping gives a good overview of the depth to bedrock of the area.

The results of the subsurface mapping have been used to create a database in GIS. Being able to have a multitude of data gathered in a 2D-visualization in GIS – and even in 3D –, makes it possible to comprehend the bedrock placement in the area as a whole – something which is difficult without this visualization. The GIS modelling and the making of the database has been a rewarding work, and it may be used in future research of the subsurface conditions and hydrogeological conditions in Revdalen.

Our study also had a focus on gaining experience in the use of the two geophysical instruments to Telemark University College. The experiences have in details been explained in the study. These experiences may be helpful for future studies and surveys made by students and personnel that can access this study and the raw data that has been gathered in this work. We hope that many students will learn to use these geophysical instruments in the future, and that they can use this study in the learning process.

Reference list

Anderson, M. P. & William, W. W (2002). *Applied groundwater modeling. Simulation of Flow and Advective Transport.* Toronto, Academic press.

Annan, A. P. (2003). *Ground Penetrating Radar Principles, Procedures & Applications.* Ontario, Sensors & Software Inc.

Bergstrøm, B. (1999). *Glacial geology, deglaciation chronology and sea-level changes in the southern Telemark and Vetfold counties, southeastern Norway.* Trondheim, Norges Geologiske Undersøkelse (NGU).

Burrough, P. A. & McDonnell R. A. (1998) Principles of Geographical Information Systems. Hertford College, Oxford

Jansen, I. J. (1979). *Kvartærgeologisk kart og kart over fjelloverflate og grunnvannsoverflate med boring, seismikk m.m.* Bø, Fylkeskartkontoret i Telemark and Telemark distriktshøgskole.

Jansen, I. J. (1982). *Lifjellområdet - Kvartærgeologisk og geomorfologisk oversikt.* Rapport, Oslo, Kontaktutvalget for vassdragsreguleringer, Universitetet i Oslo.

Jansen, I. J. (1983). *Detaljkartlegging av sand- og grusressurser i Bø kommune, Telemark.* Arbeidsrapport nr. 11. Bø, Telemark distriktshøgskole.

Jansen, I. J. (1986). *Kvartærgeologi - jord og landskap i Telemark gjennom 11000 år*. Bø, Institut for naturanalyse.

Jeppsson, H. (2012). *Geoelektriska metoder inom till-lämpad geofysik. Educational compendium GEO C04.* Lund, Geologiska institutionen, Lunds universitet. Not published material.

Klempe, H. (1988). *Eika grunnvannsmagasin. Sedimentology, hydrogeology og praktisk anvendelse.* Dr. scientavhandling, Norges landbrukshøgskole.

Klempe, H. (2001). *Årsrapport 1999, Overvåking av grunnvannsforurensning fra Revdalen kommunale avfallsfylling, Bø i Telemark*. Porsgrunn, Høgskolen i Telemark.

Koziel, J., Lauritsen, T., Mauring, E., Rønning, J. S. & Tønnesen, J. F. (1995). *Målinger med georadar. Teori, anvendelse, teknikker og eksempler på opptak.* Rapport 94.024. Trondheim, Norges geologiske undersøkelse (NGU).

Loke, M.H. (2004). *Tutorial – 2-D and 3-D electrical imaging surveys. Electrical imaging surveys for environmental and engineering studies.* Revisioned. Malaysia, Geotomo Software Inc. www.geoelectrical.com/coursenotes.zip (Accessed: 13.4.2015).

Olsen, K. S. & Jansen, I. J. (1973) Kvartærgeologien i Bø : en kartlegging og beskrivelse av kvartærgeologien i de sentrale deler av Bø kommune, Telemark distriktshøgskole

Palacky, G. J. (1987). *Resistivity characteristics of geological targets.* Tulsa, Society of Exploration Geophysicists.

Sandtak, Hellestad (2015). http://www.helle-h.no/om_oss.html. (Accessed: 13.4.2015).

Solberg, I-L., Hansen, L., Rønning, J.S., and Dalsegg, E. (2010). *Veileder for bruk av resistivitetsmålinger i potensielle kvikkleireområder*. Versjon 1.0. Rapport 2010.048. Trondheim, NGU.

Trømborg, D. (2006). *Geologi og landformer i Norge.* Grønland, Landbruksforlaget.

Wightman, W. E., Jalinoos, F., Sirles, P., and Hanna, K. (2003). *Application of Geophysical Methods to Highway Related Problems.* Publication No. FHWA-IF-04-021. Colorado, Federal Highway Administration, Central Federal Lands Highway Division.

Appendix

Inversions of resistivity profiles with other resistivity value scale:

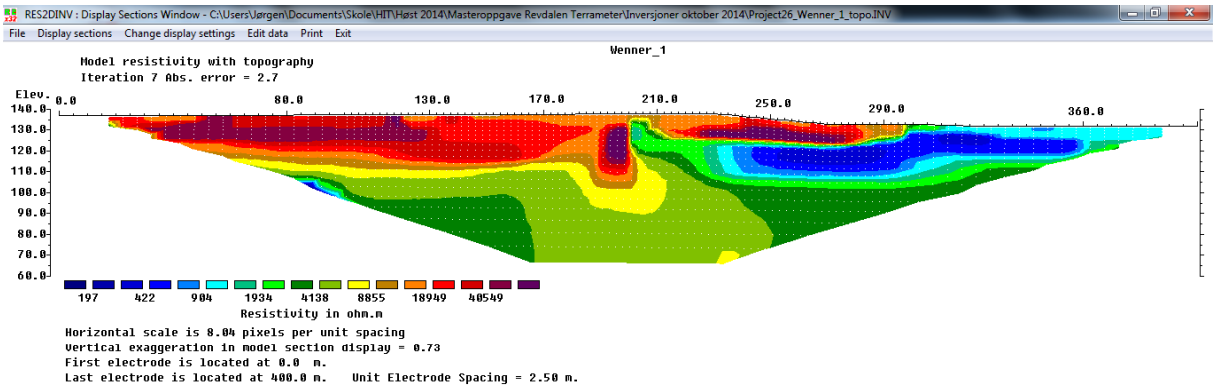

Figure 4.1: Inversion of profile 26 with a logarithmic scale of the resistivity value.

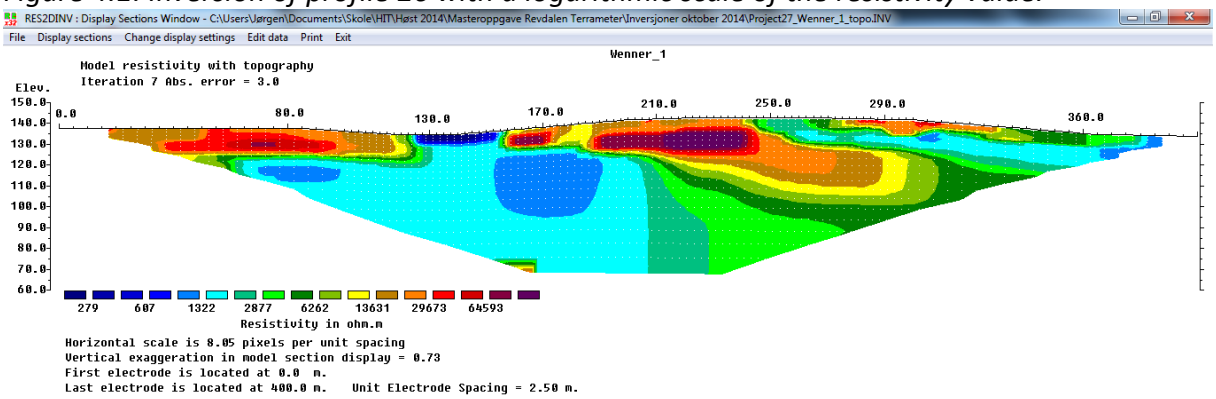

Figure 4.2: Inversion of profile 27 with a logarithmic scale of the resistivity value.

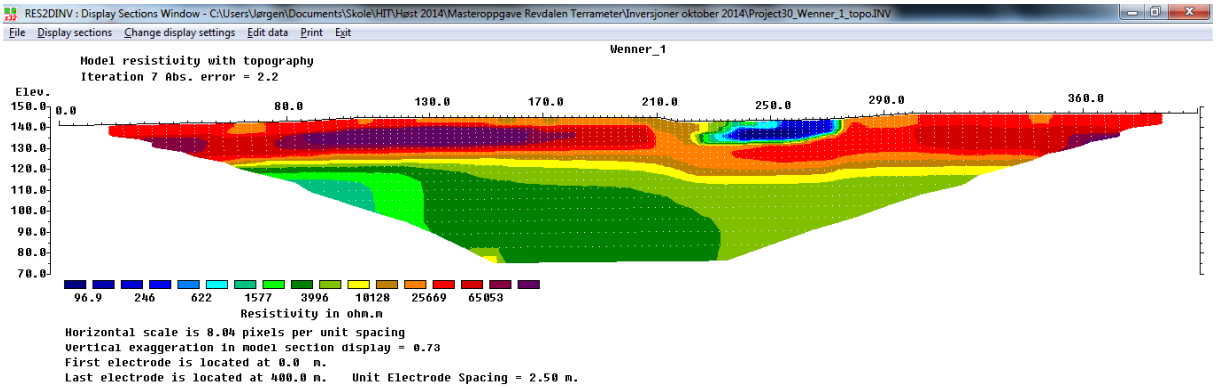

Figure 4.3: Inversion of profile 30 with a logarithmic scale of the resistivity value.

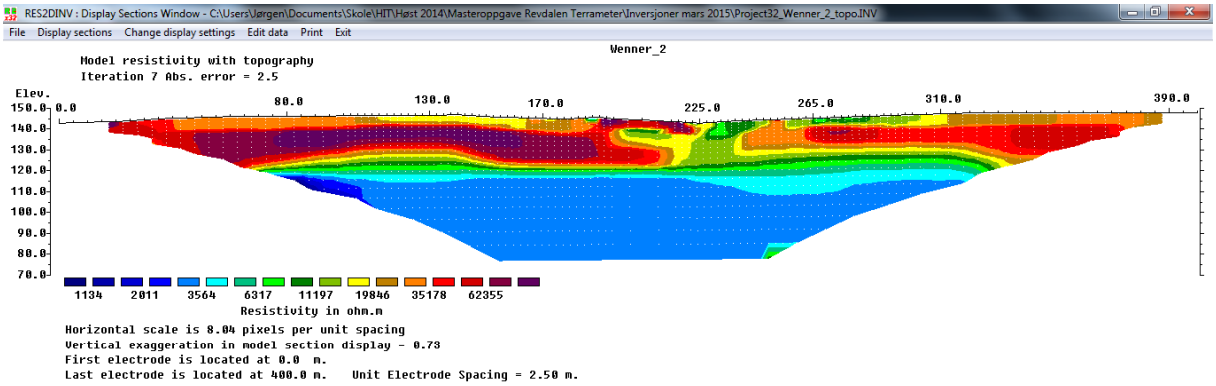

Figure 4.4: Inversion of profile 32 with a logarithmic scale of the resistivity value.

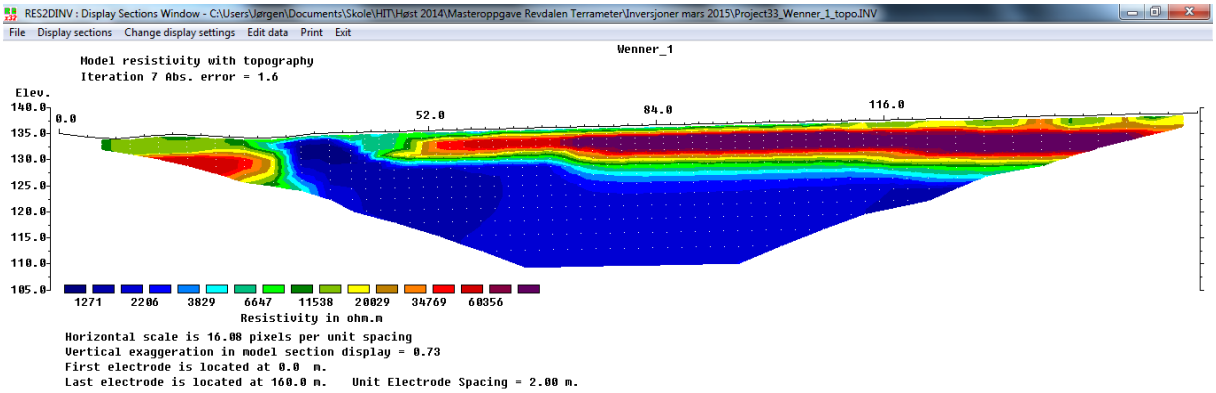

Figure 4.5: Inversion of profile 33 with a logarithmic scale of the resistivity value.

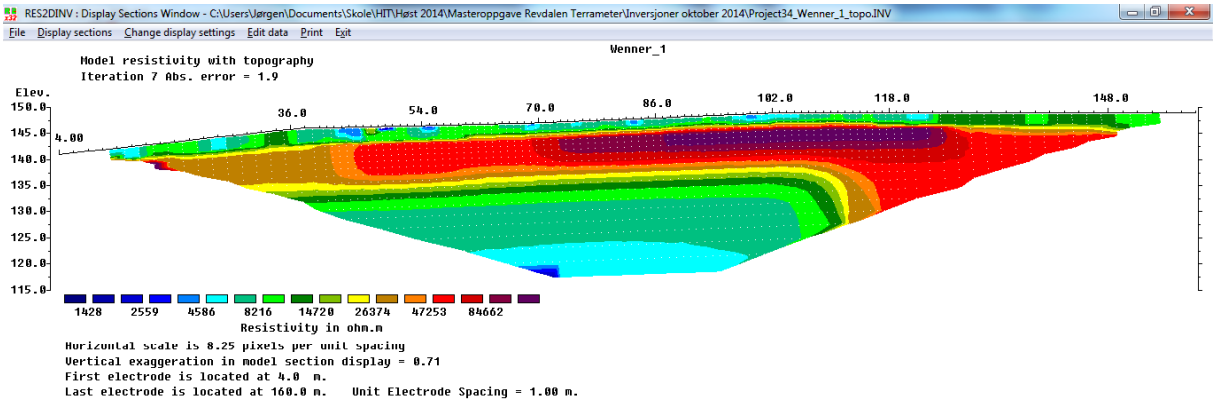

Figure 4.6: Inversion of profile 34 with a logarithmic scale of the resistivity value.

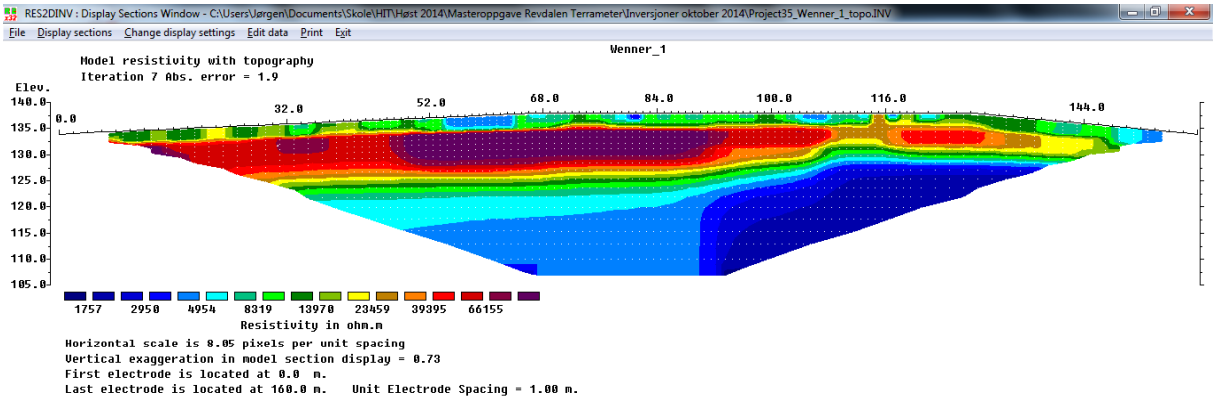

Figure 4.7: Inversion of profile 35 with a logarithmic scale of the resistivity value.

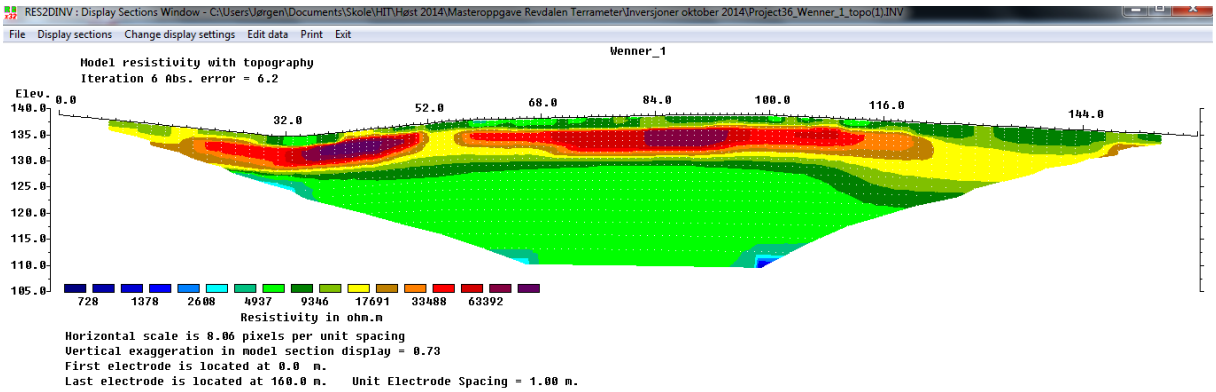

Figure 4.8: Inversion of profile 36 with a logarithmic scale of the resistivity value.

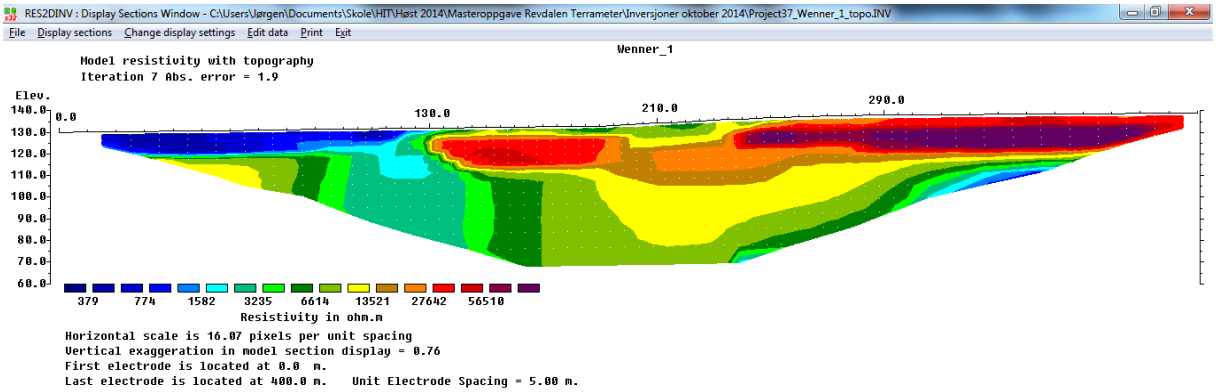

Figure 4.9: Inversion of profile 37 with a logarithmic scale of the resistivity value.

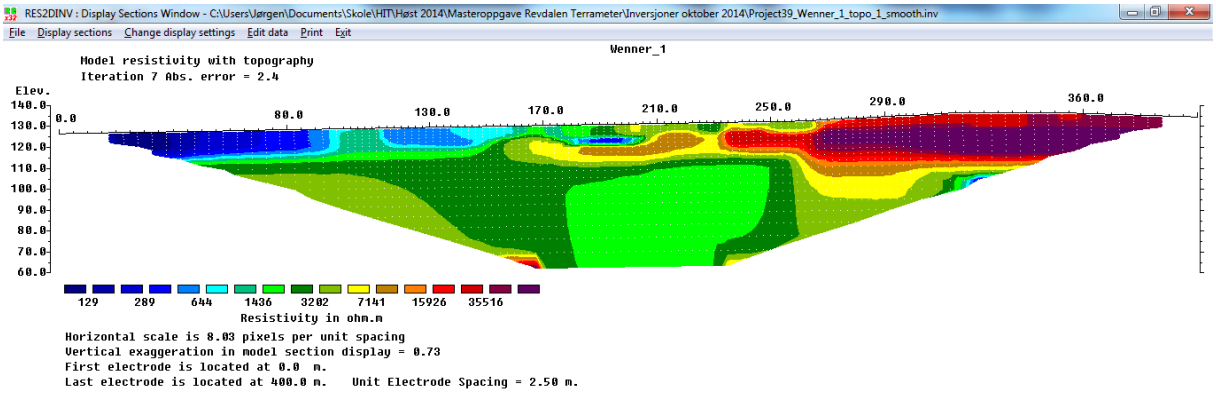

Figure 4.10: Inversion of profile 39 with a logarithmic scale of the resistivity value.

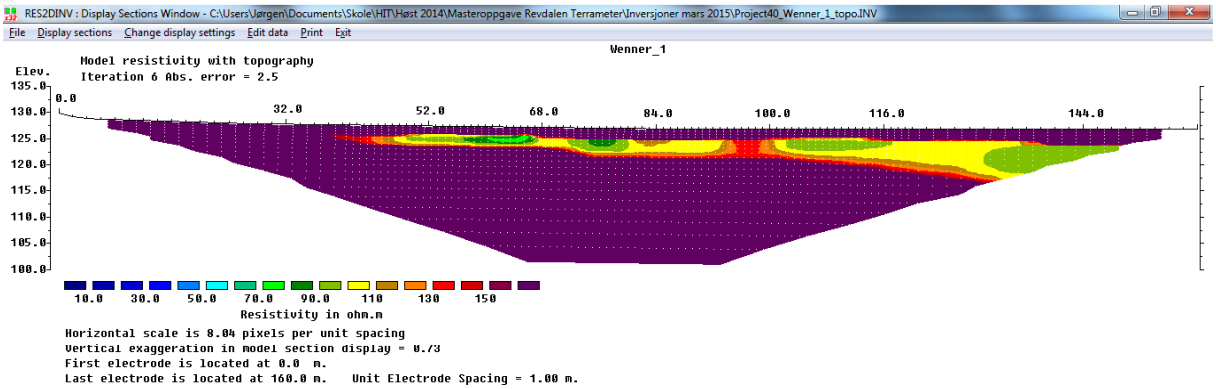

Figure 4.11: Inversion of profile 40 with a small-value scale of the resistivity value.

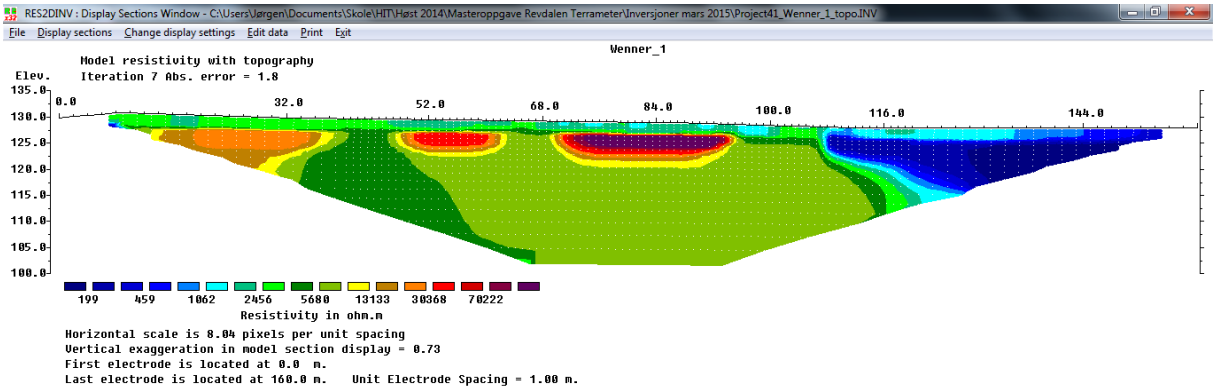

Figure 4.12: Inversion of profile 41 with a logarithmic scale of the resistivity value.

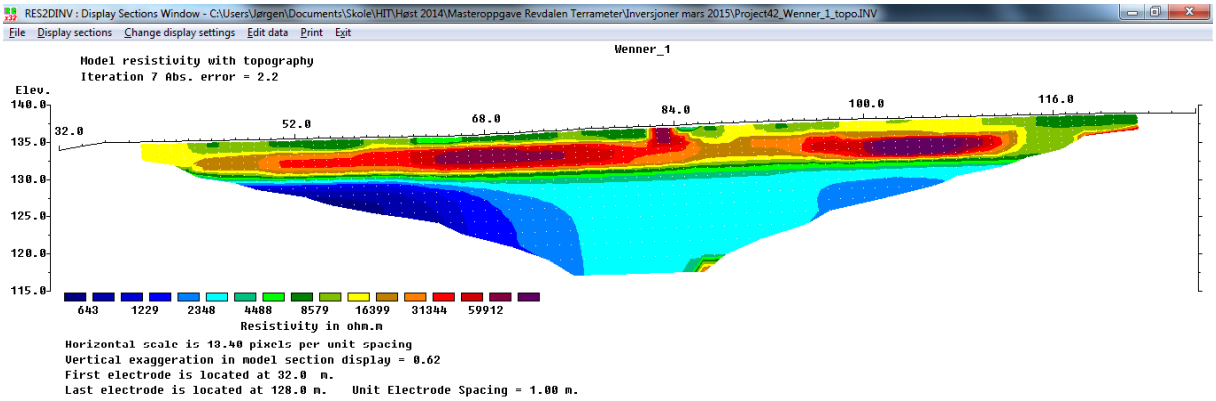

Figure 4.13: Inversion of profile 42 with a logarithmic scale of the resistivity value.

Data from earlier research

Jansen 1983

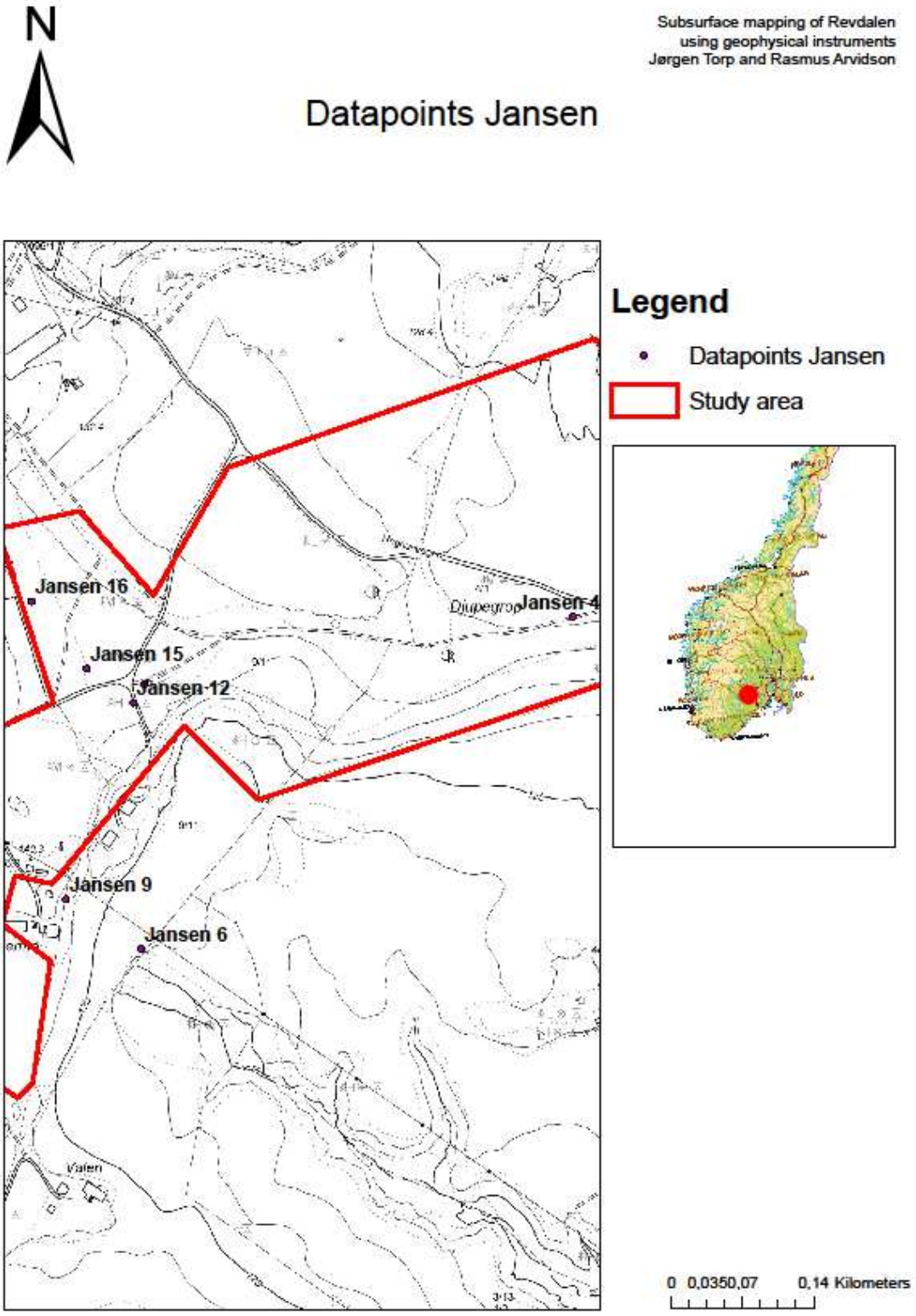

Figure 4.14: Map of Jansen's data from our project in GIS. (Jansen, 1984).

Table 4.1: Table of Jansen's data from our project in GIS.

FID	Profile	POINT_X	POINT_Y	POINT_Z	Depth_bdrc	Bdrck_ma_1
67	Jansen 6	505362,474	6587685,22	121,371574	26	95
68	Jansen 13	505366,79	6587944,83	136,719023	8	129
69	Jansen 12	505355,803	6587926,15	136	13	123
70	Jansen 15	505309,657	6587959,84	136,76843	24	113
71	Jansen 4	505789,121	6588010,95	145,779056	25	121
72	Jansen 16	505255,147	6588026,22	136,397528	22	114
73	Jansen 9	505289,44	6587732,8	132,388695	22	110

Klempe 2001.

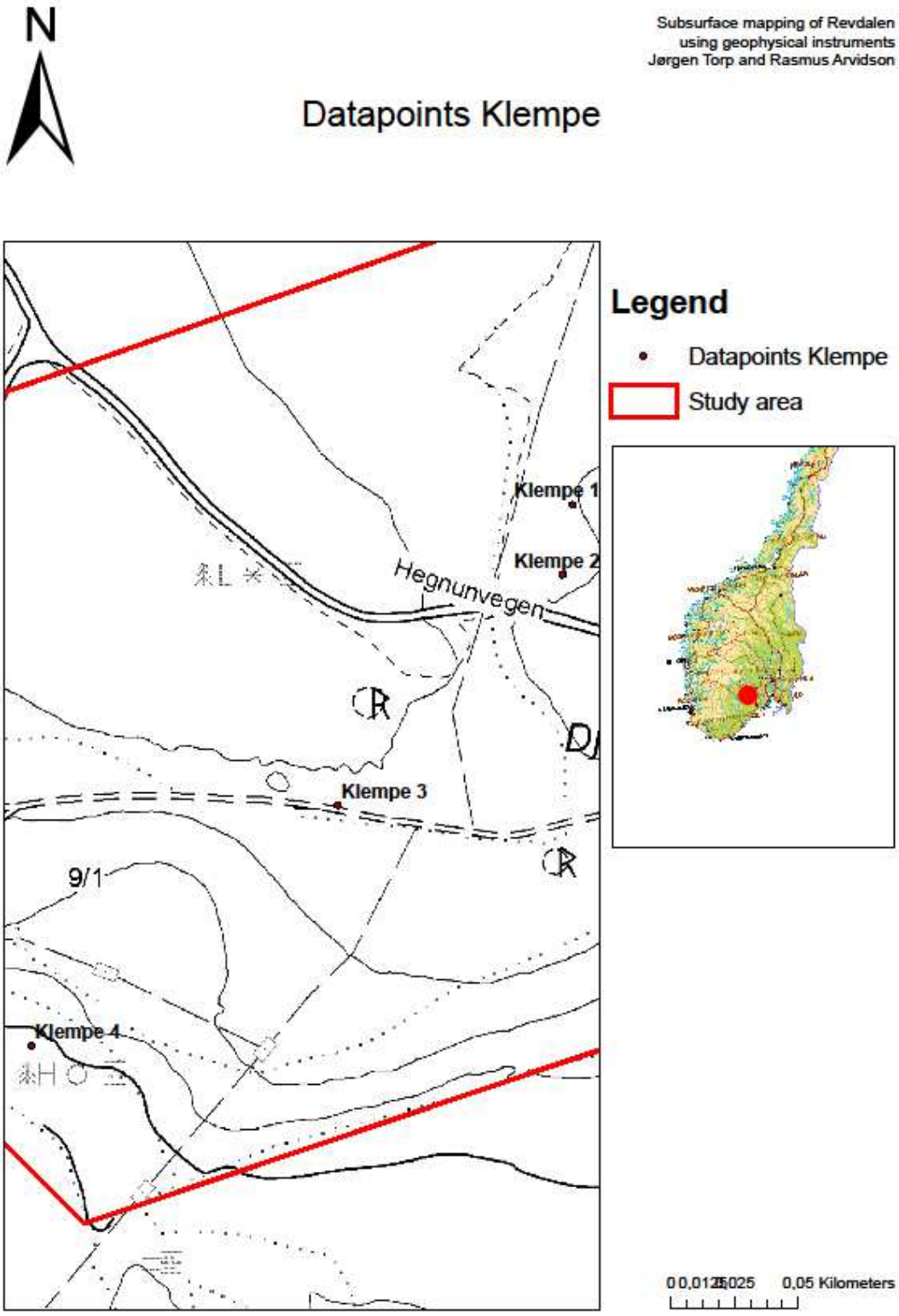

Figure 4.15: Data used from Klempe (2001) from our project in GIS. .

Table 4.2: Klempe's data (2001) from our project in GIS.

FID	Profile	POINT_X	POINT_Y	POINT_Z	Depth_bdrc	Bdrck_ma_1
86	Klempe 2	505666,976	6588085,8	144,004988	28	116
87	Klempe 1	505670,93	6588113,1	144,355606	20	124
88	Klempe 3	505578,539	6587995,24	144,88736	27	118
89	Klempe 4	505457,925	6587900,73	123,997114	12	112

Børresen et al. 1990

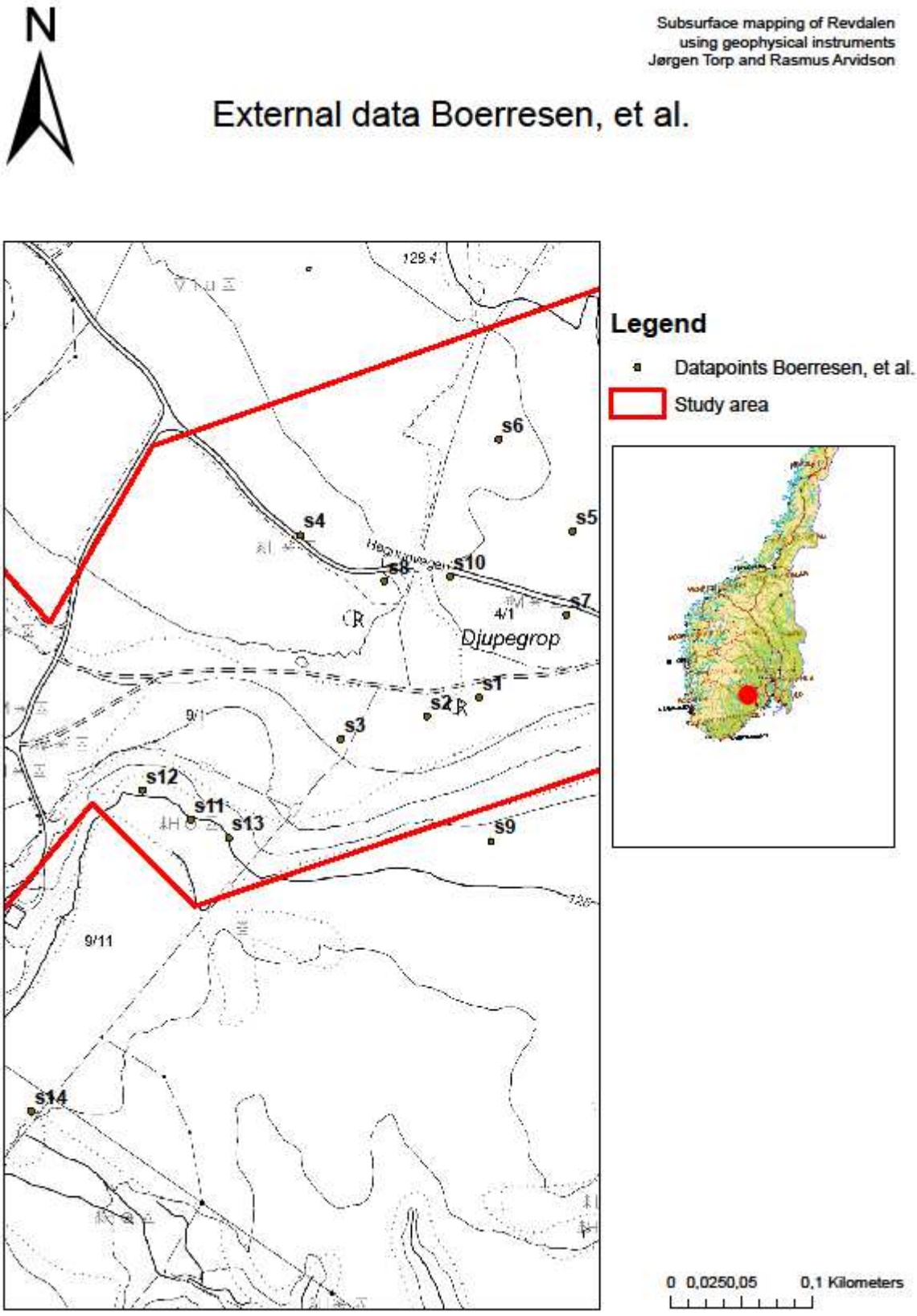

Figure 4.16: Data used from Børresen et al. (1990)from our project in GIS. .

Table 4.3: Table of data from Børresen et al. (1990) from our project in GIS.

FID	Name	POINT_X	POINT_Y	POINT_Z	Depth_bdrc	Bdrck_masl	Surface	Bdrck_ma_1
54	s1	505680,96	6587979,28	144	24	117	141	120
55	s2	505643,839	6587965,79	144	13	121	133	131
56	s3	505582,719	6587949,62	141,150292	17	121	138	124
57	s4	505553,957	6588094,33	148,528511	19	130	149	130
58	s5	505747,577	6588097,32	149	20	122	142	129
59	s6	505694,996	6588162,71	141,505161	4	129	133	138
60	s7	505743,196	6588037,66	147,802784	18	130	148	130
61	s8	505613,818	6588061,69	145,265949	31	115	146	114
62	s9	505689,656	6587876,64	128,093456	23	109	122	105
63	s10	505660,661	6588064,95	145,773 75	30	113	143	116
64	s11	505476,025	6587892,54	124,476185	9	114	123	115
65	s12	505441,87	6587913,22	125,654848	13	111	124	113
66	s13	505502,989	6587879,06	125,246826	2	123	125	123

Klempe unpublished

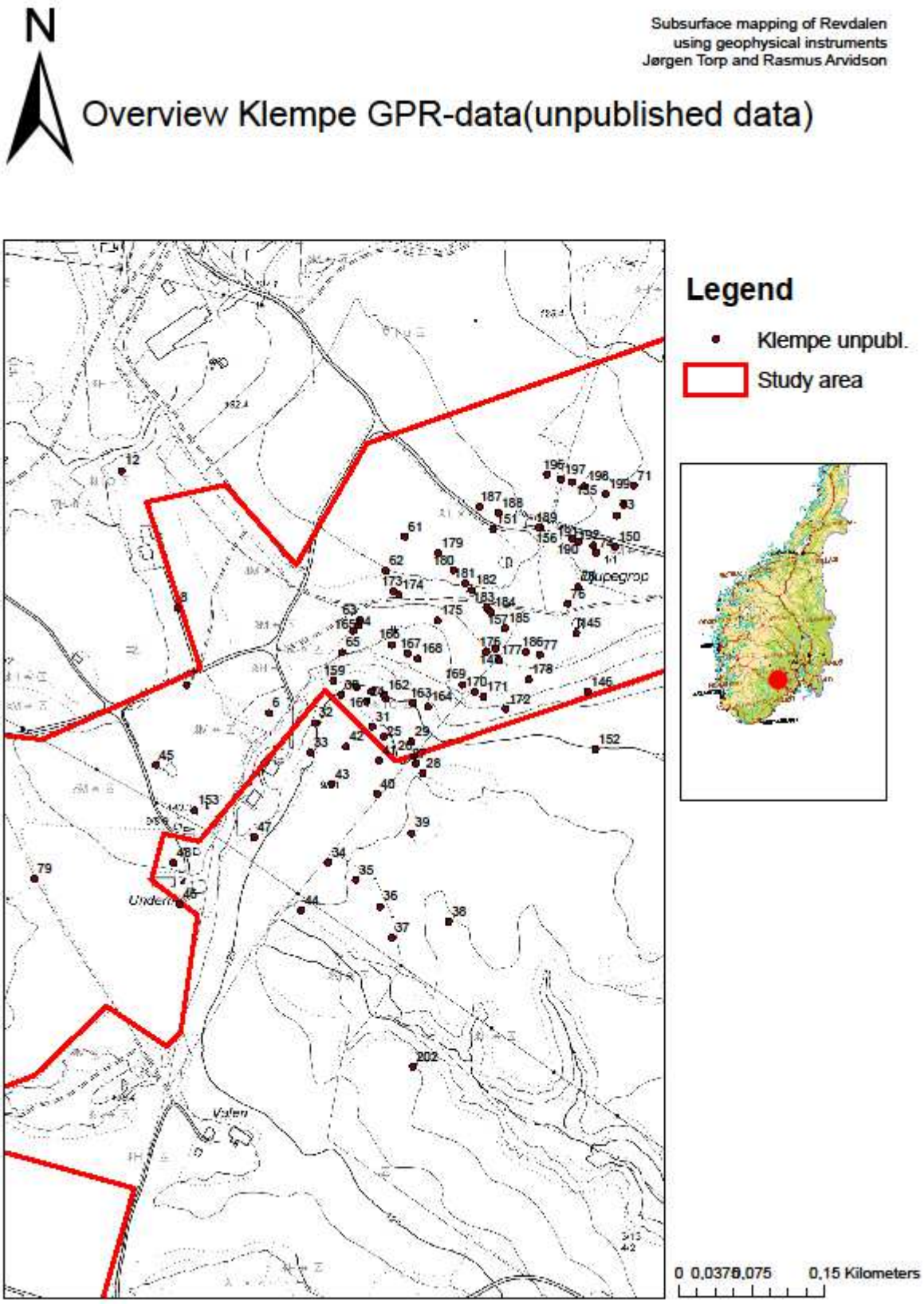

Figure 4.17: Data from Klempe (unpublished) used in our project in GIS.

Table 4.4: Data from Klempe (unpublished) used in our project in GIS.

FID	BN_ALL_ID	POINT_X	POINT_Y	POINT_Z	depth_bdrc	Bdrck_masl	BR_MASL
276	6	505347,906	6587880	136,300752	13	0	123
277	7	505262,844	6587909	136,242869	28	0	108
278	8	505253,281	6587988,5	135,749448	21	0	115
279	12	505195,875	6588129,5	137,377372	15	0	122
280	24	505448,469	6587892,5	123,547132	15	0	109
281	25	505465,719	6587856	122,040431	9	0	113
282	26	505496,688	6587835,5	121,618986	3	0	119
283	27	505499,25	6587828,5	120,98425	2	0	119
284	28	505506,281	6587818,5	120,536253	5	0	116
285	29	505494,625	6587851	122,30749	7	0	115
286	30	505422,219	6587899	124,585923	17	0	108
287	31	505454,188	6587866,5	122,225258	11	0	111
288	32	505395,188	6587870	126,749393	18	0	109
289	33	505390,313	6587839,5	126,101903	20	0	106
290	34	505408,969	6587726,5	120,894355	25	0	96
291	35	505437,188	6587708,5	119,672253	28	0	92
292	36	505461,938	6587681	118,887166	19	0	100
293	37	505474,125	6587649	117,464059	22	0	95
294	38	505532,844	6587665,5	113,756031	12	0	102
295	39	505494,5	6587756,	119,4562	20	0	99

		94	5	7			
296	40	505459,094	6587797	121,129421	6	0	115
297	41	505461,188	6587831,5	121,990663	6	0	116
298	42	505427,063	6587845,5	123,064962	10	0	113
299	43	505412,406	6587807	122,924533	16	0	107
300	44	505380,813	6587677,5	119,148109	30	0	89
301	45	505231,188	6587827	136,032121	7	0	129
302	46	505255,469	6587684	132,514483	6	0	127
303	47	505332,344	6587752,5	125,836361	37	0	89
304	48	505249,281	6587726	135,51432	31	0	105
305	61	505487,469	6588062	146,874161	32	0	115
306	62	505467,938	6588026,5	143,969463	33	0	111
307	63	505441,063	6587976	139,079902	21	0	118
308	64	505434,563	6587965	138,287512	20	0	118
309	65	505423,125	6587942,5	135,60453	20	0	116
310	71	505723,688	6588114,5	147,520524	24	0	124
311	72	505713,125	6588095	148,309483	23	0	125
312	73	505705,813	6588083,5	148,186281	20	0	128
313	74	505684,625	6588045,5	147,857865	26	0	122
314	75	505665,906	6588010	143,960142	24	0	120
315	76	505655,313	6587993	143,926571	21	0	123
316	77	505626,813	6587940,5	141,448764	26	0	115
317	79	505105,75	6587710	131,134004	23	0	108
318	145	505664,1	6587962,	143,8234	26	0	118

		56	5	78			
319	146	505676,156	6587902,5	132,504632	12	0	121
320	147	505581,188	6587947	140,771226	20	0	121
321	150	505704,219	6588052	148,054808	18	0	130
322	151	505578,531	6588069,5	146,705454	31	0	116
323	152	505683,781	6587843	124,72676	16	0	109
324	153	505270,844	6587780	138,99888	33	0	106
325	155	505659,813	6588118	143,130472	22	0	121
326	156	505626,906	6588071	144	30	0	114
327	157	505574	6587987	144,437505	28	0	116
328	158	505467,813	6587895	124,140287	13	0	111
329	159	505414,188	6587913,5	127,332281	-2	0	129
330	160	505437,563	6587907	124,715013	13	0	112
331	161	505453,156	6587902,5	124,136684	15	0	109
332	162	505466,438	6587899	124,592914	13	0	112
333	163	505496,219	6587890,5	125,389107	13	0	112
334	164	505511,344	6587886,5	127,977783	15	0	113
335	165	505439,875	6587970,5	138,637306	4	0	135
336	166	505474,25	6587950,5	133,932757	6	0	128
337	167	505490,281	6587941,5	133	14	0	119
338	168	505500,813	6587936	133	28	0	105
339	169	505547,094	6587909,5	135,977154	30	0	106
340	170	505559,938	6587902	136,560846	19	0	118
341	171	505568,6	6587897	136,6571	10	0	127

		56		04			
342	172	505591,563	6587884,5	132,883668	3	0	130
343	173	505475,625	6588005,5	141,817375	7	0	135
344	174	505481,563	6588002	141,459018	17	0	124
345	175	505521,438	6587975,5	136,701157	29	0	108
346	176	505571,406	6587943,5	139,613469	31	0	109
347	177	505584,688	6587934,5	139,90803	14	0	126
348	178	505614,938	6587915	138,669586	11	0	128
349	179	505521,906	6588045	146,217043	28	0	118
350	180	505537,938	6588027,5	145,498337	31	0	114
351	181	505549,844	6588014	145,040762	24	0	121
352	182	505556,719	6588006,5	145	24	0	121
353	183	505571,844	6587989	144,502773	30	0	115
354	184	505576,438	6587984	144,316916	28	0	116
355	185	505590,656	6587967,5	143,670831	27	0	117
356	186	505612,188	6587943	141,681472	16	0	126
357	187	505564,531	6588092,5	148,396361	21	0	127
358	188	505583,781	6588086	147,629363	32	0	116
359	189	505625,469	6588071,5	144	30	0	114
360	190	505660,313	6588060	146,072843	32	0	114
361	191	505666,719	6588057	146,670914	24	0	123
362	192	505681,844	6588052,5	147,901765	22	0	126
363	196	505634,188	6588126	137,79565	19	0	119
364	197	505648,3	6588121	142,0041	21	0	121

		75		68			
365	198	505672,688	6588113,5	144,662828	19	0	126
366	199	505694,219	6588106	146,994301	21	0	126
367	202	505496,102	6587516,32	115,413315	29	0	86

GPS coordinates

Table 4.5: GPS coordinates for GPR measurements.

GPR			**X**	**Y**
Line	0	start	505428	6587908
Line	0	stop	505479	6587881
Line	1	start	505591	6588004
Line	1	stop	505673	6588003
Line	3	start	505527	6588050
Line	3	stop	505426	6588034
Line	4	start	505557	6588054
Line	4	stop	505655	6588075
Line	5	start	505462	6587962
Line	5	stop	505550	6587942
Line	6	start	505015	6587633
Line	6	stop	504957	6587718

Table 4.6: GPS coordinates for available resistivity measurements.

RES			**X**	**Y**
Profile	26	start	505227	6588080
Profile	26	stop	505522	6587896
Profile	27	start	505381	6587986
Profile	27	stop	505766	6587938
Profile	29	start	505428	6587908
Profile	29	stop	505519	6587857

Profile	30	start	505393	6588016
Profile	30	stop	505794	6588034
Profile	32	start	505401	6588043
Profile	32	stop	505800	6588088
Profile	33	start	505324	6587913
Profile	33	stop	505458	6587955
Profile	34	start	505649	6588127
Profile	34	stop	505805	6588094
Profile	35	start	505199	6587877
Profile	35	stop	505363	6587876
Profile	36	start	505232	6587792
Profile	36	stop	505335	6587925
Profile	37	start	504883	6587867
Profile	37	stop	505221	6587788
Profile	39	start	505185	6587867
Profile	39	stop	504900	6587593
Profile	40	start	504809	6587689
Profile	40	stop	504934	6587586
Profile	41	start	504903	6587735
Profile	41	stop	505015	6587633